Functional characterisation of the lipid raft protein stomatin

by

Dorothy Kate Wilkinson

Submitted in accordance with the requirements

for the degree of Doctor of Philosophy

The University of Leeds

School of Biochemistry and Microbiology

November 2005

The candidate confirms that the work submitted is her own and that appropriate credit has been given where reference has been made to the work of others.

Acknowledgements

I would like to thank my supervisors Prof. Nigel Hooper (University of Leeds) and Prof. Gordon Stewart (University College London). Particularly Nigel for providing his continued guidance and support throughout my degree and Gordon for the many hours spent collecting and delivering patient samples at the weekends. Thank you to Nigel for reading this manuscript and offering his advice.

I would like to thank all individuals who donated their blood in the name of science.

I would like to thank all members of the Hooper lab, past and present, for their support and entertainment over the years – it's been fun! I would like to thank Daniel for his interest and help with all things calpain and Ashley for her technical guidance and patience on all things AFM.

I would greatly like to thank all fellow surfers in Leeds and the surrounding area. Between you and Mother Nature I have emerged sanity intact.

I would like to thank Rob for his love and support throughout.

Without doubt, I am most indebted to my family. Mum, dad, brother Ralph and the feline members Horace, Boris and Murphy. Without their love, support (which manifests in many forms) and confidence over the past 26 years this work would not have been possible which is why I dedicate this thesis to them.

Abstract

The function of the integral membrane protein stomatin is as yet poorly understood. Stomatin is deficient from the erythrocyte membrane of patients suffering with Over-hydrated Hereditary Stomatocytosis (OHSt). Patient erythrocytes have altered morphology and are known as stomatocytes. It is believed that stomatin is mis-trafficked in the developing stomatocyte. These patients suffer grossly abnormal cation fluxes in the stomatocyte membrane which causes increased osmotic fragility of the cell and results in haemolytic anaemia. This study set out to characterise further stomatin and to investigate its role in the cell. The membranes and lipid rafts of stomatocytes were found to have reduced actin levels as compared to erythrocytes, suggesting that stomatin may function as a structural protein linking the cytoskeleton to the membrane. Overexpression of stomatin in nucleated cells caused enhanced actin association with cell membranes and lipid rafts, further confirming the findings from stomatocytes. Calcium-induced vesiculation was found to be significantly enhanced from the stomatocyte as compared to the erythrocyte, with defective partitioning of the flotillin proteins into the vesicles. This suggests that stomatin may function as a negative regulator in this vesiculation, possibly due to its interaction with actin and that the flotillins may substitute for stomatin in this process within the stomatocyte.

Mutating the principle cysteine residue for palmitoylation within stomatin caused the protein to show less affinity for the membrane and lipid rafts but an increased affinity for the nucleus. This suggests that palmitoylation of stomatin affects the affinity of stomatin for the membrane and that this modification may be involved in regulating the shuttling of stomatin between the plasma membrane and the nucleus.

Prokaryotic stomatin exists in an operon with a serine protease, suggesting a functional link between the two. Using a reporter gene construct approach the potential for mammalian stomatin to be proteolytically processed was investigated. Stomatin was found to be proteolytically processed in the membrane by a serine protease with the subsequent release of a C-terminal fragment.

Table of Contents

List of Figures

Abbreviations

2.1	Band 2.1
4.1	Band 4.1
AFM	Atomic force microscopy
Amp	Ampicillin
APP	Amyloid precursor protein
APP-GV	APP fused to Gal4-VP16 protein
Aqp-1	Aquaporin-1
ASIC	Acid-sensing ion channel
ATP	Adenosine triphosphate
BD	Binding domain
bp	Base pairs
BU17	Glioma cells
Ca^{++}	Calcium ions
cDNA	Coding DNA
C.elegans	*Caenorhabditis elegans*
CHC	Cryohydrocytosis
CHO	Chinese hamster ovary cells
C-terminus	Carboxy-terminus
dci	3,4-dichloroisocoumarin
dH_2O	Distilled water
DHSt	Dehydrated hereditary stomatocytosis
DMEM	Dulbecco's Modified Eagle's Medium
DMSO	Dimethyl sulphoxide
DNA	Deoxyribonucleic acid
DRM	Detergent resistant membrane

dsDNA	Double stranded DNA
DTT	Dithiothreitol
E	Erythrocytes
E64	Trans-Epoxysuccinyl-L-Leucylamido-(4-Guanidino) Butane
ECP-51	Erythrocyte cytosol protein-51
ECP-54	Erythrocyte cytosol protein-54
ENaC	Epithelial sodium channel
F-1	Flotillin-1
F-2	Flotillin-2
FCS	Foetal calf serum
FP	Familial pseudohyperkalaemia
FRAP	Fluorescence recovery after photobleaching
FRET	Fluorescence resonance energy transfer
g	Gravity
GA	Glycophorin A
GLUT	Glucose transporter molecule
G6PD	Glucose-6-phosphate dehydrogenase
GPI	Glycosylphosphatidylinositol anchor
GUV	Giant unilamellar vesicle
GV	Gal4-VP16
HCl	Hydrochloric acid
HEK	Human embryonic kidney cells
HeLa	Helen Lane
HRP	Horseradish peroxidase
hSLP-1	Human stomatin like protein-1
hSLP-2	Human stomatin like protein-2

K^+	Potassium ions
kb	Kilobases
kDa	Kilodaltons
lac	Lactacystin
LB	Luria Bertani medium
L_d	liquid-disordered
L_o	liquid-ordered
LRP	Low density lipoprotein receptor-related protein
MβCD	Methyl-β-cyclodextrin
MAC	Membrane attack complex
MDCK	Mardin-Darby canine kidney cells
MBS	MES buffered saline
Mg^{++}	Magnesium ions
mRNA	Messenger RNA
Na^+	Sodium ions
NaCl	Sodium chloride
NaK	Sodium potassium pump
NEAA	Non-essential amino acids
NLS	Nuclear localisation signal
nsLTP	non-specific lipid transfer protein
N-terminus	Amino terminus
OHSt	Over-hydrated hereditary stomatocytosis
1, 10 P	1, 10-Phenanthroline
PAGE	Polyacrylamide gel electrophoresis
PBS	Phosphate buffered saline
PCR	Polymerase chain reaction

P. horikoshii	*Pyrococcus horikoshii*
PKC	Protein kinase C
PLAP	Placental alkaline phosphatase
PMA	Phorbol 12-myristate 13-acetate
PMSF	Phenylmethylsulphonyl Fluoride
PS	Phosphatidylserine
p-stomatin	Prokaryotic stomatin
PVDF	Poly (vinylidene) difluoride membrane
RNA	Ribonucleic acid
rpm	Revolutions per minute
S	Stomatocytes
SDS	Sodium dodecyl sulphate
SEM	Standard error of the mean
SH-SY5Y	Human neuroblastoma cells
Spec	Spectrin
SPFH	Stomatins, Prohibitins, Flotillins and HflK/C domain
STOPP	Stomatin operon partner protein
T	Transfected
TAE	Tris/Acetic acid/EDTA buffer
TBS	Tris buffered saline
TCR	T cell receptor
TGS	Tris/Glycine/SDS buffer
Tm	Melting temperature
ΔTMN	Stomatin protein lacking transmembrane and N-terminus
ΔTMN-GV	ΔTMN fused to Gal4-VP16 protein
TMN	Tetraploid murine neuroblastoma cells

TOPO	pcDNA3.1/V5-His©TOPO®TA
TX-100	Triton X-100
UAC	Human amniotic cells
UT	Untransfected
v/v	Volume for volume
Wt	Wild type
Wt-GV	Stomatin fused to Gal4-VP16 protein
w/v	Weight for volume

Chapter 1: Introduction

1.1 The erythrocyte

Erythrocytes serve as oxygen and carbon dioxide carriers within the blood; each litre of blood contains approximately 5 x 10^{12} erythrocytes. They are devoid of many cellular organelles, such as the nucleus, in order to maximise the volume available to the oxygen-transporting haemoglobin. Rather than being spherical, the erythrocyte is biconcave; this increases the surface area over which gas exchange can take place. Erythrocytes circulate in the blood for approximately 120 days before being phagocytosed and digested by macrophages in the liver or spleen. Low oxygen levels in the blood or a shortage of erythrocytes stimulates the kidneys to secrete erythropoietin. In humans, this stimulates erythropoiesis in the bone marrow; this causes differentiation of hematopoietic stem cells into mature erythrocytes (Richmond *et al.* 2005).

1.1.1 Organisation of the erythrocyte membrane

The membrane of the erythrocyte has to provide sufficient mechanical stability to ensure survival of the cell but also has to provide a degree of flexibility which allows deformation during transit through the narrow capillary network. The lipid bilayer is supported by a series of cytoskeletal proteins to allow this. Early work to identify the major proteins of the erythrocyte membrane used Sodium Dodecyl Sulphate Polyacrylamide Gel Electrophoresis (SDS-PAGE). Proteins were identified according to their electrophoretic mobility on the gels and given names such as 'band 3' to describe their relative position on the gel (Fairbanks *et al.* 1971).

Spectrin is thought to play a central role in maintaining cell shape whilst permitting the large reversible deformations required of the erythrocyte (figure 1.1). The two isoforms of spectrin, α and β, form heterodimers which are loosely intertwined. These heterodimers are linked head-to-head to form tetramers. The junctions between heterodimers are sites where several other proteins, as well as spectrin, can bind; this allows anchorage to the membrane via interaction with transmembrane proteins (Bennett 1989). This meshwork of spectrin covers the entire cytoplasmic surface of the erythrocyte membrane and is anchored to the membrane at two types of site. The first involves the transmembrane anion exchanger, band 3. Band 3 is responsible for the exchange of chloride and bicarbonate across the phospholipid bilayer (Fu *et al.* 2004). The protein ankyrin binds to spectrin and to the cytoplasmic domain of band 3. It is thought that protein 4.2, also bound here, stabilises this interaction. The second site at which the spectrin meshwork is anchored to the membrane is through interaction with protein 4.1 which in turn binds to glycophorin. Spectrin is also able to associate with actin, this is stabilised by protein 4.1 and adducin. Bundles of filamentous actin crosslinked by protein 4.9 associate with tropomyosin and tropomodulin (Tse *et al.* 1999). Many of the major cytoskeletal proteins are phosphorylated; this reduces the binding affinity of the components and weakens the rigidity of the membrane. How phosphorylation regulates the mechanical stability of the membrane is unknown (Manno *et al.* 2005). Mutations in the genes that encode major erythrocyte membrane-associated proteins can cause complete or partial protein deficiencies within the membrane. Alternatively, some mutations can allow the protein to locate to the membrane but show an incorrect function (Low *et al.* 2001). This can compromise the shape of the erythrocyte, its stability and function. Frequently the mutations will hinder the association with binding-partners in the membrane. In a

secondary manner these binding partners are then diminished in the erythrocyte membrane (McMullin 1999). For example, hereditary spherocytosis is a haemolytic anaemia in which the erythrocyte shows increased osmotic fragility and spherocytic morphology. Mutations in ankyrin, band 3, band 4.2 and spectrin are all known to cause this condition (Delaunay 2002).

The lipid distribution across the bilayer is under tight control; aminophospholipids (e.g. phosphatidylserine and phosphatidylethanolamine) are maintained on the inner surface of the bilayer whereas the cholinephospholipids are predominantly located in the outer leaflet. Scramblase, translocase and flippase proteins ensure transbilayer asymmetry (Zwaal *et al.* 1997). This lipid maintenance provides the erythrocyte with mechanical stability through phosphatidylserine-cytoskeletal protein interactions and ensures cell survival; phosphatidylserine on the outer surface marks a cell for destruction by macrophages (Manno *et al.* 2002).

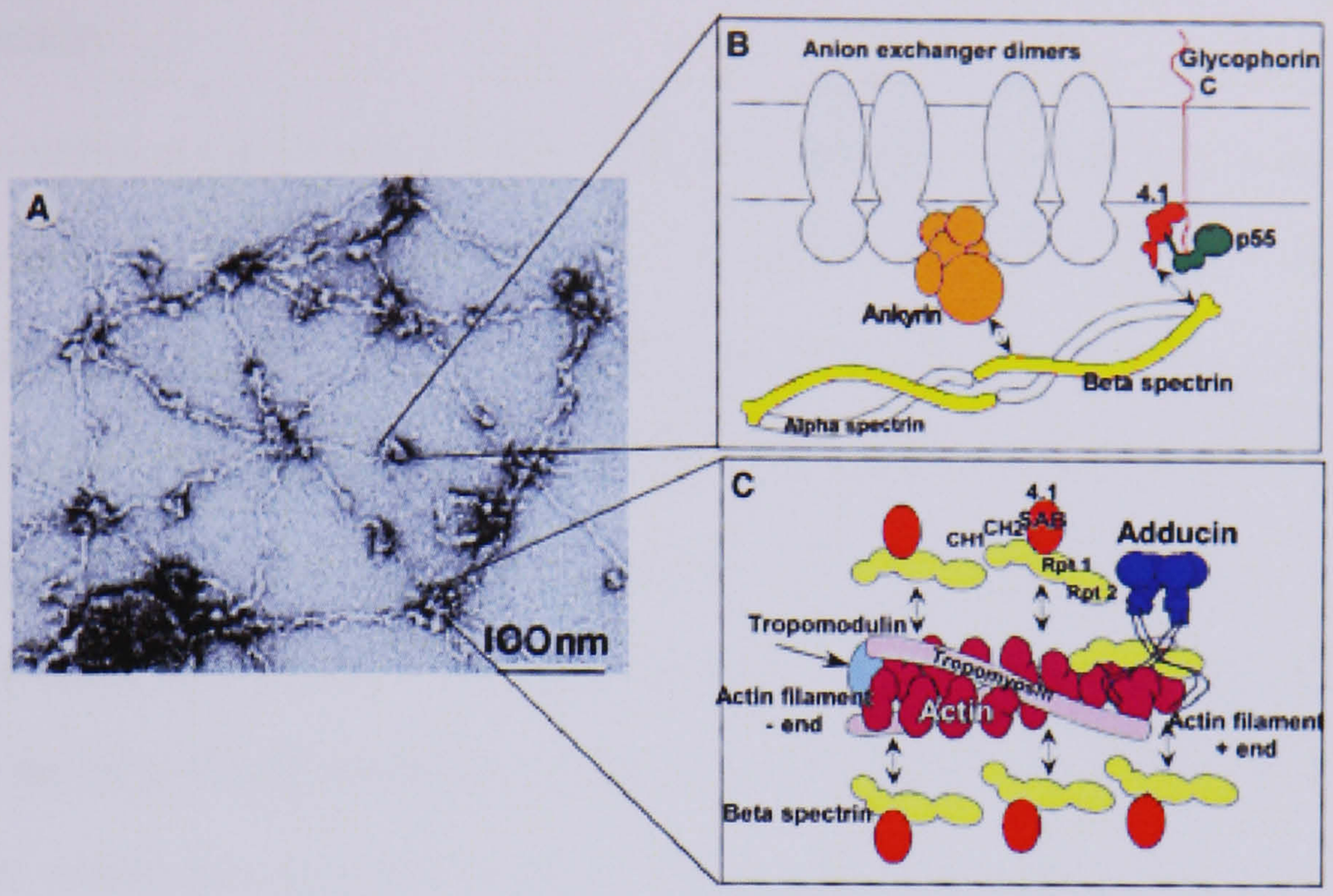

Figure 1.1 Organisation of the erythrocyte membrane skeleton

(A) Electron microscopy of the erythrocyte membrane skeleton. (B) Junctions where spectrin is anchored to the membrane via band 3 and glycophorin. (C) The spectrin-actin junction. Figure taken from (Bennett *et al.* 2001).

1.2 Stomatin

The membrane protein stomatin was originally identified due to its absence from the erythrocyte membrane in patients suffering Over-hydrated Hereditary Stomatocytosis (OHSt). The erythrocytes of OHSt patients were observed to have altered morphology and adopt a mouth-like shape rather than the traditional disc-like shape and were thus called stomatocytes. Stoma, being the Greek for mouth, gave the name to the protein and the condition. Due to its relative electrophoretic mobility on SDS-PAGE stomatin is also known as band 7.2b (Lande *et al.* 1982). Although widely expressed in animals, plants and microorganisms, and in many tissues, the function of stomatin is as yet unclear (Stewart *et al.* 1992).

1.2.1 Characteristics of stomatin

Purification of band 7.2b revealed an integral membrane phosphoprotein of 32kDa (Wang *et al.* 1991). In situ proteolytic fragmentation of the protein revealed an intracellular domain larger than 12 kDa (Hiebl-Dirschmied *et al.* 1991a). Cloning of the cDNA encoding stomatin showed that the protein contained a stretch of 29 hydrophobic residues, amino acids 26-54 inclusive. The hydrophobic stretch is preceded by a highly charged 24 residue long N-terminus and followed by the relatively large C-terminus accounting for the remaining 234 residues and the previously identified 12 kDa intracellular domain (Hiebl-Dirschmied *et al.* 1991b; Stewart *et al.* 1992). The N-terminus of stomatin was initially considered to be exoplasmic forming a bitopic membrane protein. However, the identification of a phosphorylation site at Ser-9 proved that the N-terminus also faced the cytoplasm, resulting in an entirely cytofacial monotopic membrane conformation (figure 1.2). This formation of a protein in the membrane is known as a hairpin loop (Salzer *et al.*

1993). Stomatin is palmitoylated at cysteine 29 (Cys-29) and cysteine 86 (Cys-86). Cys-29 forms the major palmitoylation site and, due to its positioning relative to the transmembrane domain, is suggested to enhance the affinity of the protein for the membrane (Snyers *et al.* 1999b). In the human amniotic cell line UAC, stomatin is present in membrane-protruding folds and extensions at high concentrations where it co-localises with actin microfilaments even after disruption of the filaments with cytochalasin D. This prompted suggestions that stomatin functions as a structural protein which anchors the actin cytoskeleton to the membrane (Snyers *et al.* 1997). Stomatin is able to form homo-oligomers which comprise of between 9 and 12 subunits; truncation mutants suggest the C-terminus is critical for this association. As many other oligomeric proteins are associated with cellular roles in morphogenesis, it was suggested that stomatin may function similarly (Snyers *et al.* 1998).

Stomatin shows similar trafficking to glycosylphosphatidylinositol (GPI)-anchored proteins in polarised epithelial cells, co-localising to the apical membrane (Snyers *et al.* 1999). Whilst in the Golgi complex GPI-anchored proteins become associated with sphingolipid and cholesterol-enriched lipid rafts, this is thought to cause apical targeting of the proteins (Simons *et al.* 1997). Lipid rafts are resistant to non-ionic detergents at cold temperatures; this allows their isolation from the rest of the plasma membrane. Stomatin too can be isolated in detergent resistant complexes of the plasma membrane, suggesting the protein resides within lipid rafts (Salzer *et al.* 2001). Caveolae form a well characterised subset of lipid rafts, so-called due to the high concentration of the structural protein caveolin. They are implicated in endocytosis and cell signalling (Hooper 1999). Stomatin does not co-localise with caveolin and therefore functions in a separate lipid microdomain perhaps providing

a critical structural element required for formation and integrity of this stomatin-specific microdomain (Snyers *et al.* 1999a). Stomatin does share some structural similarities with caveolin; both contain multiple sites of palmitoylation, both oligomerise and both assume a hairpin loop in the lipid bilayer. This again prompted suggestions of a structural role for stomatin (Snyers *et al.* 1999b). As well as being located in the plasma membrane, stomatin has also been found in the nucleus (Fricke *et al.* 2005), mitochondria (Argent *et al.* 2004), endosomes (Snyers *et al.* 1999a) and lipid bodies (Umlauf *et al.* 2004). The role of stomatin in the nucleus and mitochondria has never been investigated. Lipid bodies are implicated in the storage and turnover of lipids, protecting the cell membrane from lipid overload (van Meer 2001). It is as yet unknown what role stomatin has in the lipid bodies; lipid organisation and cargo selection are amongst the possibilities (Umlauf *et al.* 2004). Two chaperones of stomatin have been isolated from human erythrocyte cytosol, ECP-51 and ECP-54. They contain ATP-binding sites, interact with each other and are found in both the cytosol and nucleus (Salzer *et al.* 1999).

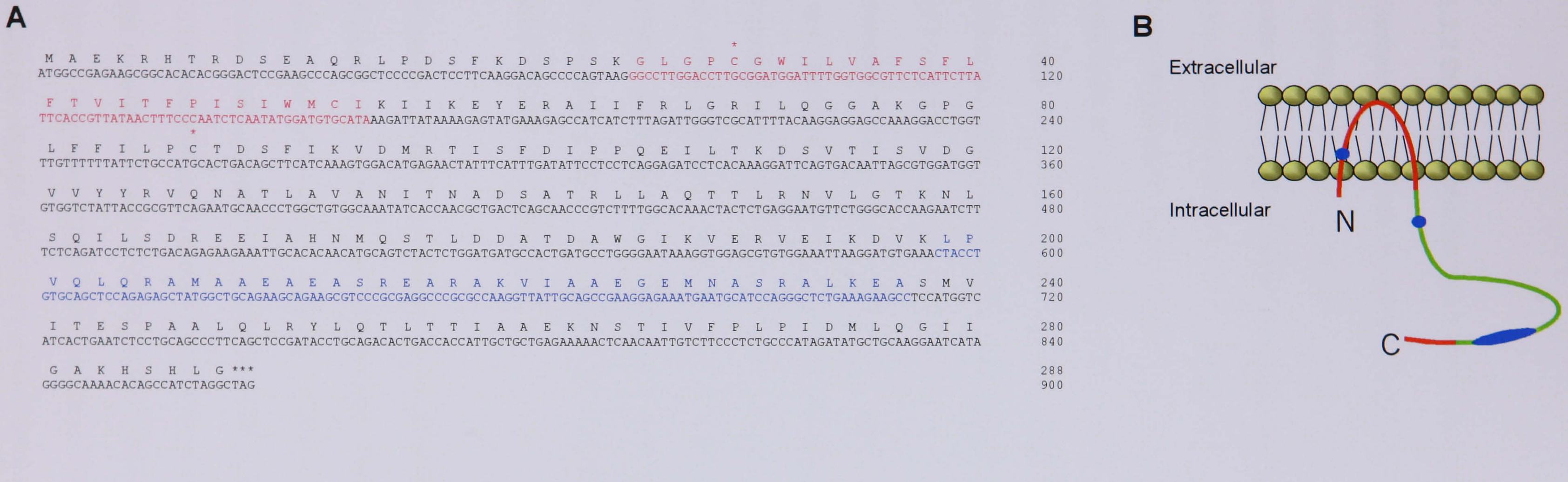

Figure 1. 1 Sequence and membrane topology of stomatin

(A) Amino acid and nucleotide sequence of human stomatin. The SPFH domain begins at amino acid position 55 and ends position 256. The hydrophobic transmembrane region is highlighted red. Oligomerisation of stomatin is mediated by coiled coils in the AE-rich sequence shown in blue. * indicates a palmitoylated cysteine.

(B) Stomatin adopts a hairpin loop configuration in the lipid bilayer. Both the N and C terminii are cytosolic. Caveolin, podocin and the flotillins are also known to adopt a hairpin loop configuration in the bilayer (Langhorst *et al.* 2005). The SPFH domain is shown in green. Blue spheres indicate palmitoylated cysteines. Blue oval shows AE-rich region.

1.2.2 Stomatin and the movement of ions across the membrane

Stomatin is deficient in the erythrocyte membranes from patients suffering Over-hydrated Hereditary Stomatocytosis (OHSt) (discussed in detail below). The patient's erythrocytes suffer increased intracellular cation concentration due to an as yet uncharacterised leak in the membrane. It is unclear if the deficiency in stomatin is the direct cause of the cation leak but this has prompted speculation that stomatin may have an ion channel regulatory role (Lande *et al.* 1982). Although this role for stomatin has never been proven, other studies have linked stomatin with ion channels, particularly the epithelial sodium channel (ENaC). Stomatin and subunits of ENaC have been found expressed in the same dorsal root ganglion of rats; this is consistent with a role for stomatin in mechanotransduction (Fricke *et al.* 2000). The stomatin homologue MEC-2 in the nematode *Caenorhabditis elegans* (*C.elegans*) interacts with and regulates the ion channel degenerin, the mammalian equivalent of which is ENaC. This has been linked to mechanotransduction (Goodman *et al.* 2002). As the activation of ENaC requires the channel activating protease xCAP-1, it has been suggested that stomatin may function to regulate this activity (Vallet *et al.* 2002; Green *et al.* 2004).

Patients suffering from Liddle's syndrome have a congenitally leaky ENaC. In this disease the domain associated with Nedd-4 ubiquitination protein turnover is destroyed by mutation, causing increased numbers of the channel and elevated mean open probability (Abriel *et al.* 1999; Stewart *et al.* 1999). Na^+ and K^+ transport in the patient's erythrocytes is accelerated suggesting there may be a few copies of the protein functioning in the erythrocyte under normal conditions (Gardner *et al.* 1971). However, ENaC has never been found in the erythrocyte and treatment to inhibit the channel fails to correct the leak seen in OHSt cells (Stewart *et al.* 1992).

Stomatin is expressed in mammalian sensory neurons (Mannsfeldt *et al.* 1999). Here stomatin is known to bind and alter the activity of acid-sensing ion channels (ASICs). These Na^+ channels are members of the ENaC family expressed in the central and peripheral nervous systems of mammals and other vertebrates, where they are thought to function as transducers of sensory stimuli. It is unclear if this is a direct association, i.e. stomatin forms a subunit of the channel, or indirect association facilitated by the presence of stomatin in lipid rafts (Price *et al.* 2004).

Stomatin has been shown to exhibit an affinity for the GLUT-1 glucose transporter and is the first known protein to exert a regulatory effect on this transporter (Zhang *et al.* 1999). Overexpression of stomatin depresses the transporter's activity. These data imply a possible link between stomatin and glucose transport across the cell membrane (Zhang *et al.* 2001).

1.2.3 Stomatin and proteolysis

Protein-protein BLAST searching of prokaryotic genomes identified 23 organisms with stomatin homologues (p-stomatin). In every genome found to encode p-stomatin, the gene encoding 'stomatin operon partner protein' (STOPP) was also found. In 19 of these genomes *stopp* was found adjacent to *p-stomatin* where they are thought to share the same operon (Green *et al.* 2004). Genes found in operons often code for components involved in the same multimolecular process (Lawrence *et al.* 1996). Prokaryotic STOPP is a membrane-bound serine protease. As p-stomatin shares an operon with STOPP, it is thought that stomatin may act as either a chaperone to the enzyme, a regulator to the enzyme, or as a substrate to the enzyme (Green *et al.* 2004). Further studies on one of these genomes, *Pyrococcus horikoshii* (*P. horikoshii*), suggested that stomatin forms the substrate to the

membrane-bound serine protease. The stomatin homologue (PH1511) is cleaved by the protease homologue (PH1510) which is hypothesised to cause the opening of an ion channel (figure 1.3) (Yokoyama *et al.* 2005).

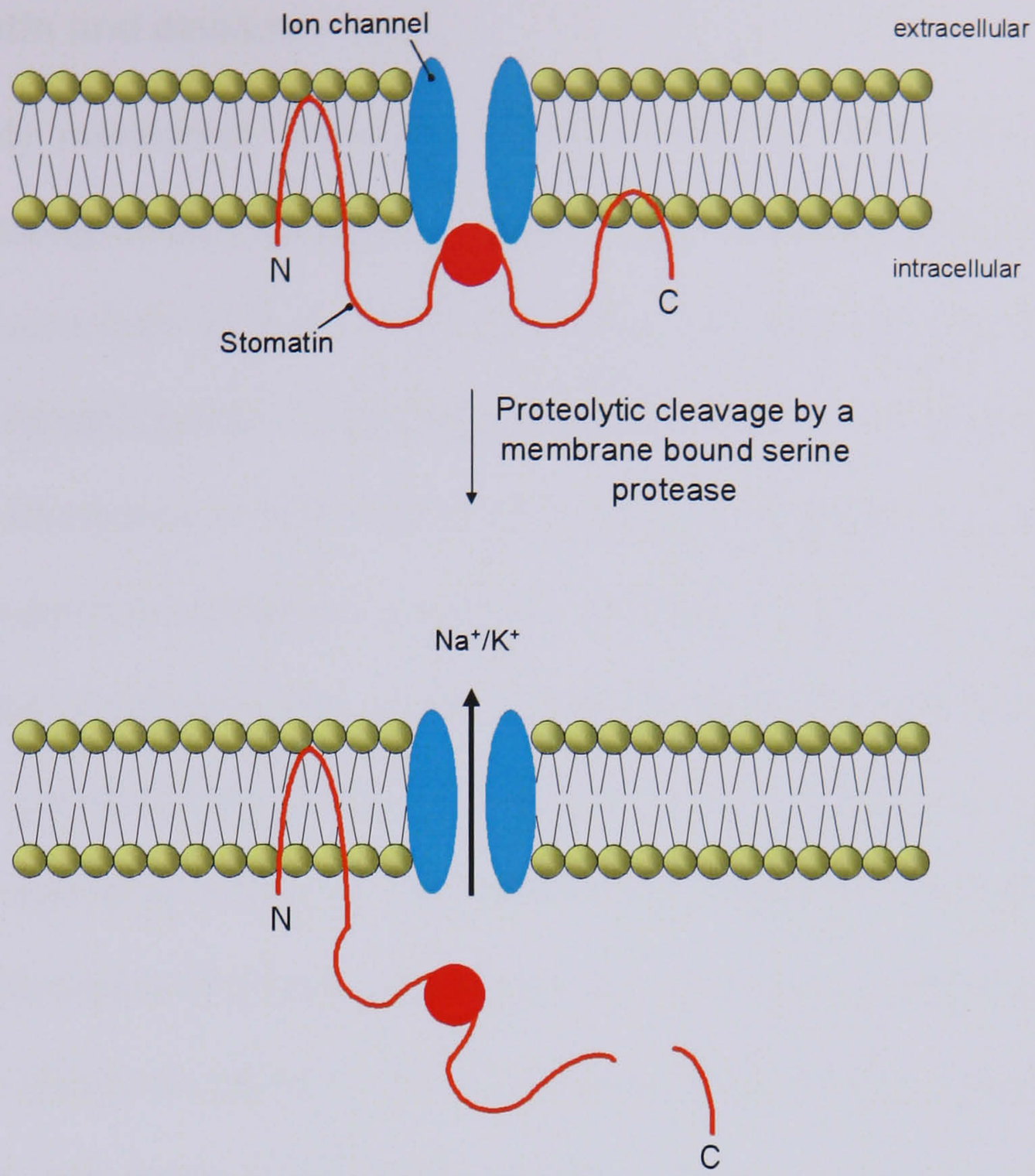

Figure 1.3 Schematic showing proteolysis of stomatin resulting in ion channel opening

In *Pyrococcus horikoshii* the stomatin homologue PH1511 is cleaved by a membrane-bound serine protease, and it is hypothesised that this cleavage results in the opening of an ion channel (Yokoyama *et al.* 2005). The C-terminal domain of stomatin contains a proposed serine protease cleavage site in a region rich in hydrophobic residues. Interaction of this region with the membrane is proposed to block ion channel function. Upon cleavage within the domain a C-terminal fragment is released from the parent protein and allows the opening of an ion channel.

1.2.4 Stomatin and disease

As previously mentioned, stomatin is deficient in the erythrocyte membrane of patients suffering OHSt (Lande *et al.* 1982). This condition has been found to be the most severe form of a group of dominantly inherited anaemias known as the hereditary stomatocytoses (discussed in detail below). In these diseases the erythrocyte membrane is 'leaky' to cations and as a result the cell shows elevated cation and water concentrations leading to premature lysis of the erythrocyte. The stomatin gene is not mutated and the molecular basis of OHSt remains unknown. Patients are generally able to lead normal lives but can require transfusions in times of crisis (Stewart *et al.* 1999). It is believed that stomatin is trafficked wrongly in the maturing erythrocyte and fails to locate to the plasma membrane (Fricke *et al.* 2005). The knockout stomatin mouse is without phenotype, suggesting that the deficiency of stomatin in stomatocyte membranes is not responsible for the cation leak (Zhu *et al.* 1999). Whether other proteins of the erythrocyte membrane can function in place of stomatin is unknown.

A French child born to healthy first cousins of Tunisian origin showed a severe multisystem disease. Suffering many problems including altered erythrocyte morphology, anaemia, delayed growth, delayed neurological development, mitochondrial dysfunction and convulsions; the child died aged six. It was realised that stomatin was deficient in the erythrocyte membrane. As with the OHSt cases, sequencing found no mutation in the gene. However, the mRNA showed a series of spliceforms. Five siblings to the same parents were still born or died soon after birth, one is alive and well. The exact cause of this condition remains unknown (Argent *et al.* 2004).

1.2.5 Human stomatin-like proteins

Stomatin-like protein 1 (hSLP-1) is a bipartite protein containing a stomatin-like domain at the N-terminus and a non-specific lipid transfer protein (nsLTP) domain at the C-terminal end. The *C.elegans* protein UNC-24 also shows the same bipartite structure and is thought to be the hSLP-1 homologue in this organism. hSLP-1 is not present in erythrocytes. The highest levels of expression were detected in the brain, an organ where stomatin is not expressed and thus hSLP-1 is thought to represent 'brain-specific stomatin' (Seidel *et al.* 1998). The second human stomatin-like protein (hSLP-2) is widely expressed in many tissues and is also found in mature erythrocytes. It is the first member of the stomatin family to lack a hydrophobic stretch at the N-terminus and is only peripherally associated with the membrane. The high homology between the C-terminal domains of stomatin and hSLP-2 suggests the two could potentially associate in mixed oligomers forming cytoskeletal associated structural components of the membrane (Wang *et al.* 2000). hSLP-2 has been found overexpressed in an oesophageal carcinoma where it is thought it may have a role in hyperproliferation. Antisense transfection of *hSLP-2* suppressed cell growth and proliferation due to S phase arrest (Zhang *et al.* 2005).

1.3 SPFH domain proteins

Stomatin contains an SPFH (Stomatins, Prohibitins, Flotillins and HflK/C) domain that spans 200 of the 234 residues that form the C-terminus (Tavernarakis *et al.* 1999). Sharing this domain with stomatin, as the name suggests, are the prohibitins, flotillins, HflK and HflC as well as three *C.elegans* homologues and podocin. It is as yet unclear what purpose this domain serves in stomatin but observations on the other SPFH domain members suggest that it may be critical in membrane protein degradation (Kaser *et al.* 2000) or as a scaffold protein for the assembly of multiprotein complexes (Langhorst *et al.* 2005). SPFH domain proteins tend to be associated with the actin cytoskeleton, oligomerise and reside within lipid rafts.

1.3.1 Prohibitins

The two prohibitin proteins, prohibitin 1 and prohibitin 2, are highly conserved and found in bacteria, plants, yeast, worms, flies and humans (Nijtmans *et al.* 2002). They are interdependent; a decreased level of one corresponds with a similar decrease in the other. They are found mainly in the inner membrane of the mitochondria where they are believed to chaperone the m-AAA protease. This is thought to form part of the quality control system within mitochondria and protect non-assembled membrane proteins (Tatsuta *et al.* 2005). Cells with decreased levels of the prohibitins show a decreased lifespan; as cells age the prohibitin expression lowers. This implicates prohibitin in cellular ageing (Coates *et al.* 2001). Prohibitins are also found in the nucleus where they can regulate cell-cycle progression through interaction with E2F transcription factors and Rb proteins (suppressors of E2F-mediated transcription). Interaction with E2F prevents the

protein binding to E2F promotor sites present in many of the genes involved in progression through S phase (Wang *et al.* 2002). The prohibitins are tumour suppressors and are found overexpressed in many tumours. This is believed to aid the tumour cells in reducing oxidative stress and allowing their continued growth (Nijtmans *et al.* 2002). The 3' untranslated region of the prohibitin gene is known to act as a tumour suppressor in breast cancers (Manjeshwar *et al.* 2003).

1.3.2 Flotillins

Flotillins are highly conserved and found in bacteria, plants, fungi, flies and humans (Langhorst *et al.* 2005). They are interdependent and normally associated with the plasma membrane where they assume a hairpin loop in the bilayer. Flotillin-1 is known to translocate to the nucleus particularly at the beginning of S-phase; its role here is unknown (Santamaria *et al.* 2005). Flotillin-2 has not yet been reported to locate to the nucleus. As yet, the function of the flotillins is unclear but they have been implicated in cell signalling, trafficking and cytoskeletal rearrangement (Langhorst *et al.* 2005).

1.3.3 HflK and HflC

The bacterial membrane proteins HflK and HflC (high frequency of lysogenisation) associate with and regulate the AAA protease, FtsH. This influences the choice between the lysogenic and lytic cycle during λ-phage infection. FtsH affects the stability of the transcriptional regulator cII. When cII levels are high lysogeny is favoured; when cII levels are low lysis is favoured (Saikawa *et al.* 2004). They show the same interdependence as seen for the prohibitins (Banuett *et al.* 1987).

1.3.4 Podocin

Podocin is a membrane protein exclusively expressed in podocytes, specialised renal epithelial cells involved in plasma ultrafiltration during urine formation. It assumes a hairpin loop in the bilayer where it is linked to the actin cytoskeleton by the adapter protein CD2AP. The role of podocin is unclear but it is thought to be responsible for the recruitment of nephrin to lipid rafts followed by subsequent nephrin signalling (Schwarz *et al.* 2001; Huber *et al.* 2003). The *podocin*-knockout mouse dies soon after birth due to renal failure (Roselli *et al.* 2004). Expression levels and subcellular localisation of nephrin are affected in several renal diseases such as diabetes (Liu *et al.* 2004).

1.3.5 UNC and MEC proteins in *C.elegans*

Three homologues of stomatin have been found in *Caenorhabditis elegans* (*C.elegans*), all of which, if mutated, cause neuronal dysfunction of some form. The two most similar to stomatin are MEC-2, which when mutated causes mechanoinsensitivity, and UNC1, the mutated form of which causes sensitivity to volatile anaesthetics.

MEC-2 (65% identity, 85% amino acid similarity to stomatin) is required for mechanosensation through its interaction with the epithelial sodium channels (ENaC) and the actin cytoskeleton; mutations in the *mec-2* gene result in animals unresponsive to light touch (Huang *et al.* 1995). MEC-2 interacts with MEC-4, a homolog of a subunit of ENaC (Suzuki *et al.* 2003).

UNC-1 (52% identity, 87% amino acid similarity to stomatin) is required for the normal locomotion of the nematode. Mutations in the *unc-1* gene result in animals with the abnormal motion described as kinked. Mutations in this gene also result in animals which show altered sensitivity to volatile anaesthetics. This led researchers to suggest UNC-1 may represent a site of interaction between the cell and the lipophilic anaesthetics (Rajaram *et al.* 1998). Interestingly, the lipophilic quinoline antimalarials are known to interact with stomatin (Foley *et al.* 1997). UNC-1 is known to interact with UNC-8, a sodium channel subunit (Sedensky *et al.* 2004).

UNC-24 is less like stomatin (32% identity, 64% amino acid similarity to stomatin across residues 25-198). Mutations in the *unc-24* gene result in animals which show difficulty in moving forward. It is a bipartite protein, as well as containing a domain similar to stomatin; it also contains a domain similar to the non-specific lipid transfer protein (nsLTP). These proteins are found in animals, plants and microorganisms and transport phospholipids between membranes (Wang *et al.* 2005). UNC-24 is proposed to be membrane-bound via its stomatin-like domain and to regulate lipid transfer between closely associated membranes with its nsLTP domain (Barnes *et al.* 1996). This protein is most like the bipartite brain-specific form of stomatin, stomatin-like protein 1 (Seidel *et al.* 1998).

1.4 Hereditary stomatocytoses

As with many mammalian cells, erythrocytes maintain low intracellular sodium (Na^+) levels and high potassium (K^+) levels. This requires the action of the ATP-driven NaK pump which exports Na^+ and imports K^+ against their concentration gradients (Stewart *et al.* 1999). The action of the NaK pump balances a diffusional process in the erythrocyte which is poorly understood. It is this diffusional process which is considered to be responsible for the cation leak in patients with hereditary stomatocytosis. Patients show increased NaK pump rates; this is thought to be the erythrocytes compensatory response to the uncontrollable leak.

This set of autosomal dominant anaemias are grouped on account of abnormal erythrocyte membrane permeability to Na^+ and K^+ (Stewart *et al.* 1999). To date, twelve different phenotypes have been identified with 33 different pedigrees. The severity of the cation leak ranges from the mild barely detectable familial pseudohyperkalaemia, to the severe overhydrated hereditary stomatocytosis where ion flux rates are 40x those in a control erythrocyte. Distinguishing between the phenotypes takes into account the severity of the cation leak, the temperature dependence of the leak (figure 1.4), degree of hydration of the cell, phospholipid content and presence of stomatin in the erythrocyte membrane (Stewart 2004). Often patient blood films will reveal abnormally shaped erythrocytes (figure 1.5). The swollen, mouth-shaped 'stomatocytes' were described in the first case of this group (Lock *et al.* 1961). The altered morphology is likely due to excessive lipid packing of the inner leaflet, although this has never been shown in hereditary stomatocytoses patients (Coles *et al.* 1999). Patients can generally lead normal lives, however, in times of crisis such as infection, transfusions may be necessary. This has proved fatal when religious principles disallow such medical intervention.

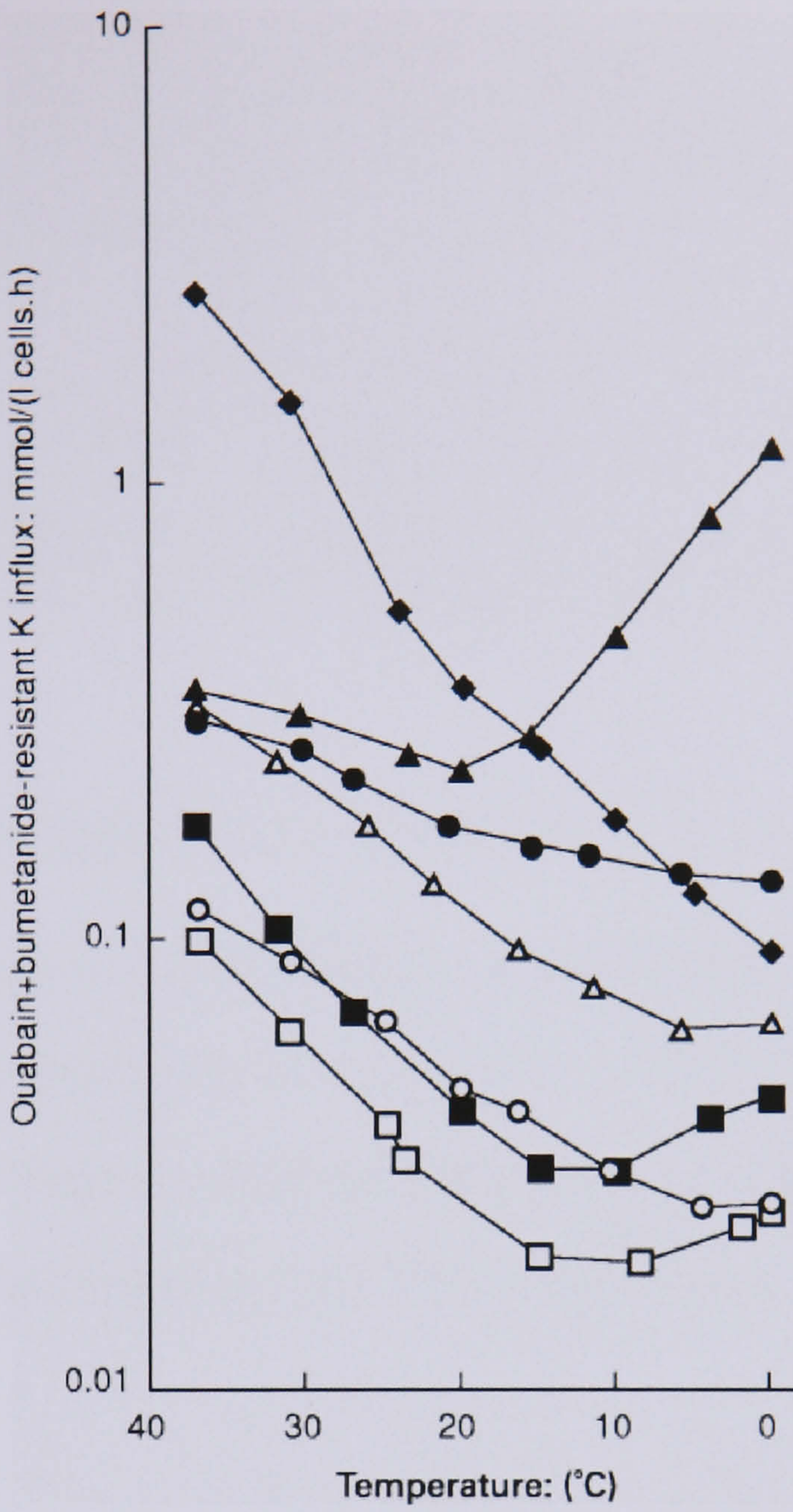

Figure 1.4 Temperature dependence of cation leak in different hereditary stomatocytoses variants

Graph showing K^+ influx at various temperatures following inhibition of NaK pump with ouabain and bumetanide treatment. Not all hereditary stomatocytoses phenotypes are represented. □ - normal; ○ - Familial pseudohyperkalaemia; ■ - Dehydrated hereditary stomatocytosis; △ - Woking phenotype; ◆ - Overhydrated hereditary stomatocytosis; ● - Blackburn phenotype; ▲ - Cryohydrocytosis. Figure taken from (Stewart *et al.* 1999).

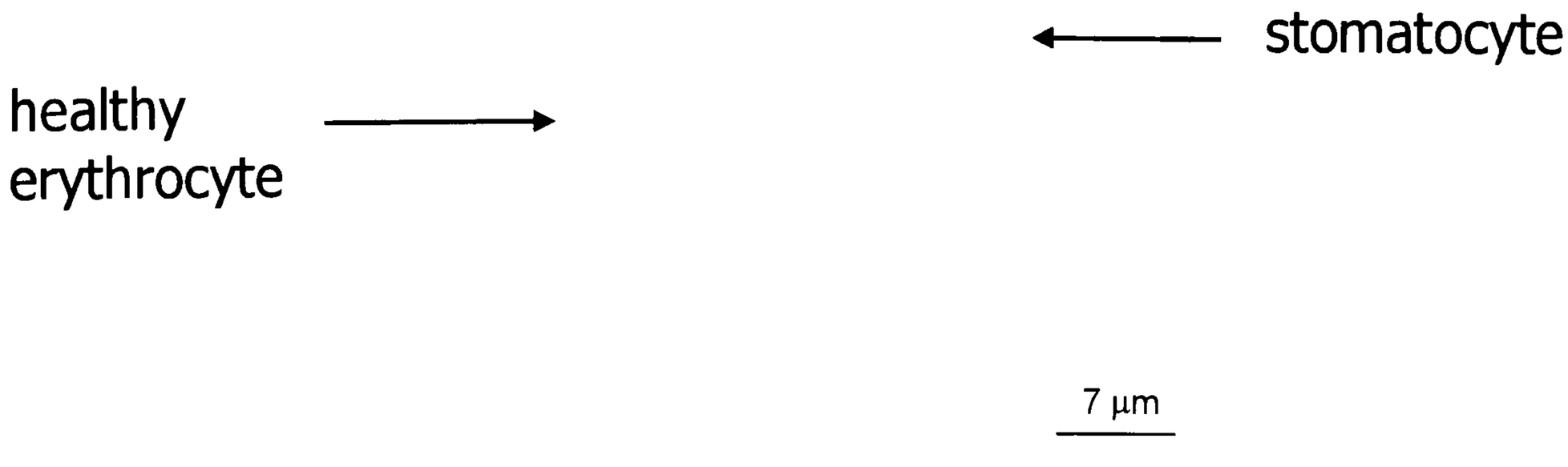

Figure 1.5 Blood film taken from an individual with OHSt

The healthy erythrocyte is a disc/biconcave structure allowing for maximum surface area for gaseous exchange. The stomatocyte in hereditary stomatocytoses patients is mouth-shaped; this may be due to excessive packing of lipids in the inner leaflet of the lipid bilayer. Figure adapted from (Fricke *et al.* 2003).

1.4.1 Overhydrated hereditary stomatocytosis

Over-hydrated Hereditary Stomatocytosis (OHSt) is rare and was the original hereditary stomatocytoses condition described (Lock *et al.* 1961). Patients show ion flux rates 40x that of a control erythrocyte, making this the most severe phenotype of the group. Intracellular Na^+ is over ten times greater in patient's stomatocytes than in normal erythrocytes and K^+ four times lower. The overall increase in intracellular cation concentration is accompanied by increased intracellular water concentration, which results in swelling and premature lysis of the erythrocyte (Stewart *et al.* 1999). Haemoglobin levels are two thirds of that in a control erythrocyte. Patients are chronically jaundiced. The integral membrane protein stomatin is deficient in all cases. This deficiency is isolated to the erythrocyte membrane; patient's brain, liver, kidney, gut and muscle samples show normal levels of stomatin (Stewart *et al.* 1993). Messenger RNA levels are normal within the maturing erythrocytes of patients and sequencing has revealed no mutation in the stomatin gene (Stewart 1997). Cultured cells from OHSt patients reveal that the protein is unable to reach the plasma membrane and appears to be restricted to an area of multivesicular complexes and in the nucleus (Fricke *et al.* 2005). When the condition was first realised, patients underwent therapeutic splenectomy in an attempt to reduce splenic destruction of the stomatocytes (Stewart *et al.* 1999). This treatment was adopted due to similarities to hereditary spherocytosis; in these cases prevention of the splenic destruction of abnormal erythrocytes eases the anaemia (Reliene *et al.* 2002). It was gradually realised that OHSt patients who underwent this procedure suffered with thrombotic problems and this has recently been attributed to the possible appearance of phosphatidylserine (PS) at the surface of the stomatocyte (Stewart 2004). The phospholipid PS is usually contained on the inner surface of the erythrocyte by the action of the lipid transport

system within the membrane, appearance of PS at the surface can initiate thrombosis (Zwaal *et al.* 1997). Studies on lipid movement between the two leaflets of the bilayer in OHSt cells showed reduced movement of PS from the inner to the outer leaflet but lipid movements were otherwise normal (Ho *et al.* 1997).

1.4.2 Dehydrated hereditary stomatocytosis

Dehydrated Hereditary Stomatocytosis (DHSt) is less severe than OHSt but more common. Ion flux rates are only twice that of control erythrocyte rates. Patient's erythrocytes show mildly decreased levels in Na^+ and K^+ ions, which accounts for the dehydration. The erythrocyte membrane shows normal levels of stomatin but shows elevated levels of phosphatidylcholine. This is thought possibly to be caused by a defect in the lipid transport system of the erythrocyte membrane which maintains asymmetrical phospholipid distribution between the two leaflets of the bilayer (Stewart *et al.* 1999). As with OHSt, haemoglobin levels are low. Thrombotic problems have developed in patients which underwent therapeutic splenectomy. Two pedigrees are described as DHSt with ascites (the build up of fluid in the abdominal cavity); this variant shows mental retardation (Stewart 2004).

1.4.3 Cryohydrocytosis

Cryohydrocytosis (CHC) is less severe than OHSt but slightly more severe than DHSt. Ion flux rates are 4x that of a control erythrocyte. Two pedigrees have been identified which show stomatin deficiency in the erythrocyte membrane. In these cases ion flux rates are slightly more abnormal at 10x the control level. These two pedigrees show neurological abnormalities, including seizures and mental retardation (Fricke *et al.* 2004). If left to stand at room temperature, the erythrocytes

gain Na^+ and lose K^+, this effect is enhanced if the sample is stored chilled. As the gain in Na^+ outweighs the loss in K^+, the cells gain water, swell and lyse. Patient's cells show increased sensitivity to phospholipid degradation by phospholipase at low temperatures. It has been suggested that this may be as a result of improperly packed lipids. In some cases the erythrocyte membrane shows increased ether content. No thrombotic problems have been described following splenectomy in these patients (Stewart *et al.* 1999).

1.4.4 Familial pseudohyperkalaemia

Patients with Familial pseudohyperkalaemia (FP) are essentially symptomless. Ion flux rates vary between being normal to 4x greater than control erythrocytes. At physiological temperatures intracellular Na^+ is moderately increased and K^+ decreased. Following storage at room temperature, the erythrocytes show a loss of K^+. Such storage could be expected during a routine blood test; the results prompting further investigation and eventual diagnosis. Haemoglobin levels are normal. Thrombotic problems have developed in patients which underwent therapeutic splenectomy (Delaunay 2004).

1.4.5 Other phenotypes

The other less frequent phenotypes are so called following patient location. Blackburn phenotype suffers ion flux rates 4x that of control erythrocytes but is distinguishable from CHC due to different temperature dependence of the leak (figure 1.4). Chiswick phenotypes show ion flux rates 1.5x that of control erythrocytes; the temperature dependence is unique to this phenotype. Woking phenotype suffers ion flux rates 4x that of control erythrocytes but is distinguishable

from CHC and Blackburn phenotype again due to different temperature dependence of the leak. There are two Middlesbrough phenotypes suffering with 2x and 4x ion flux rates which have a temperature-dependent leak unique to their phenotype (Stewart 2004).

1.5 Lipid Rafts

Polarised cells e.g. epithelial cells, form and maintain two functionally different membrane domains. The apical membrane faces the lumen of an internal organ and the basolateral membrane contacts surrounding cells. Tight junctions link the cells and seal the epithelium; they also prevent the mixing of components between the two membrane domains. The distinct character of each domain requires sorting of proteins and lipids in the Golgi complex. The concept of lipid rafts was introduced to describe how the protein and lipid distribution between the apical and basolateral domains of polarised epithelial cells could differ (Simons *et al.* 1997). Specialised rafts concentrated in cholesterol and sphingolipids form in the Golgi complex and are specifically trafficked to the apical membrane. Proteins destined for the apical side of the cell would associate with the rafts and traffic with them. In support of this model, glycosylphosphatidylinositol (GPI)-anchored proteins which are specifically apically located were found to become insoluble in non-ionic detergents following their association with the cholesterol and sphingolipid in the Golgi complex. It was found that the detergent isolated GPI-protein complexes were rich in cholesterol and sphingolipids (Brown *et al.* 1992). As well as existing in mammalian cells, rafts have also been reported in plants and yeast (Bhat *et al.* 2005; Malinska *et al.* 2003). The fluid mosaic model described the plasma membrane as a lipid bilayer where proteins are randomly distributed and free to diffuse. Lipid rafts are proposed to introduce a degree of organisation to the plasma membrane. The model proposes that clusters of lipid form heterogeneous platforms which exist in a different phase to the bulk of the plasma membrane. These microdomains are able to diffuse as intact structures (Simons *et al.* 1997). Since the introduction of the lipid raft model, the microdomains have been implicated in many cellular roles including sorting,

trafficking, signalling and polarisation (Simons *et al.* 1997; Meiri 2005; Gomez-Mouton *et al.* 2004).

Signalling

Lipid rafts are implicated in many signalling events in a variety of cell types. They are considered to act as platforms where the crucial elements for a signalling event can organise in space and time (Bickel 2002; Magnani *et al.* 2004). Perhaps the best characterised raft-based events leading to a signalling event are in T-cells during their activation (Meiri 2005). Many proteins involved in T cell signalling such as the T cell antigen receptor (TCR) and kinases are concentrated in lipid rafts (Harder *et al.* 2000). Displacement of proteins critical for the signalling event from microdomains can inhibit T cell signalling (Zeyda *et al.* 2002). Rafts are thought to be responsible for the recruitment of binding partners, with the eventual assembly of a mature immunological synapse. They also recruit proteins associated with the underlying actin cytoskeleton, thought to provide the mechanical stability critical for the signalling event to be sustained (Valensin *et al.* 2002).

Proteolysis

Neuronal lipid raft integrity is required for the proteolytic activation of plasminogen to plasmin. The active plasmin is thought to influence neuronal plasticity (Ledesma *et al.* 2003). Lipid rafts are known to provide the cellular site in which the amyloidogenic pathway leading to Alzheimer's disease occurs (Cordy *et al.* 2003).

Cell migration

In mammalian cells it has been demonstrated that lipid rafts redistribute and accumulate at the leading edge of a migrating cell. The raft-based receptors

involved in the spatially restricted signalling show similar redistribution suggesting key signalling events for migration preferentially occur in lipid rafts. Cholesterol depletion produced cells which fail to migrate successfully (Gomez-Mouton *et al.* 2004).

Disease and microbes

Many viruses gain access to the host cell via interaction with proteins which are lipid raft based; in some cases disruption of the lipid rafts with cholesterol depletion prevents viral entry (Pietiainen *et al.* 2005). Rafts have also been found to contain high proportions of structural proteins from enveloped viruses; this may aid assembly and budding of the virus (Suomalainen 2002). Increasing numbers of bacteria are also found to enter host cells via lipid rafts, a process in some bacteria thought to be initiated by the secretion of cholesterol-binding proteins (Lafont *et al.* 2005). Rafts are also thought to play a role in the endovacuolation of the protozoa *Plasmodium falciparum* (Haldar *et al.* 2001). As well as being hijacked by pathogens, rafts have been implicated in various diseases. For example, the conversion of the normal cellular form of the prion protein into the pathogenic form occurs preferentially in lipid rafts (Hooper 2005). Depletion of cellular cholesterol and thus disruption of lipid rafts reduces the level of the pathogenic form. Also the amyloidogenic pathway leading to Alzheimer's disease preferentially occurs in lipid rafts (see above).

1.5.1 Structure of lipid rafts

Lipid rafts are glycosphingolipid and cholesterol-enriched discrete microdomains. Sphingolipids have highly saturated long acyl chains which allow them to pack tightly in the membrane. Space beneath the head group is filled with cholesterol

molecules, largely responsible for stabilisation of these domains (figure 1.6) (Simons *et al.* 1997). Whilst the exoplasmic leaflet lipid content of rafts is well documented, the content of the cytoplasmic leaflet is not clear. As well as enrichment in certain lipids, the same can be said for various proteins, specifically GPI-anchored and acylated proteins within rafts. The partitioning of certain proteins into lipid rafts is thought, in part, to involve hydrophobic mismatch. As the lipids in rafts are saturated they sit taller in the membrane; the length of the transmembrane domain of a protein can therefore influence their partitioning and sorting in the Golgi complex (Allende *et al.* 2004).

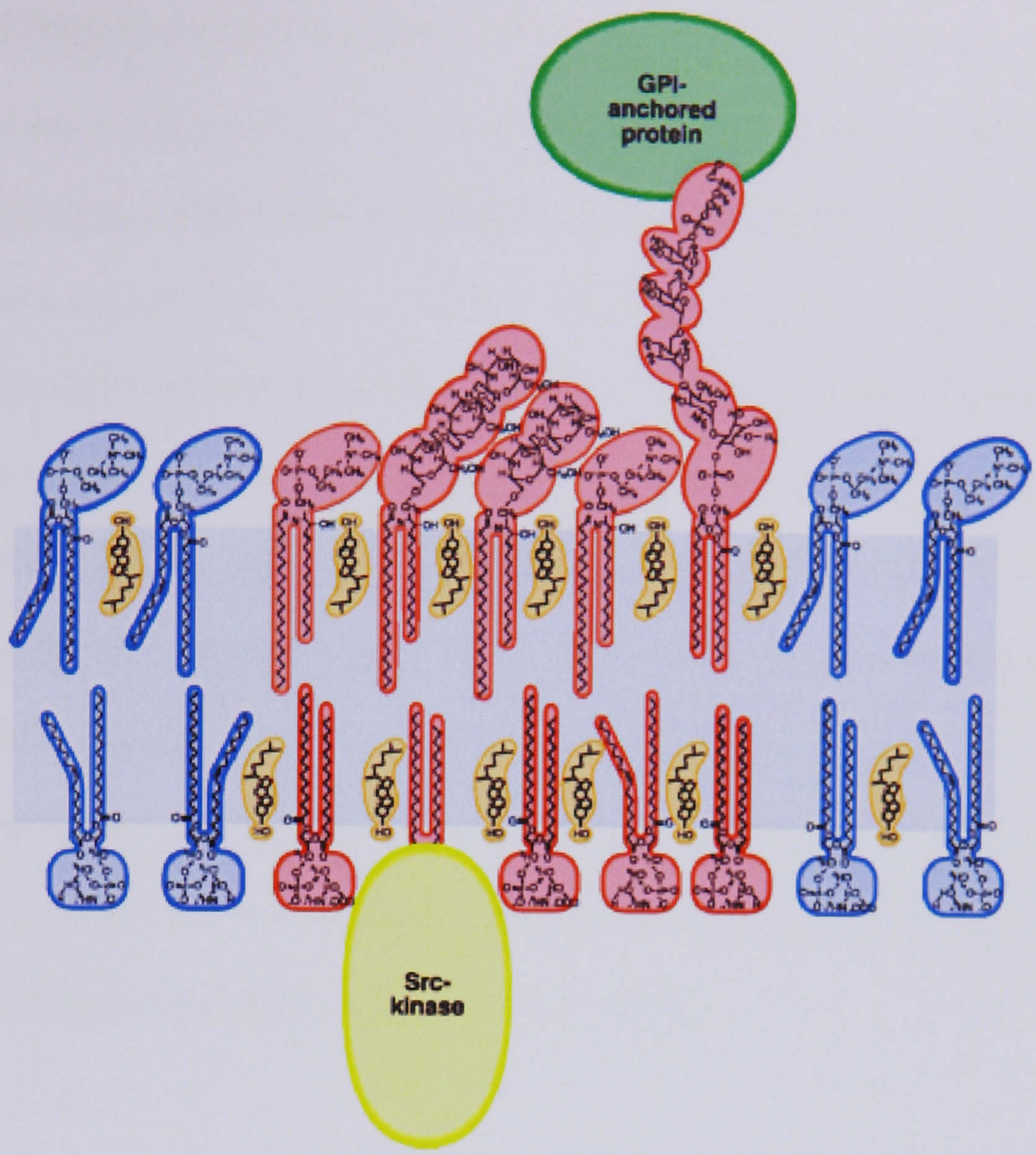

Figure 1.6 Structure of a lipid raft

Lipid rafts are discrete microdomains enriched in cholesterol (orange) and lipids with saturated acyl chains (red). They are packed tighter than the surrounding membrane (blue) and associate with acylated and GPI-anchored proteins. Figure taken from (Simons *et al.* 2000).

1.5.2 Lipid rafts in the erythrocyte

The erythrocyte membrane is known to contain at least two distinct subsets of cholesterol and glycosphingolipid-rich lipid rafts. Upon calcium-induced vesiculation of the erythrocyte, stomatin vesiculates in the microvesicles and the flotillins remain within the erythrocyte membrane (Salzer *et al.* 2002). Both stomatin and the flotillins are known raft proteins and their segregation during this vesiculation is considered to indicate the existence of separate microdomains (Salzer *et al.* 2001). This suggests that some lipid rafts within the erythrocyte are sites where exovesiculation can occur. During malarial infection many DRM-associated proteins are found enriched in the vacuole that forms around the parasite. This suggests that some lipid rafts in the erythrocyte can also be sites of endovesiculation that are hijacked by invading pathogens (Murphy *et al.* 2004).

1.5.3 Phase Separation of lipid bilayers

Model membranes of phospholipid bilayers were shown to contain a solid-like gel phase co-existing with a fluid phase (Lee 1977). Lipids which contain saturated (lack double bonds) acyl chains, e.g. most sphingolipids, form bilayers with high melting temperatures (T_m) which exist in the gel phase. Lipids with unsaturated acyl chains, e.g. most phospholipids, form bilayers with low T_m. The low T_m, due to a cis double bond in the acyl chain, ensures fluidity of the membrane which exists in the fluid/liquid disordered (l_d) phase (Parasassi *et al.* 1993). The introduction of cholesterol into model membranes with saturated lipids such as sphingomyelin resulted in the formation of an intermediate phase. It was tightly packed and ordered as in the gel phase, yet displayed the lateral mobility almost identical to that seen in l_d phase (Almeida *et al.* 1992). This state is known as the liquid ordered

state (l_o). In this phase the haphazard acyl chains of phospholipids as seen in the l_d phase are extended and more tightly packed, this causes a thickening of the bilayer. Tighter packing causes the membrane to be less permeable but still allows lateral mobility of both lipids and proteins within this phase. As the gel and l_d phases can co-exist in model membranes, so too can the l_o and l_d phases (Silvius *et al.* 1996; Ahmed *et al.* 1997).

1.5.4 L_o phase and detergent insolubility

GPI-anchored proteins are insoluble in cold, non-ionic detergents such as Triton X-100 (TX-100) following transit through the Golgi apparatus where they associate with sphingolipids and cholesterol (Brown *et al.* 1992). Glycosphingolipids and GPI-anchored proteins were found to be associated in the same detergent-insoluble complexes. This supported the lipid raft model of sphingolipid microdomains sorting associated proteins such as GPI-anchored proteins, to the apical surface of polarised epithelial cells (Brown *et al.* 1992; Simons *et al.* 1997). Cholesterol shows a particular affinity for sphingolipids and both are required for detergent insolubility of the l_o domains (Silvius 2003; Hanada *et al.* 1995). Model membranes similar in composition to the isolated detergent-resistant membranes are in the l_o phase (Ahmed *et al.* 1997). Detergent insolubility is seen in model membranes in the l_o phase; membranes not in this phase lose detergent resistance (Schroeder *et al.* 1998). The detergent resistance of domains in the l_o phase, considered to be the *in vivo* lipid raft, have made them simple to isolate via detergent extraction.

1.5.5 Detergent extraction of lipid rafts

Detergent extraction is the most widely used technique in the biochemical study of lipid rafts. Membranes are solubilised in a cold non-ionic detergent such as TX-100. The membrane-detergent mix is then placed at the bottom of a sucrose density gradient. Following high speed centrifugation overnight the insoluble low density raft material floats away from the solubilised non-raft material and is segregated upon fractionation of the sucrose gradient (figure 1.7). It is thought detergent insolubility is a consequence of the tight packing of lipids in the l_o phase and the low density is caused by the high cholesterol content (London *et al.* 2000). It is still unclear how accurately the isolated detergent resistant-membranes (DRMs) reflect *in vivo* lipid rafts and the limitations of this protocol are a concern (Lichtenberg *et al.* 2005). DRMs could possibly represent an artefact of the extraction process. Firstly, extraction is performed at 4°C rather than physiological temperature; at 37°C most DRMs are solubilised. It is possible that the lower temperature could promote alteration in tighter lipid organisation in the bilayer, a phenomenon not present under physiological conditions (Brown *et al.* 1992). Secondly, the detergents themselves could promote l_o formation or cause fusion of native rafts into larger membrane aggregates (Heerklotz 2002). Finally, proteins associate with DRMs to different extents. Physical properties of certain proteins, such as hydrophobicity, may be responsible for DRM association rather than *in vivo* raft residency (Ferguson 1999).

Many other detergents besides TX-100 have been used in the isolation of DRMs including Lubrol WX, CHAPS, TX-114, Brij 96, Brij 98 and octylglucoside (Chamberlain 2004). Varying concentrations and temperatures have been used to produce a range of results. Depending on detergent, DRMs isolated from the same

membrane show varying degrees of solubilisation and can vary in protein, cholesterol and sphingolipid content. These differences have been attributed to 'DRM selectivity' of the different detergents (Schuck *et al.* 2003), subpopulations of raft within any given cell (raft heterogeneity) (Madore *et al.* 1999) and varying degrees of fusion between native rafts (Pike 2004). In an attempt to avoid the criticisms of detergent extraction, detergent-free methods have been developed using sonication (Smart *et al.* 1995). However, whilst there are concerns over the validity of DRM extraction, it remains by far the most popular protocol in lipid raft analysis.

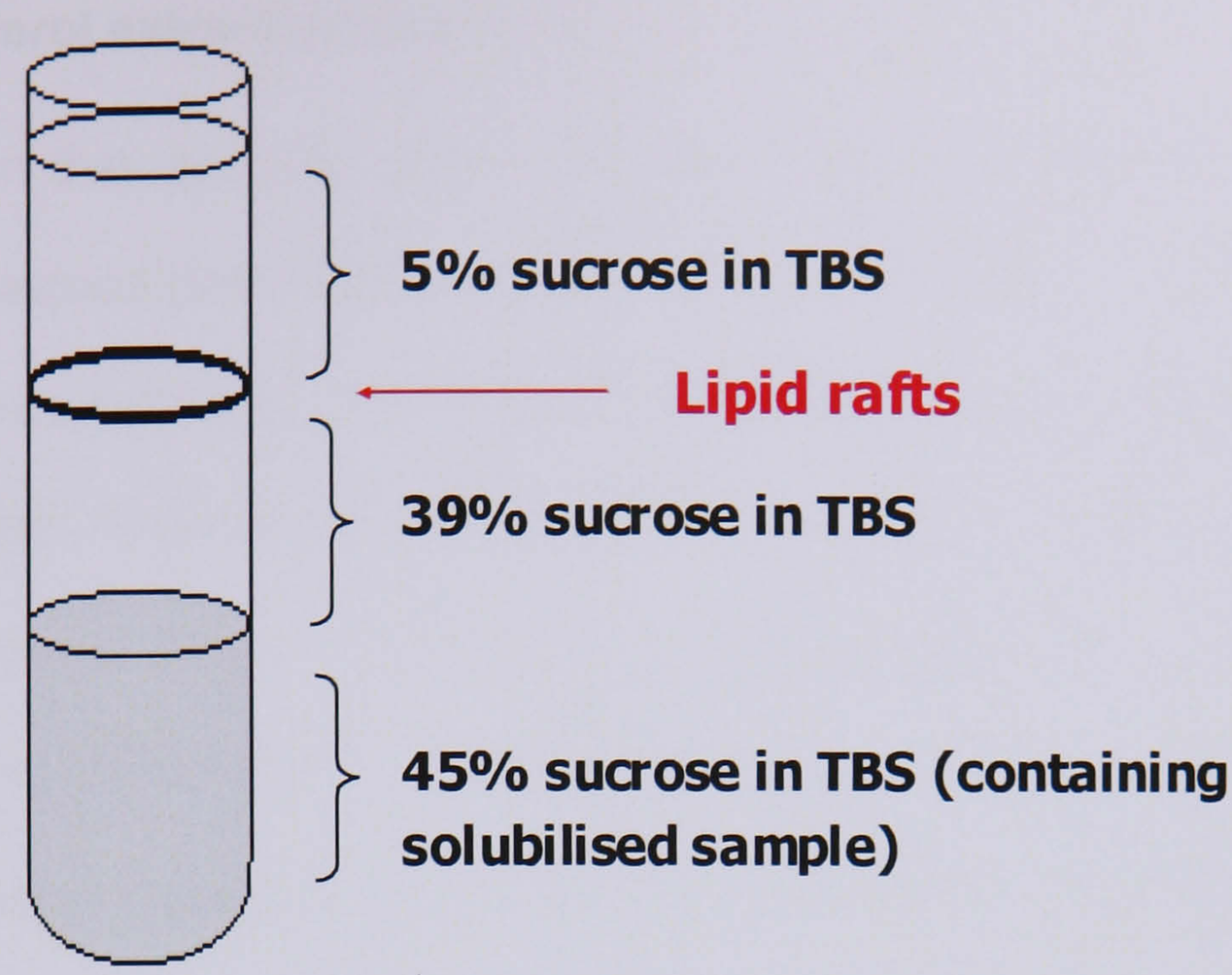

Figure 1.7 Detergent extraction of lipid rafts

Membranes are first solubilised in a cold non-ionic detergent such as Triton X-100. The solubilised sample is placed underneath a sucrose gradient (diagram shows a non-continuous gradient). The gradient is subjected to high speed centrifugation overnight at 4°C. Fractionation of the gradient from the base upwards allows the isolation of lipid rafts. TBS – Tris-buffered saline.

1.5.6 Cholesterol extraction/depletion

The realisation that lipid rafts are concentrated in cholesterol led to many studies involving cholesterol depletion to perturb these microdomains. Various techniques have been used including cholesterol deprivation in cultured cells (Hannan *et al.* 1996), inhibiting synthesis of cholesterol (Rothberg *et al.* 1990) and depletion of cholesterol using various compounds to directly remove it form the bilayer (Schnitzer *et al.* 1994; Smart *et al.* 1994). The use of methyl-β-cyclodextrin (MβCD) to deplete cells of cholesterol is commonly used in raft studies (Ilangumaran *et al.* 1998). This compound acts by extracting the cholesterol peripherally rather than becoming incorporated into the membrane (Christian *et al.* 1997). DRM isolation from cholesterol-depleted cells often results in a normally insoluble protein being found in the soluble region of the gradient. It is thought this phenomenon is due to the dissociation of the protein from the raft *in vivo* (Scheiffele *et al.* 1997; Hao *et al.* 2001).

1.5.7 Atomic Force Microscopy of lipid rafts

A bilayer of phosphatidylcholine is 3.5 nm thick; a bilayer of sphingomyelin is 4.6 nm thick. This height difference is easily detected by atomic force microscopy (AFM) and has made it popular in the study of lipid rafts (Henderson *et al.* 2004). Model membranes show sphingomyelin-enriched domains increase in size as cholesterol concentration is raised. Likewise, if the system is depleted of cholesterol, these domains shrink (Rinia *et al.* 2001; Milhiet *et al.* 2001; Lawrence *et al.* 2003). AFM has provided convincing images of distinct microdomains, estimated to be between 40-100 nm (Yuan *et al.* 2002). AFM has also shown GPI-anchored proteins known

to be enriched in DRMs, e.g. placental alkaline phosphatase (PLAP), are targeted to these domains (Saslowsky *et al.* 2002).

1.5.8 Fluorescent studies of lipid rafts

Fluorescent lipid analogues have been used to investigate phase separation in planar model membranes. Many have reported domain formation consistent with phase separation of the lipid bilayer (Samsonov *et al.* 2001; Brown 2001). Giant unilamellar vesicles (GUVs) are model membranes which require no support as with the planar models and rules out any effect the support may have on the lipids. They have been used to demonstrate lateral heterogeneity, glycosphingolipid content and that the use of detergents neither induces the formation of domains nor coalesces existing domains (Staneva *et al.* 2005).

Laurdan is a fluorescent probe used to measure phase separation. Due to altered water penetration in the lipid bilayer, laurdan exhibits a greater fluorescence in disordered than ordered domains in model membranes. Use of this probe in GUVs supports domain formation in model membranes (Dietrich *et al.* 2001). Live macrophages labelled with this probe show domain-like structures. This study predicts 10-15% of the macrophage cell surface is raft-like at physiological temperature (Gaus *et al.* 2003).

Fluorescence resonance energy transfer (FRET) is able to detect nanoscale distribution *in vivo*. Energy transfer from the donor to the acceptor occurs at distances less than 12 nm. The degree of fluorescence reflects the surface density of the fluorophores; this is used to measure clustering in live cells. Although the early studies supported the existence of lipid rafts < 70 nm in diameter in live cells

which could be disrupted following cholesterol depletion, some more recent studies have reported the possibility that some of these data may have been misinterpreted concluding that the density of fluorescence was most likely due to membrane topology and not the clustering of lipid rafts (Varma *et al.* 1998; Glebov *et al.* 2004a). Analysis of the distribution of GPI-anchored proteins showed no clustering in live cells, even after stimulation of T-cells. The common use of MβCD to disrupt lipid rafts has no effect on the distribution of GPI-anchored proteins, as measured by FRET. For these reasons FRET analysis favours the lipid shell theory rather than lipid rafts (Glebov *et al.* 2004b). The lipid shell theory suggests that each protein exists in its own lipid microenvironment rather than being associated with larger more stable rafts (Anderson *et al.* 2002).

Fluorescence recovery after photobleaching (FRAP) measures a protein's ability to laterally diffuse across a membrane. A section of the membrane is bleached and recovery of unbleached molecules is monitored. Various raft and nonraft proteins have been investigated and found to exhibit similar diffusional behaviour. This suggests raft association is not a dominant factor in determining the ability of a protein to laterally diffuse across the membrane (Kenworthy *et al.* 2004).

1.6 Aims of this study

The overall aim of this study is to investigate the role(s) of stomatin in erythrocytes and nucleated cells. As the stomatocyte is deficient in stomatin it represents an easily obtainable model to investigate the role of stomatin in the membrane. Given the abundance of stomatin in lipid rafts, the role of stomatin in these microdomains will be of particular interest.

The roles of stomatin homologues collectively suggest a role as a scaffold protein, ion channel regulator or as a regulator of membrane protein degradation. Site-directed mutagenesis of conserved residues within the SPFH domain of stomatin that are shared by these proteins may reveal residues crucial in the function of stomatin.

Finally, the proposed proteolysis of mammalian stomatin will be investigated. It has been suggested that stomatin may be a substrate for a membrane-bound serine protease. This study aims to identify if a C-terminal fragment is released from the membrane and to characterise the enzyme responsible.

Chapter 2: Materials and Methods

2.1 Materials

All materials were purchased from Sigma-Aldrich Ltd (Poole, UK) unless otherwise indicated.

10 X Phosphate Buffered Saline	Invitrogen Ltd, Paisley, UK
10 X TGS Buffer	Biorad Laboratories, CA, USA
10 X Trypsin-EDTA	Cambrex Bio Science, Nottingham, UK
6 X Loading Buffer	Promega, Southampton, UK
Acetic acid	Fisher
Acrylamide	Severn Biotech Ltd., Kidderminster, UK
Actin antibody	Santa Cruz Biotechnology Inc. CA, USA
Agar	Oxoid Ltd, Basingstoke, UK
Ankyrin antibody	Calbiochem, Nottingham, UK
Annexin V antibody	Santa Cruz
Aquaporin-1 antibody	Santa Cruz
Band 2.1 antibody	Santa Cruz
Band 3 antibody	Santa Cruz
Band 4.1 antibody	J.Pinder, King's college London, UK
Caveolin antibody	BD Biosciences, ON, Canada
Di-Sodium Hydrogen Orthophosphate	Fisher
Dithiothreitol	Melford Laboratories, Ipswich, UK
Dpn I	Stratagene
Dual-Luciferase® Reporter Assay	Promega

Dulbecco's Modified Eagle's Medium - Cambrex	
ECL Reagent	Amersham Biosciences, Little Chalfont, UK
Enhanced chemiluminescence kit	Amersham Biosciences
Ethanol	Fisher
Flotillin-1 antibody	BD Biosciences
Flotillin-2 antibody	BD Biosciences
Foetal Bovine Serum	Cambrex
GLUT-1 antibody	S.Baldwin, University of Leeds, UK
Glycine	BDH, Poole, UK
Glycophorin A antibody	J.Pinder, King's college London, UK
Glycophorin C	Santa Cruz
Ham's F-12 Medium	Cambrex
HRP-conjugated antibodies	Sigma
Isopropanol	Fisher
Lipofectamine	Invitrogen
Marvel skimmed milk power	Local food outlet
Methanol	Fisher Scientific, Loughborough, UK
Molecular Weight Markers	Amersham
Non-essential amino acid mixture	Cambrex
OptiMEM with GLUTAMAX	Invitrogen
pcDNA3.1/V5-His©TOPO®TA Kit	Invitrogen
Penicillin-Streptomycin	Cambrex
Pfu Turbo DNA Polymerase	Stratagene, Amsterdam, The Netherlands
Phosphate Buffered Saline	Invitrogen
Plasmid DNA preparation kits	Qiagen Ltd, Crawley, UK
Poly (vinylidene) difluoride membrane - Amersham	

Primer mix	Promega
Propan-2-ol	Fisher
QuikChange® Site-Directed Mutagenesis kit - Stratagene	
Restriction enzymes	Promega
Sodium Chloride	Fisher
Sodium Dihydrogen Orthophosphate	Fisher
Sodium Dodecyl Sulphate	Fisher
Spectrin antibody	Santa Cruz
Stomatin antibody	G.W.Stewart, University College London, UK
T4 DNA ligase	Promega
Tissue culture flasks	Fisher
Tris	Fisher
Trypsin-EDTA	Cambrex
Tryptone	Oxoid
Tween-20	Lancaster Synthesis, Morecambe, UK
XL-1 Blue competent cells	Stratagene
Yeast Extract	Oxoid

2.2 Cell culture

2.2.1 Culture of mammalian cells

Cells were cultured in Dulbecco's Modified Eagle's Medium (DMEM) with 4.5g/L Glucose with L-Glutamine. Chinese Hamster Ovary (CHO) cells were cultured in Ham's – F12. All media were supplemented with 10% foetal bovine serum (FBS) and 1% penicillin (10, 000 U/ml)/streptomycin (10, 000 µg/ml). The culture medium of HEK cells was also supplemented with 1% non-essential amino acids. Cells were maintained at 37°C, with 5% CO_2 in humidified air and kept viable using standard cell culture techniques.

Once confluent, the cells were passaged, harvested or prepared for storage in liquid nitrogen. Cells were first washed twice with phosphate buffered saline (PBS) then treated with trypsin-EDTA. Madin Darby Canine Kidney (MDCK) cells were treated with 10X trypsin-EDTA. Both trypsin-EDTA and 10X trypsin-EDTA were purchased from Cambrex. Cells were incubated at 37°C until they became dislodged. Once the cells had detached, an equal volume of medium was then added and the cell suspension centrifuged at 1000*g* for 5 min. For passage, the resultant pellet was re-suspended in an appropriate volume of medium and split accordingly into separate culture flasks. If the cells were to be used in investigation, the supernatant was removed and the cells used accordingly. For storage in liquid nitrogen, the resultant pellet was re-suspended in filter-sterilised 50% FBS, 40% medium, 10% Dimethyl Sulphoxide (DMSO) and transferred to cryo-vials. The cells were placed at – 70°C overnight in a cryogenic cooler and then transferred to liquid nitrogen for long term storage.

2.2.2 Transient transfection of mammalian cells using Lipofectamine

Ethanol precipitated DNA was mixed with 600μl Opti-MEM. This was added to a mixture containing 25μl Lipofectamine and 75μl Opti-MEM. The Lipofectamine/DNA solution was incubated at room temperature for 15 min to allow formation of the DNA-cationic lipid complex. During the incubation period, cells at 50% confluency were washed twice with the appropriate volume of Opti-MEM. The Lipofectamine/DNA solution was then added to the cells and incubated at 37°C for 4.5 h. Medium supplemented with 20% foetal bovine serum (FBS) and 1% penicillin (10, 000 U/ml)/streptomycin (10, 000 μg/ml) was then added and the cells incubated at 37°C for 19 h. Medium was then removed and replaced with standard growth media.

2.3 Mammalian cell preparations

2.3.1 Preparation of cell lysates

Cells were washed twice with Phosphate Buffered Saline (PBS) and then dislodged from the tissue culture flask using a cell scraper. The cell suspension was centrifuged at 1500*g* for 5 min at 4°C and the PBS removed. Cells were then resuspended in lysis buffer (50mM Tris/HCl pH 7.4, 1% (v/v) Triton X-100, 1% (v/v) protease inhibitor cocktail), 2ml for each T80 tissue culture flask was used. The cell suspension was sonicated for 30 sec, full cycle - power setting 3 (Branson Sonifier 450). Samples were then centrifuged at 13,000*g* for 5 min at 4°C and the supernatant isolated. Lysates were stored at -20°C.

2.3.2 Preparation of cell membranes

Cells were washed twice with Phosphate Buffered Saline (PBS) and then dislodged from the tissue culture flask using a cell scraper. The cell suspension was centrifuged at 1500*g* for 5 min at 4°C and the PBS removed. All stages were carried out on ice to minimise protease activity. Cells were resuspended in 4ml of cold 100mM Tris/HCl pH7.4. The cell suspension was then sonicated for 1 min (Branson Sonifier 450; output control – 2; duty cycle % - constant). The sample was then centrifuged at 2000*g* for 5 min at 4ºC. The supernatant was then removed and centrifuged at 50,000*g* for 1 h at 4ºC. The resultant pellet was resuspended in cold 100mM Tris/HCl pH7.4.

2.3.3 Isolation of nuclei

Cells were washed twice with Phosphate Buffered Saline (PBS) and then dislodged from the tissue culture flask using a cell scraper. The cell suspension was centrifuged at 1500*g* for 5 min at 4°C and the PBS removed. A Nuclei Pure Prep Nuclei Isolation Kit (Sigma-Aldrich Ltd) was used to isolate nuclei; the protocol was followed as suggested by the manufacturer. Briefly, cells were lysed in a solution containing Dithiothreitol (DTT) and Triton X-100. Nuclei were purified from the lysate by centrifugation at 30,000*g* for 45 min at 4°C, through a sucrose cushion. A pre-cooled Beckman Ultracentrifuge SW28 rotor and 35.5ml buckets were used. Nuclei were resuspended in the storage buffer supplied with the kit and stored at -20°C.

2.3.4 Lysis of nuclei

One volume of nuclei suspended in storage buffer was centrifuged at 5000*g* for 5 min at 4°C, nuclei were resuspended in one volume of lysis buffer (10mM Pipes pH 6.8, 100mM NaCl, 300mM Sucrose, 1mM Magnesium Chloride, 1 mM EGTA, 1mM DTT, 1mM PMSF, 1% (v/v) protease inhibitor cocktail (Sigma # P-8346), 0.1% (v/v) Triton X-100). Lysates were stored at -20°C.

2.3.5 Isolation of detergent-resistant membranes (DRMs)

Cells were washed twice with Phosphate Buffered Saline (PBS) and then dislodged from the tissue culture flask using a cell scraper. The cell suspension was centrifuged at 1500*g* for 5 min at 4°C and the PBS removed. The resultant pellet was incubated on ice for 30 min. All buffers were pre-cooled and work carried out at

4°C. For each T175 culture flask used, the cell pellet was resuspended in 2 ml MES buffered saline (MBS) (25mM MES, 130mM NaCl, pH 6.5) containing 1% (v/v) Triton X-100. The suspension was homogenised by passing through a 21G needle (30 times). Cell nuclei and debris were removed by centrifugation at 1000*g* for 10 min at 4°C. An equal volume of 80% (w/v) sucrose in MBS was added to the supernatant and mixed well. The protein solution with final sucrose concentration of 45% (2.5 ml) was placed at the bottom of a 5ml centrifuge tube and overlaid with 2ml 30% (w/v) sucrose in MBS and 0.5ml 10% (w/v) sucrose in MBS. The gradient was subject to ultracentrifugation using a pre-cooled SW-55 Beckman rotor at 140,000*g* for 18 h at 4°C. The gradient was fractionated from the base upward. Fraction zero represents the insoluble pellet at the base resuspended in MBS. Fractions were stored at -20°C.

2.4 Blood

2.4.1 Blood collection

Blood was harvested from healthy donors and one patient suffering Over-hydrated Hereditary Stomatocytosis by venipuncture into heparinised tubes. Erythrocytes were used same day.

2.4.2 Isolation of erythrocyte membranes

Erythrocytes were isolated from whole blood by centrifugation at 200*g* for 10 min at 4°C and washed 5 times with three volumes of 0.9% (w/v) NaCl, 5 mM Sodium Phosphate, pH 8. Erythrocytes were then lysed in 5 mM Sodium Phosphate, pH 8 and the membranes pelleted by centrifugation at 12,000*g* for 10 min at 4°C. The lysis step was repeated twice more. Ghosts were stored at -20°C.

2.4.3 Isolation of DRMs from erythrocytes

Erythrocytes were isolated from whole blood by centrifugation at 200*g* for 10 min at 4°C and washed 5 times with Tris-buffered saline (TBS), (150mM Sodium Chloride, 10mM Tris/HCl pH 7.5). All buffers were pre-cooled and work carried out at 4°C. The erythrocytes were then lysed in 9 volumes of 0.5% (v/v) Triton X-100 in TBS and incubated on ice for 20 min. The resultant solution was centrifuged at 15,000*g* for 10 min at 4°C and the pellet resuspended in 10ml of 0.5% (v/v) Triton X-100 in TBS. The solution was incubated on ice for 5 min and then centrifuged at 15,000*g* for 10 min at 4°C. The pellet was resuspended in 2 ml TBS and the protein concentration determined. The protein solution was diluted (2 mg/ml) with TBS and one volume of 90% (w/v) sucrose in TBS added. The protein solution with final

sucrose concentration of 45% (4 ml) was placed at the bottom of a 17.5ml centrifuge tube and overlaid with 5ml 30% (w/v) sucrose in TBS and 5ml 10% (w/v) sucrose in TBS. The sucrose gradient was then centrifuged using a pre-cooled SW-28 Beckman rotor at 140,000*g* for 18 h at 4°C and fractionated from the base upward. Fraction zero represents the insoluble pellet at the base resuspended in TBS. Fractions were stored at -20°C.

2.4.4 Calcium-induced vesiculation of erythrocytes

As used previously by Salzer *et al.* 2002. Erythrocytes were isolated from whole blood by centrifugation at 200*g* for 10 min at 4°C and washed 5 times with Tris-buffered saline (TBS) (150mM NaCl, 10mM Tris/HCl pH 7.5). Erythrocytes were resuspended in 9 volumes of TBS containing 1 mM $CaCl_2$, 5 μM calcium ionophore A23187 and incubated at 37°C for 30 min. Following incubation, EDTA was added to a final concentration of 5 mM. Erythrocytes were pelleted by centrifugation at 15,000*g* for 30 sec at 4°C and the supernatant subjected to 4 centrifugation steps. The first three steps were at 15,000*g* for 10, 20 and 30 min respectively at 4°C. This is followed by the final ultracentrifugation using a pre-cooled SW-55 Beckman rotor at 100,000g for 1 h at 4°C. Each vesicle pellet was resuspended in the appropriate volume of TBS; the 30 min pellet was discarded. Vesicles were stored at -20°C.

2.4.5 Cholesterol depletion of erythrocytes

Erythrocytes were isolated from whole blood by centrifugation at 200*g* for 10 min at 4°C and washed twice with phosphate buffered saline (PBS) (0.02M NaH_2PO_4,

0.0015M Na_2HPO_4, 0.15M NaCl, pH 7.4). Erythrocytes were then incubated at 5% concentration in 3 mM methyl-β-cyclodextrin in PBS for 30 min at 37°C. This treatment has been reported to reduce membrane cholesterol by 40% (Rivas MG *et al.* 2003).

2.4.6 AFM and vesicle fixing

Vesicles were prepared from whole erythrocytes as detailed in section 2.4.4 and resuspended in Hepes-buffered saline (5mM Hepes, 150mM NaCl, pH 7.3). The vesicles were applied to freshly cleaved mica (Agar Scientific, Stansted, UK) and imaged at room temperature using a multimode atomic force microscope with a Nanoscope IIIa controller and an E-scanner (Digital Instruments, Santa Barbara, CA). Images were recorded in intermittent tapping mode using oxide-sharpened silicon nitride tips mounted on cantilevers with nominal spring constants of 0.32 Newton/m, oscillating to a frequency between 7 and 9KHz. The set point was adjusted during imaging to minimise the force whilst scanning at a rate of 1Hz.

2.5 Biochemistry

2.5.1 Bicinchoninic acid Protein Assay

Protein concentrations were determined using the bicinchoninic acid protein assay with bovine serum albumin as standard (Smith *et al.* 1985).

2.5.2 Sodium Dodecyl Sulphate Polyacrylamide Gel Electrophoresis (SDS-PAGE)

Polyacrylamide gels were cast and subsequently electrophoresed using Hoefer Mighty Small mini gel apparatus obtained from Amersham Biosciences (Little Chalfont, UK). Proteins were resolved on either a 10% acrylamide (30%; acrylamide ratio 37.5:1 bis acrylamide) gel or 7-17% gradient gel for larger proteins. Samples were prepared using 2x Lamelli buffer (62.5mM Tris-HCl pH 6.8, 2% (w/v) SDS, 25% (v/v) glycerol, 10% (w/v) beta Mercaptoethanol, 0.01% (w/v) bromophenol blue), followed by subsequent boiling for 5 min. Samples were electrophoresed alongside the appropriate molecular weight markers in Tris/Glycine/SDS (TGS) buffer. The acrylamide gels were electrophoresed at a constant 40mA until the front had eluted.

2.5.3 Immunoblot analysis

Resolved proteins were transferred electrophoretically onto an activated poly (vinylidene) difluoride (PVDF) membrane. The gel and membrane assembly were immersed in Towbin transfer buffer (20mM Tris/HCl pH 8.3, 150mM glycine, 20% (v/v) methanol) and subjected to a constant 115 volts for 75 min. Blotting equipment from Biorad Laboratories (CA, U.S.A.) was used. Following transfer, the

membrane was blocked for 1 h at room temperature in 5% (w/v) milk, 2% (w/v) bovine serum albumin and 0.05% (v/v) Tween 20 in Phosphate-buffered saline (PBS) (20mM NaH_2PO_4, 200mM Na_2HPO_4, 0.15M NaCl, pH 7.4). The membrane was then washed in PBS for 15 min. Incubation with the primary antibody for 1 h was performed in blocking solution. Three 15 min washes in 0.05% (v/v) Tween 20 in PBS were followed by incubation for 1 h with the appropriate peroxidase – conjugated secondary antibody. This was then followed by the detection using the enhanced chemiluminescence detection kit from Amersham Biosciences (Little Chalfont, UK) and autoradiography film (blue sensitive).

2.5.4 Coomassie blue staining

Electrophoresed gels were stained using Coomassie blue stain (25% (v/v) isopropanol, 10% (v/v) acetic acid, 0.5% (w/v) Coomassie brilliant blue G250) overnight at room temperature on a rocking platform. Excess staining was removed using a destain solution (5% (v/v) isopropanol, 10% (v/v) acetic acid) at room temperature on a rocking platform.

2.5.5 Amido black staining

Following chemiluminescence detection, PVDF membranes were stained using amido black stain (0.1% (w/v) amido black, 1% (v/v) acetic acid, 40% (v/v) methanol, 60% (v/v) water).

2.5.6 Densitometric analysis

Immunoblots were scanned using a flatbed scanner and saved as Tiff files. The image was viewed using the imaging programme ScionImage (Scion Corporation). The 'threshold' function was used to convert the greyscale image to pure black and white. The black pixels in selected bands were counted and the values compared using Excel. Results are semi quantitative.

2.6 Molecular Biology

2.6.1 Preparation of Luria-Bertani (LB) medium

The following were dissolved in dH_2O, 1% (w/v) tryptone, 0.5% (w/v) yeast extract and 0.5% (w/v) NaCl. The medium was autoclaved at 121°C for 20 min. Before use, the selective antibiotic ampicillin was added to a final concentration of 100μg/ml.

2.6.2 Preparation of LB-ampicillin plates

The LB medium was made as in section 2.6.1 with 1.5% agar (w/v). Following autoclaving, the medium was let to cool to 55°C before ampicillin was added. The plates were then poured and allowed to set overnight. They were then stored at 4°C for no more than a month. Plates were prewarmed to 37°C before use.

2.6.3 Preparation of plasmid DNA

Selective LB media was inoculated with a single colony picked from a selective agar plate. For a small preparation of DNA 5ml of LB media was used, larger

preparations required 50ml of LB media. Media was incubated shaking overnight at 37°C. Cells were centrifuged at 6000*g* for 15 min at 4°C. Plasmid DNA was isolated using Qiagen® Plasmid Purification kits (Crawley, UK); the protocol was followed as suggested by the manufacturer. All buffers were supplied in the kit. Briefly, cells were lysed using a buffer containing Sodium Hydroxide and Sodium Dodecyl Sulphate. The cleared lysate was applied to an anion-exchange column. Bound DNA was washed and then eluted using a high-salt buffer. DNA was precipitated by the addition of isopropanol and then desalted with 70% ethanol. The DNA was resuspended in dH_2O and quantified by absorbance measurement at 260nm. DNA was stored at -20°C.

2.6.4 Restriction digest of DNA

Promega restriction enzymes were used in all cases according to manufacturer's guidelines. Briefly, 10μg of DNA was incubated with the desired enzyme in the buffer supplied by the manufacturer. Incubation at the temperature selected according to the manufacturer was for 1 h.

2.6.5 Ligation of DNA

Amount of DNA used was calculated thus:

$$\frac{\text{ng of vector} \times \text{kb size of insert} \times \text{molar ratio of insert}}{\text{kb size of vector}} = \frac{\text{ng of insert}}{\text{vector}}$$

Vector and insert DNA was incubated with T4 DNA Ligase in manufacturer's buffer at 14°C overnight.

2.6.6 Transformation of XL1-Blue competent cells

XL1-Blue Cells were thawed on ice. Cells were aliquoted into 50µl samples and incubated on ice for 30 min with the appropriate amount of DNA. Samples were heat pulsed at 42°C for 45 sec and then returned to ice for 2 min. LB medium (0.5ml) was added to each transformation reaction and then incubated with shaking (225rpm) at 37°C for 1 h. Cells were then collected by centrifugation at 1000*g* for 1 min. All but 50 µl of the supernatant was removed; cells were then resuspended and plated on LB-ampicillin selective agar plates. Plates were incubated overnight at 37°C. Colonies were selected the following morning, DNA isolated and sequenced.

2.6.7 Agarose gel electrophoresis

Agarose at the desired concentration was dissolved in TAE buffer (40mM Tris/HCl pH 8.0, 0.1% (v/v) acetic acid, 1mM EDTA) with warming. The agarose solution was let to cool before 1µl of a 10mg/ml solution of Ethidium Bromide was added. The solution was mixed well and the gel cast using Anachem Ltd gel equipment (Luton, UK). Once set, the gel was placed in a horizontal gel tank where it was immersed in TAE buffer. Samples were prepared using 6X loading buffer and loaded onto the gel. The gel was electrophoresed at a constant 100V for 30 min.

2.6.8 TOPO cloning system

The pcDNA3.1/V5-His©TOPO®TA Expression Kit was purchased from Invitrogen (Paisley, UK), the protocol was followed as suggested by the manufacturer. Briefly, 1µl of fresh PCR product was incubated with the TOPO© cloning vector for 5 min at

room temperature. The cloning reaction was then placed on ice. A single vial of One Shot® cells was thawed and to it, 2µl of the cloning reaction added. Cells were incubated on ice for 30 min. They were then heat-shocked at 42°C for 30 sec without shaking and then immediately placed on ice. To each vial, 250µl of room temperature SOC medium was added. The cells were then incubated shaking, at 37°C for 1 h. For each transformation, 100µl of the cell solution was spread onto prewarmed ampicillin selective plates. The plates were incubated overnight at 37°C. Colonies were selected; the DNA isolated and sent for sequencing.

2.6.9 Dual-Luciferase® Reporter Assay

The Dual-Luciferase® Reporter Assay kit was purchased from Promega (Southampton, UK), the protocol was followed as suggested by the manufacturer. Cells grown in 6-well culture plate were washed twice with 5ml of PBS. The passive lysis buffer supplied in the kit was diluted appropriately and 500µl applied to each well. The plates were incubated on a rocking platform at room temperature for 15 min. The lysates were transferred to an eppendorf and stored at -20°C. Sufficient Luciferase Assay Reagent II, Stop & Glo® Reagent and lysates were warmed to room temperature. Luciferase readings were taken on a Berthold Lumat LB 9501 luminometer.

Chapter 3: The role of stomatin in the plasma membrane

3.1 Stomatin in the erythrocyte

Although stomatin is found in abundance in the erythrocyte membrane (410,000 copies per cell) (Desneves *et al.* 1996), its role here is unclear. The erythrocyte membranes from Over-hydrated Hereditary Stomatocytosis (OHSt) patients are deficient in this protein (Fricke *et al.* 2003). The usual biconcave morphology of erythrocyte becomes mouth-shaped and is commonly known as a stomatocyte. The reason for this deficiency of stomatin is as yet unknown; trafficking problems, failure to locate a binding partner within the membrane and rapid degradation have all been suggested (Stewart 1997). Stomatin resides in lipid rafts within the membrane (Salzer *et al.* 2001). Membrane lipids and proteins are known to exist in domains (Parsegian 1995); the lipid raft hypothesis was put forward to explain this heterogeneity (Simons *et al.* 1997). Cholesterol, glycosphingolipids and some proteins, particularly those which are GPI-linked, appear to concentrate into rafts (Hooper 1999). In some instances this selective association can cluster crucial elements to initiate a signalling event (Magee *et al.* 2005) or enzymatic reaction (Morford *et al.* 2002). Rafts are thought to exist in both leaflets of the membrane and function cooperatively to initiate spatially directed signals in response to extracellular stimuli (Gri *et al.* 2004). Rafts are often represented in the literature as sections of membrane isolated on a sucrose density gradient following detergent extraction, more commonly known as detergent-resistant membranes (DRMs). In many instances, including for stomatin, DRM association has been used to indicate raft residence *in vivo* (Salzer *et al.* 2001).

In this project, membranes and DRMs were isolated from erythrocytes and stomatocytes to investigate their protein content. Comparing the membrane content and DRM protein profiles may show consequential differences in the stomatocyte due to the deficiency in stomatin, or possibly reveal a cause for this deficiency. A protein which partitions into DRMs containing stomatin may do so because of some tethering between itself and stomatin. Identification of possible binding partners may provide some indication as to a possible function for stomatin in the membrane.

ATP-dependent vesiculation is defective in the stomatocyte, although whether stomatin has a direct involvement in this is unclear (Turner *et al.* 2003). During calcium-induced vesiculation stomatin is known to leave the erythrocyte membrane and concentrate into microvesicles (Salzer *et al.* 2002). This process was investigated further with the aim of defining a role for stomatin.

3.1.1 Comparison of membrane-associated proteins in erythrocytes and stomatocytes

Membranes were prepared from erythrocytes and stomatocytes (section 2.4.2). Samples were subjected to SDS-PAGE (section 2.5.2) followed by subsequent immunoblot analysis (section 2.5.3) using antibodies against known erythrocyte proteins (figure 3.1). For further detail on some of these proteins see section 1.1.1.

As previously reported (Lande *et al.* 1982) stomatin was deficient in the stomatocyte membrane. Flotillin-1 was present in erythrocyte and stomatocyte membranes at a similar concentration; however, more of the phosphorylated form was present in the stomatocyte membrane (lower band on flotillin-1 immunoblot in figure 3.1). The reason for this is unknown. Actin showed decreased membrane association in the

stomatocyte. All other proteins examined were present in approximately equal concentration in the erythrocyte and stomatocyte membranes.

To quantify these results, densitometric analysis (section 2.5.6) was carried out on the immunoblots in figure 3.1 and one other representative immunoblot. The density of the protein band in the erythrocyte sample was set at 100% in each case and the equivalent stomatocyte band compared. Stomatin was present in the stomatocyte membrane at 5% of the amount in the erythrocyte membrane, whilst actin was reduced to 50% in the stomatocyte membrane (figure 3.2). All other proteins were present in the two membrane systems at essentially the same amount.

This result suggests that the deficiency of stomatin seen in the stomatocyte has no global effect on the protein content of the membrane. It does, however, suggest a possible link between the deficiency of stomatin and the lowered amount of actin in the membrane. This link between stomatin and actin was investigated further by isolating DRMs from erythrocytes and stomatocytes.

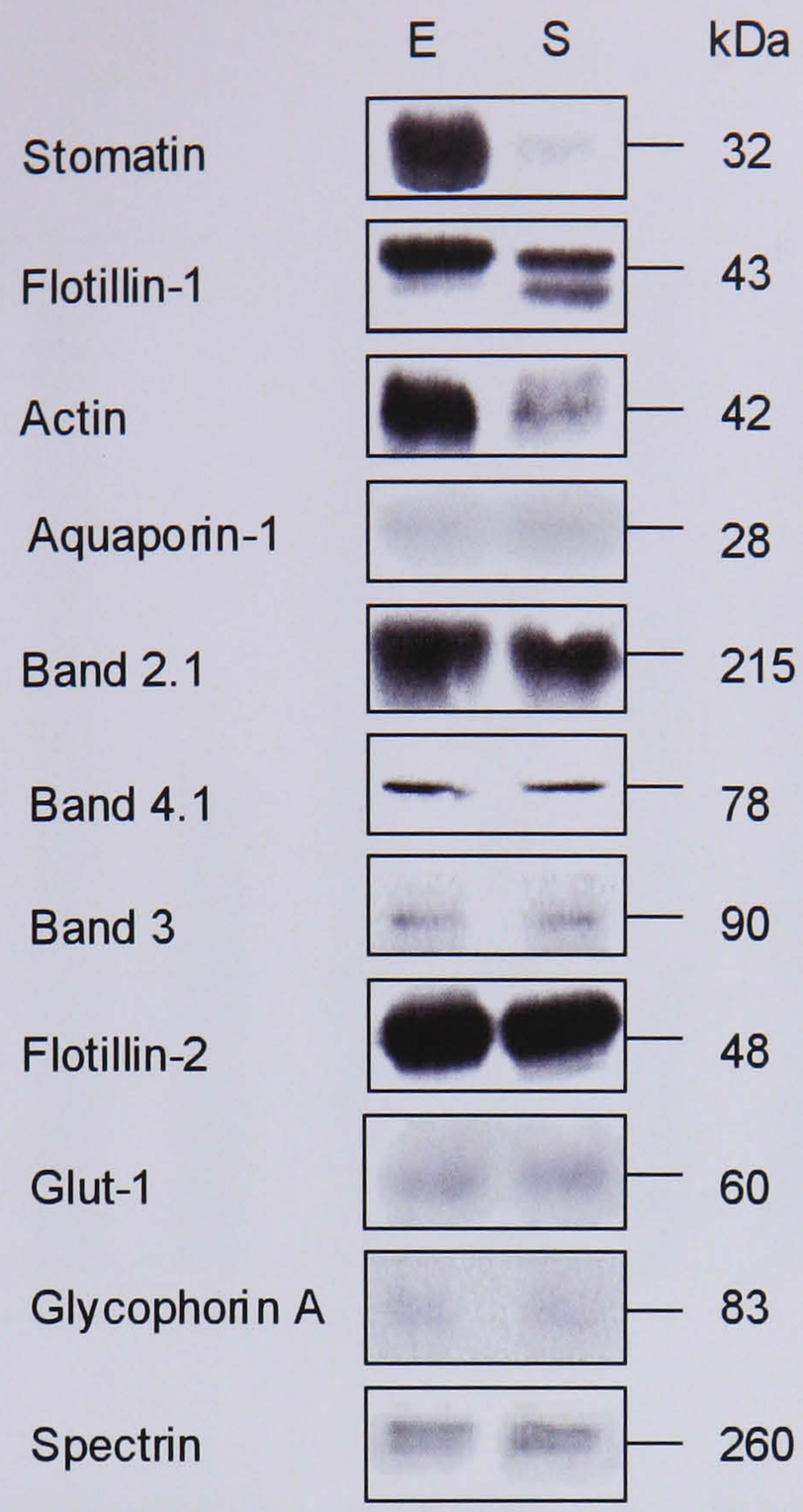

Figure 3.1 Protein content of erythrocytes and stomatocytes

Membranes were isolated from erythrocytes (E) and stomatocytes (S) (section 2.4.2) and subjected to SDS-PAGE (equal protein loading; 10µg), followed by subsequent immunoblot analysis using antibodies against the indicated proteins. The blots are representative of two separate isolations. Molecular weights are shown to the right of each immunoblot (kDa).

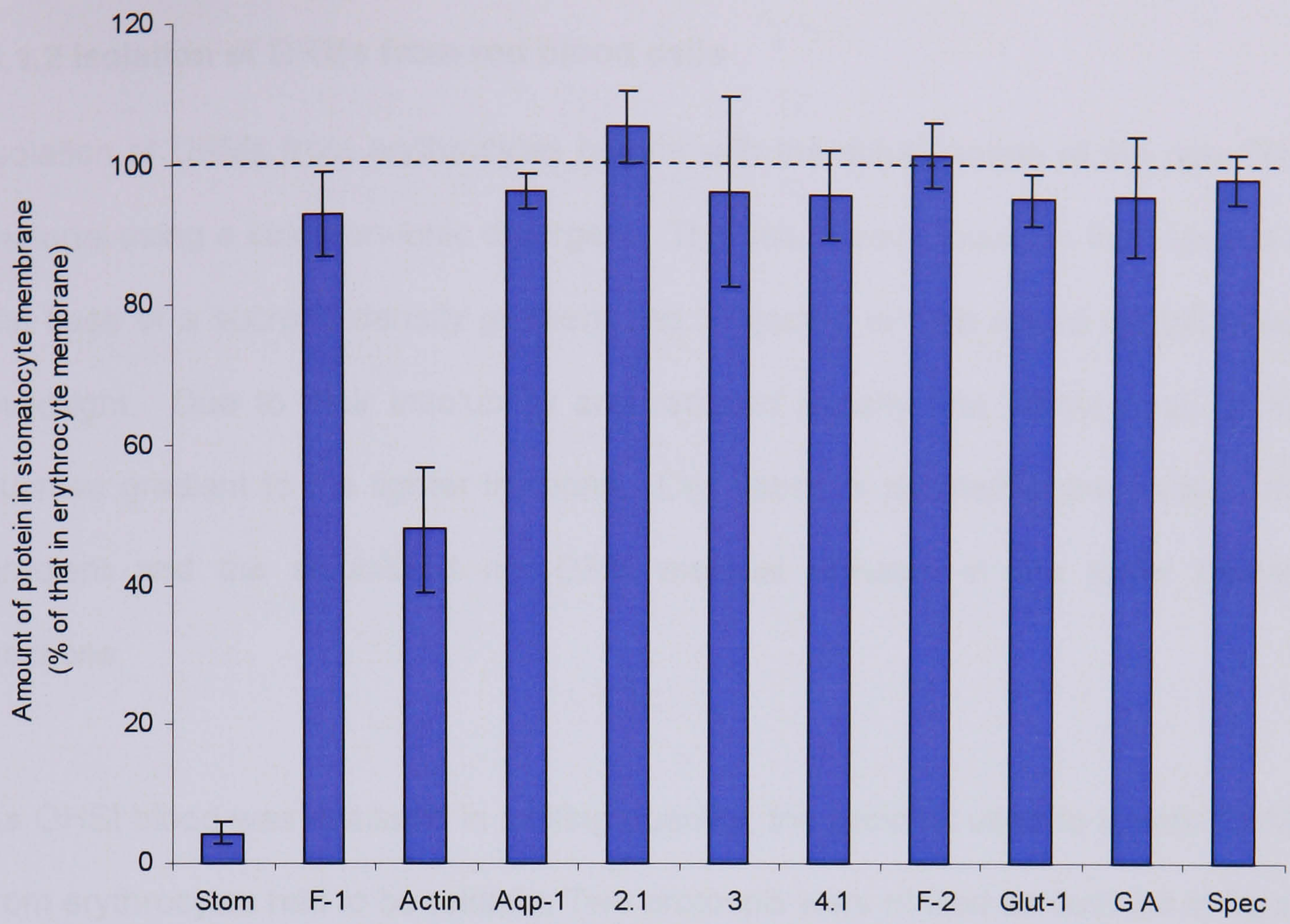

Figure 3.2 Densitometric analysis of proteins in erythrocytes and stomatocytes

The densities of the protein bands on the immunoblots of the erythrocyte and stomatocyte membranes (figure 3.1) were measured using Scion Image software. Results shown represent the percentage content of the protein in the stomatocyte compared to that in the erythrocyte (set to 100%). Stom – stomatin; F-1 – flotillin-1; Actin – actin; Aqp-1 – aquaporin-1; 2.1 – band 2.1; 3 – band 3; 4.1 – band 4.1; F-2 – flotillin-2; Glut-1 – glucose transporter molecule-1; GA – Glycophorin A; Spec – spectrin. Results are the mean (± range) of two separate experiments.

3.1.2 Isolation of DRMs from red blood cells

Isolation of DRMs from erythrocytes begins with the solubilisation of the non-DRM material using a cold non-ionic detergent. The solubilised mixture is then loaded at the base of a sucrose density gradient and subjected to high speed centrifugation overnight. Due to their insolubility and reduced density, the DRMs float up the sucrose gradient to the lighter fractions. Cell debris is pelleted at the base of the gradient and the solubilised non-DRM material remains in the lower heavier fractions.

As OHSt blood was available in limiting quantity, the protocol used to isolate DRMs from erythrocytes had to be reliable. Two protocols were trialled as outlined in figure 3.3. The first was sourced through personal communication with Prof. GW Stewart (University College London) and the second is adapted from a protocol from the Prohaska group (Salzer *et al.* 2001). Both are based on the use of cold Triton X-100 and a sucrose density gradient as mentioned above.

The success of each protocol was determined by positioning of the DRM marker protein flotillin-1 across the fractionated sucrose gradient. Fractions were subjected to SDS-PAGE (section 2.5.2) followed by subsequent immunoblot analysis (section 2.5.3) using antibodies against flotillin-1 (figure 3.4). Each protocol was carried out several times to assess its reliability. In my hands protocol 1 rarely isolated DRMs. Immunoblot analysis for flotillin-1 commonly detected the protein in lower fractions containing solubilised material and in the pellet fraction. The presence of flotillin-1 in the soluble regions of the gradient using protocol 1 may indicate partial solubilisation of the DRMs during preparation. The Triton X-100 concentration was considered to be a possible problem and lowered from 1% to 0.5%. Again, similar

problems were experienced. This distribution across a gradient is seen in some instances when a protein shows partial DRM association. However, flotillin-1 should be restricted to the DRM fractions. It was critical to ensure complete separation of DRMs from non-DRM material for future comparison of erythrocytes with stomatocytes. Protocol 1 was trialled in four separate experiments; on one occasion DRMs were successfully isolated.

Protocol 2 successfully isolated DRMs from erythrocytes (figure 3.4). Flotillin-1 was detected only in the lighter density fractions (7-10), demonstrating the insolubility and reduced density of the DRMs. Protocol 2 was trialled in four separate experiments; each successfully isolated DRMs. Due to its reliability, protocol 2 was used for the subsequent isolation of DRMs. For further experimental detail on protocol 2, see section 2.4.3.

	Protocol 1	Protocol 2
Source	Prof. GW Stewart (UCL)	(Salzer *et al.* 2001)
Isolation	Erythrocytes isolated from whole blood (200*g*; 10 min; 4°C)	
Wash	Packed erythrocytes were washed three times in an equal volume of phosphate buffered saline (PBS) (pH 7.4) (1000*g*; 10 min; 4°C)	Packed erythrocytes were washed three times in an equal volume of Tris buffered saline (TBS) (pH 7.5) (1000*g*; 10 min; 4°C)
Lysis	1 volume packed erythrocytes lysed in 100 volume of 20 mM hypotonic phosphate buffer (pH 7.4) (12,000*g*; 10 min; 4°C) (repeated up to four times)	1 volume packed erythrocytes lysed in 9 volume of 0.5% Triton X-100 in TBS. Incubated on ice 20 min; (15,000*g*; 10 min; 4°C) Pellet resuspended in 10ml 0.5% Triton X-100 (TBS), incubated on ice 5 min; (15,000*g*; 10 min; 4°C)
Pellet resuspension	2ml PBS	2ml TBS
Solubilisation	1 volume of 1% Triton X-100 in PBS; incubated on ice 10 min; sonication (30 sec; 80% total time; 1.5 power level)	Previously solubilised when erythrocytes lysed
Sucrose gradient	1 volume 90% sucrose added then loaded at base of discontinuous sucrose gradient; 18 hrs; 140,000*g*; 4°C	
Fractionation	Fractionation from base; 0 – insoluble pellet; 12 – top fraction	

Figure 3.1 Two protocols trialled in the isolation of DRMs from erythrocytes

Protocol 1 was kindly gained through personal communication with Prof. GW Stewart (University College London, UK). Protocol 2 was adapted from the Prohaska research group (Salzer *et al.* 2001). All buffers were pre-chilled and each stage carried out at 4°C.

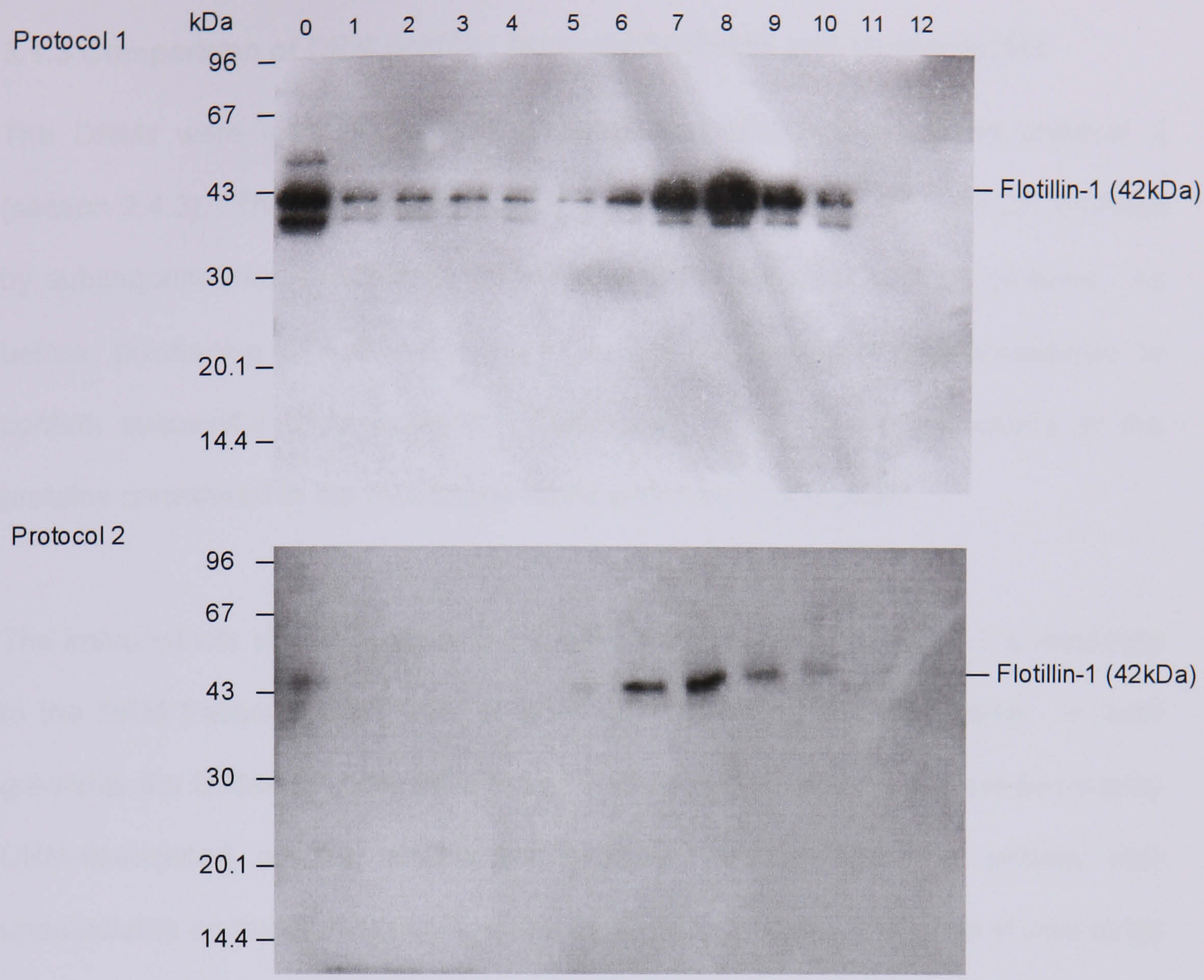

Figure 3.4 Immunoblot analysis of gradients produced using each protocol

Whole erythrocytes were subjected to the treatments indicated in figure 3.3. Fractionated gradients were subjected to SDS-PAGE (equal volume of each fraction loaded) followed by subsequent immunoblot analysis using an antibody against flotillin-1. The upper panel shows the immunoblot analysis for protocol 1 and the lower shows the immunoblot analysis for protocol 2 (0-pellet, 12-top fraction). Molecular weight markers are shown to the left of each immunoblot (kDa). The immunoblots are representative of four separate isolations.

3.1.3 Comparison of DRM profiles from erythrocytes and stomatocytes

The DRMs were isolated from erythrocytes and stomatocytes using protocol 2 (section 2.4.3). The fractionated gradients were subjected to SDS-PAGE followed by subsequent immunoblot analysis using antibodies against various proteins. As before, positioning of flotillin-1 across the gradient was primarily considered to confirm successful DRM isolation. Distribution in the gradient fractions of the proteins considered in the membrane study was then investigated.

The immunoblots shown in figure 3.5 clearly demonstrate that flotillin-1 is restricted to the DRM fractions in both the erythrocyte and stomatocyte gradients. In both gradients the DRMs are present mainly in fractions 6-8. Stomatin is predominantly DRM-associated on the erythrocyte gradient; as expected the protein was undetectable on the stomatocyte gradient (data not shown). Actin was shown to be partially DRM-associated in the erythrocyte with significant proportions of the protein detected in most fractions. There was a clear reduction in actin levels across the stomatocyte gradient, particularly in the DRM fractions. To quantify this reduction, the DRM fractions on the immunoblots seen in figure 3.5 and one other representative immunoblot were subjected to densitometric analysis (section 2.5.6). The actin content in these fractions on the erythrocyte gradient was set at 100%. The equivalent stomatocyte fractions had only 10% (mean value) of the actin level of the erythrocyte (figure 3.6).

Aquaporin-1, flotillin-2 and glut-1 were also shown to be DRM-associated, although minor amounts of flotillin-2 were present in the non-DRM fractions in both erythrocytes and stomatocytes (figure 3.5). Band 2.1, band 3, band 4.1 and spectrin were all shown to be non-DRM-associated proteins. They remained in the

solubilised material at the base of the gradient. There was no co-localisation of flotillin-1 with these solubilised proteins, indicating that the DRMs were completely segregated from the solubilised material at the base of the gradient.

Together these results suggest that stomatin deficiency in the stomatocyte has little effect on the partitioning of several proteins into DRMs. The only difference noted in this study was the reduced association of actin across the stomatocyte gradient, particularly in the DRM regions. This suggests stomatin may be linked to the actin cytoskeleton and thus form part of a tethering mechanism between the membrane and the cytoskeleton. This result agrees with the decreased actin content in the stomatocyte membrane (figure 3.1) and was further investigated through the overexpression of stomatin in mammalian cells.

A summary of the distribution of proteins in erythrocyte and stomatocyte membranes and DRMs is shown in figure 3.7. Additional proteins investigated with inconclusive results are also noted there.

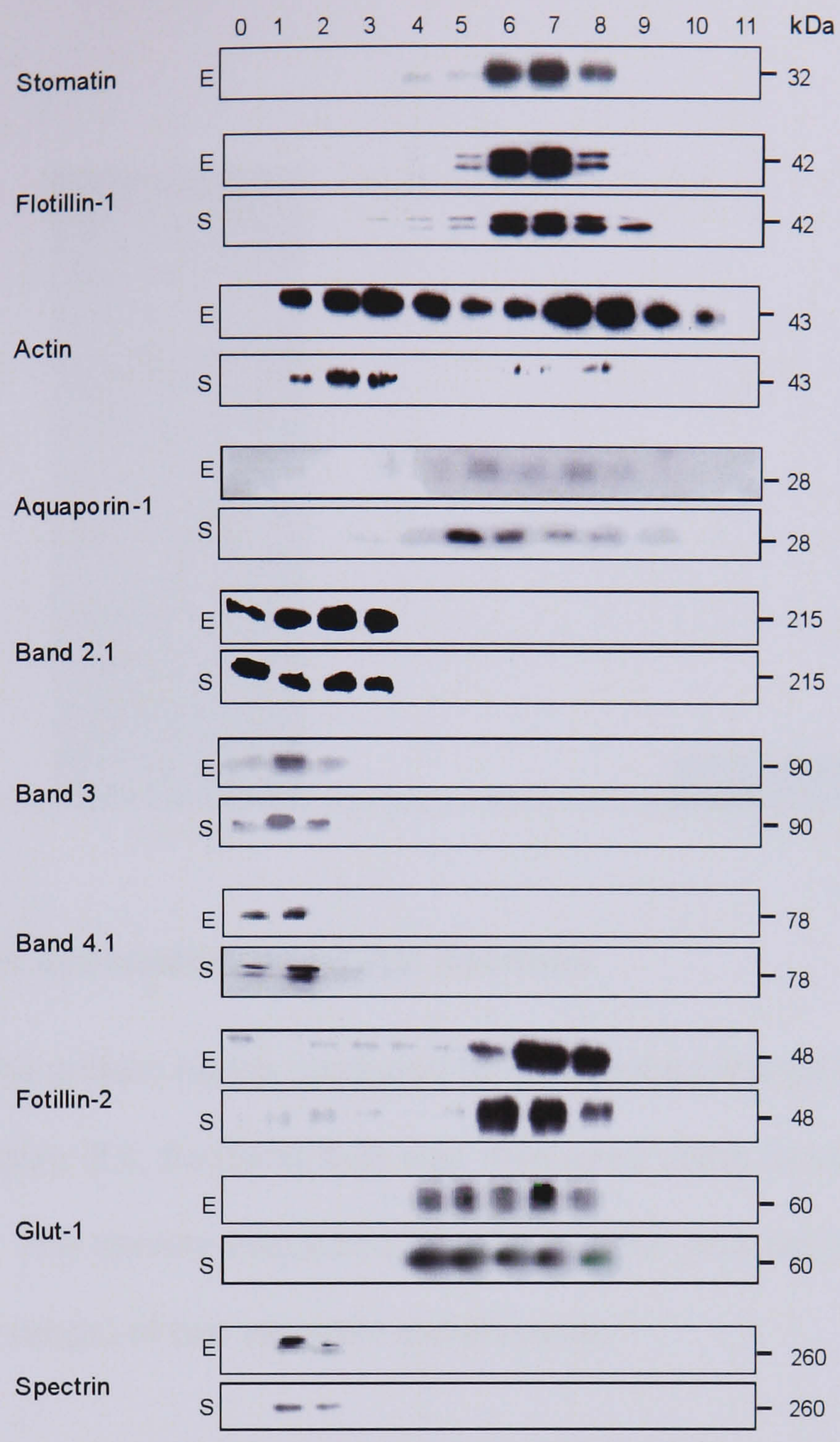

Figure 3.5 Distribution of proteins across erythrocyte and stomatocyte gradients

DRMs were isolated using a discontinuous buoyant sucrose density gradient in the presence of Triton X-100 (section 2.4.3). The gradients were fractionated base upwards and the pelleted material resuspended (0-pellet; 11-top fraction). The gradients were subjected to SDS-PAGE (equal volume of each fraction loaded) and subsequent immunoblot analysis using antibodies against the indicated proteins. Blots are representative of 2 separate isolations. E – erythrocyte; S – stomatocyte. Molecular weights are shown to the right of each immunoblot (kDa).

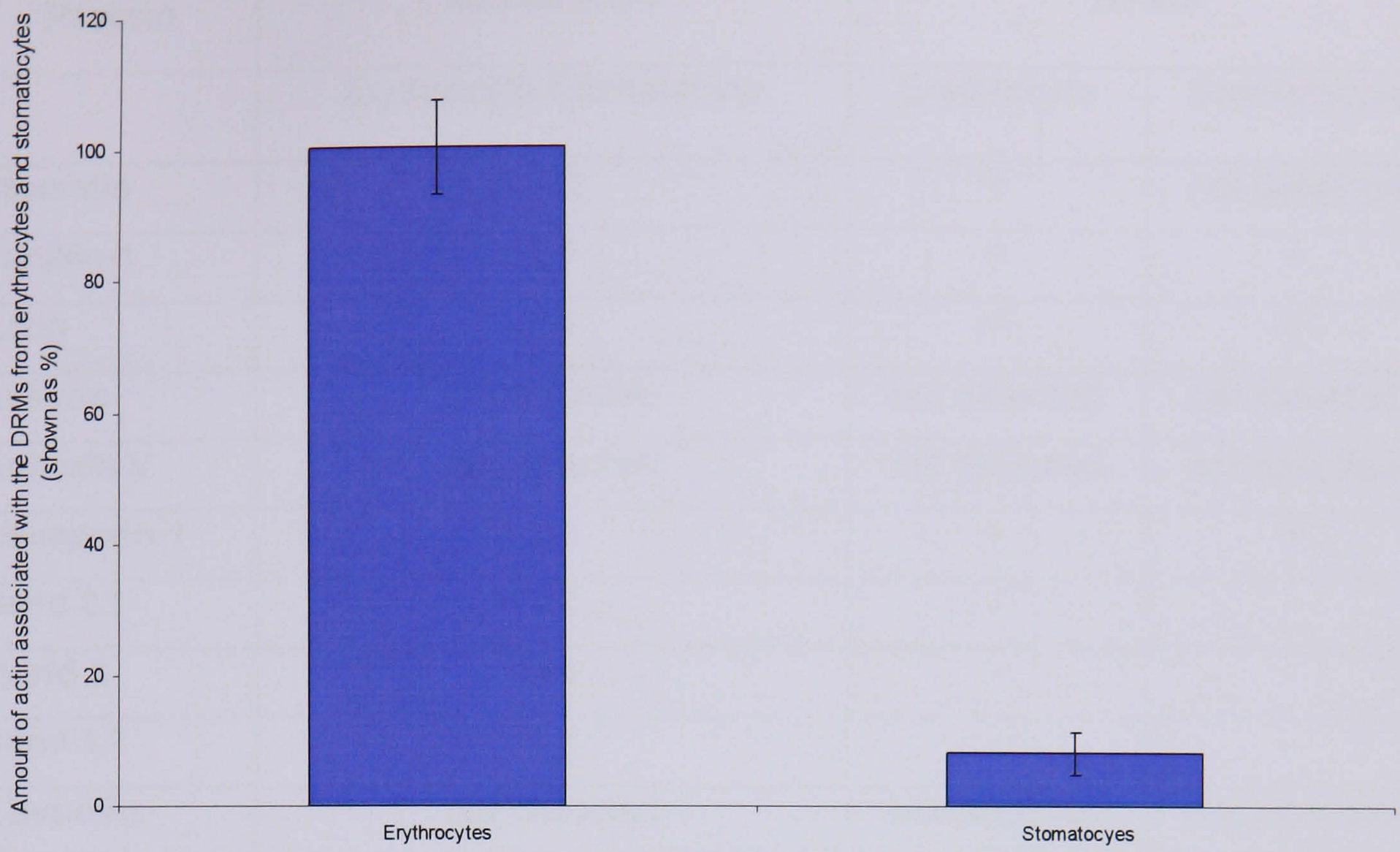

Figure 3.6 Actin association with DRM fractions

The density of the protein bands produced by immunoblot analysis for actin content of the DRMs (figure 3.5; fractions 6-8) was measured using Scion Image software (section 2.5.6). The density measured for erythrocytes was set to 100%. Results are the mean (± range) of two separate experiments.

Protein	Membranes	DRMs	
	Erythrocyte:Stomatocyte	Erythrocyte	Stomatocyte
Stomatin	1:0	+	not detected
Flotillin-1	1:1	+	+
Actin	2:1	+/-	+/-
Ankyrin	not detected	not detected	not detected
Annexin V	not detected	not detected	not detected
Aquaporin-1	1:1	+	+
Band 2.1	1:1	-	-
Band 3	1:1	-	-
Band 4.1	1:1	-	-
Caveolin	not detected	not detected	not detected
Flotillin-2	1:1	+	+
Glut-1	1:1	+	+
Glycophorin A	1:1	not detected	not detected
Glycophorin C	not detected	not detected	not detected
Spectrin α	1:1	-	-

Figure 3.7 Protein ratio in membranes and their distribution across the sucrose gradient in erythrocytes and stomatocytes

Membranes were isolated from erythrocytes and stomatocytes (section 2.4.2), subjected to SDS-PAGE (equal protein loading; 10µg) and subsequent immunoblot analysis using antibodies against the proteins indicated. Results shown represent the ratio of protein content between the erythrocyte and stomatocyte.

DRMs were isolated from erythrocytes and stomatocytes. The fractionated gradients were subjected to SDS-PAGE (equal volume of each fraction loaded) followed by subsequent immunoblot analysis using antibodies against the proteins shown (+ DRM associated, - no DRM association; +/- partially DRM association).

3.2 Overexpression of stomatin in mammalian cells

The results obtained from the analysis of the erythrocyte and stomatocyte membranes and DRMs suggest that stomatin may be linked to the actin cytoskeleton. To further investigate this, stomatin was overexpressed in mammalian cells and the actin levels assessed. Various mammalian cell lines were cultured using standard cell culture techniques (section 2.2.1). Once confluent, they were washed and harvested. Membranes were isolated from each cell line (section 2.3.2) and subjected to SDS-PAGE (section 2.5.2) followed by subsequent immunoblot analysis (section 2.5.3) using an antibody against stomatin (figure 3.8). Madin-Darby canine kidney (MDCK) cells showed low endogenous expression of stomatin and so were selected for this study. The protein content of MDCK cell lysates, membranes and DRMs following the overexpression of stomatin was investigated.

3.2.1 Cloning of stomatin into the expression vector pcDNA3.1

In order to overexpress stomatin transiently in MDCK cells, the DNA of stomatin was first cloned into the expression vector pcDNA3.1/V5-His©TOPO®TA (TOPO). Full-length human stomatin cDNA was purchased from OriGene Technologies Inc. (MD, USA). The clone was supplied as plasmid DNA and retrieved according to the manufacturer's instructions. The DNA was sequenced and subsequently used as a template in the amplification of the cDNA encoding stomatin. Accutaq LA DNA Polymerase (Sigma-Aldrich Ltd., Poole, UK) was selected due to the proofreading system attached to this enzyme. The enzyme and reagents supplied were used as suggested by the manufacturer; 200ng of template DNA was used. Cycling parameters were set according to the manufacturer.

Freshly generated stomatin cDNA was cloned into the expression vector TOPO. The vector was supplied as a component of the pcDNA3.1/V5-His©TOPO®TA Expression Kit (Invitrogen Ltd, Paisley, UK). The kit was used as suggested by the manufacturer (section 2.6.8). The ligation reactions were then transformed into the TOP10 competent *E.coli* cells supplied in the kit. The cells were plated on selective media containing ampicillin (section 2.6.2). Colonies were selected and the plasmid DNA isolated (section 2.6.3) and sequenced. MDCK cells were transiently transfected (section 2.2.2) with 10µg of the expression vector TOPO containing the cDNA encoding human stomatin. Lysates (section 2.3.1), membranes (section 2.3.2) and DRMs (section 2.3.5) were prepared from the cells 48 hours post-transfection.

3.2.2 Comparison of actin levels in cells overexpressing stomatin

Lysate samples from untransfected and transfected MDCK cells were subjected to SDS-PAGE (section 2.5.2) followed by subsequent immunoblot analysis (section 2.5.3) using antibodies against stomatin, flotillin-1 and actin. Under these conditions no endogenous stomatin was detected in the untransfected MDCK cells (figure 3.9). This is likely due to the low level at which the protein is usually expressed. An increased signal was detected for stomatin in the transfected cells confirming overexpression of this protein. The levels of flotillin-1 and actin were unaltered following overexpression of stomatin. Densitometric analysis (section 2.5.6) to confirm this observation was carried out using the immunoblots shown in figure 3.9 and other representative data. The untransfected sample was set at 100% and the transfected sample compared to it. The levels of both flotillin-1 and actin were essentially the same in the transfected cells as in the untransfected cells (figure 3.9).

Membrane samples isolated from untransfected and transfected cells were immunoblotted similarly to the aforementioned lysate samples. Again, no endogenous stomatin was detected (figure 3.9). An increased signal for stomatin was detected in the transfected cells, again confirming overexpression of this protein and demonstrating correct cellular localisation. The level of membrane flotillin-1 was unaltered in the transfected cells, confirmed by densitometric analysis. The signal for membrane-associated actin was greater in the transfected cells as compared to the untransfected cells. Densitometric analysis showed there to be a 50% increase in membrane-associated actin in the transfected as compared to the untransfected cells (figure 3.9). The densitometric analysis was carried out on the immunoblot shown in figure 3.9 and one other representative immunoblot produced in a separate experiment, the mean result was taken.

Fractionated sucrose gradients prepared from transfected and untransfected cells were subjected to SDS-PAGE followed by subsequent immunoblot analysis using antibodies against stomatin, flotillin-1 and actin. Distribution of the proteins across the gradient was determined with particular interest shown to the DRM fractions (figure 3.10). Positioning of the DRM marker protein flotillin-1 showed the DRMs to be present in fractions 7-9 in both the untransfected and transfected cells. Stomatin was also found in the DRM fractions from the transfected cells. No stomatin was detected in the gradient prepared from the untransfected cells (data not shown). The actin content was significantly higher in the DRMs from the transfected cells; a 20% increase as shown by densitometric analysis of the immunoblot in figure 3.10 and one other representative immunoblot (figure 3.10).

These data agree with the analysis of membranes and DRMs isolated from erythrocytes and stomatocytes. The results obtained following the overexpression of stomatin in MDCK cells provides further evidence for a link between stomatin and actin. This link may serve to tether the cytoskeleton to the membrane.

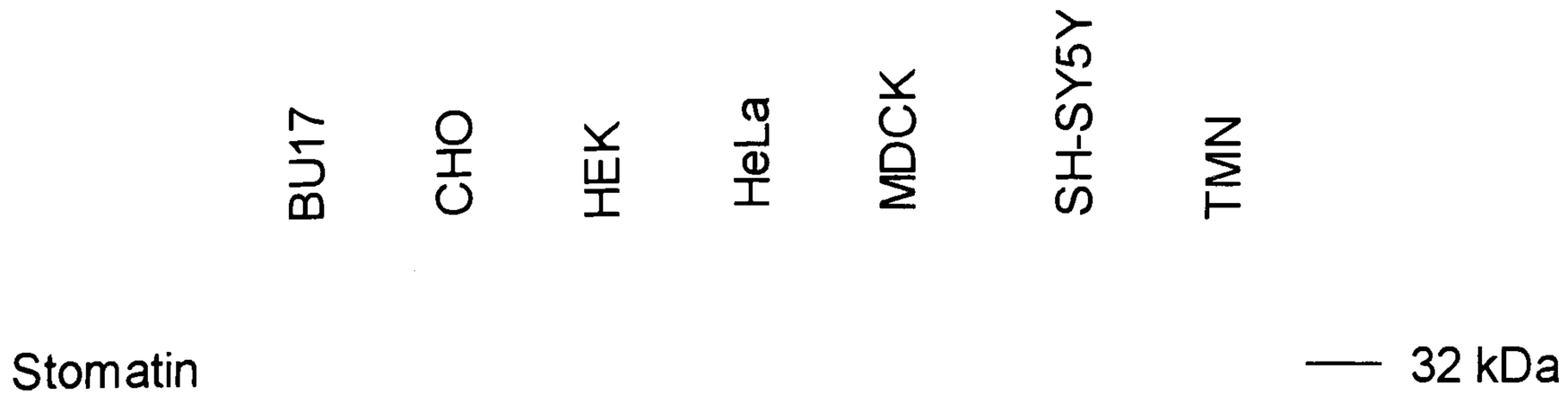

Figure 3.8 Immunoblot analysis for stomatin in various mammalian cell lines

Membranes were isolated from mammalian cells (section 2.3.2) that were cultured using standard cell culture techniques (section 2.2.1). Membrane samples from each cell line were subjected to SDS-PAGE (equal protein loading; 10µg) followed by subsequent immunoblot analysis using an antibody against stomatin. Glioma (BU17), Chinese hamster ovary (CHO), cervical carcinoma (HeLa), human embryonic kidney (HEK), Madin-Darby canine kidney (MDCK), human neuroblastoma (SH-SY5Y), tetraploid murine neuroblastoma (TMN).

Lysates

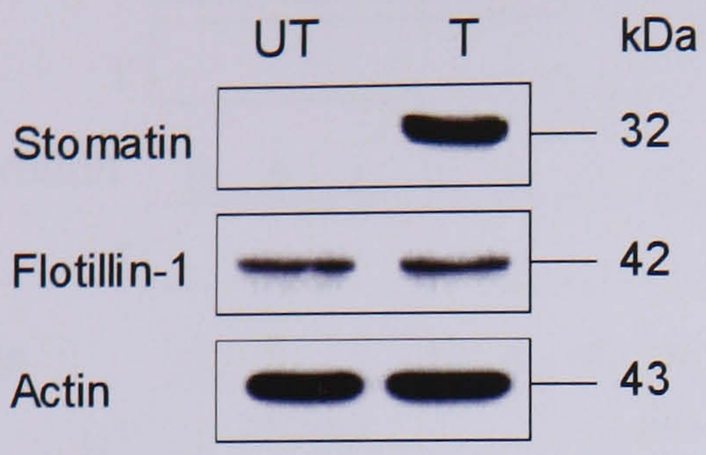

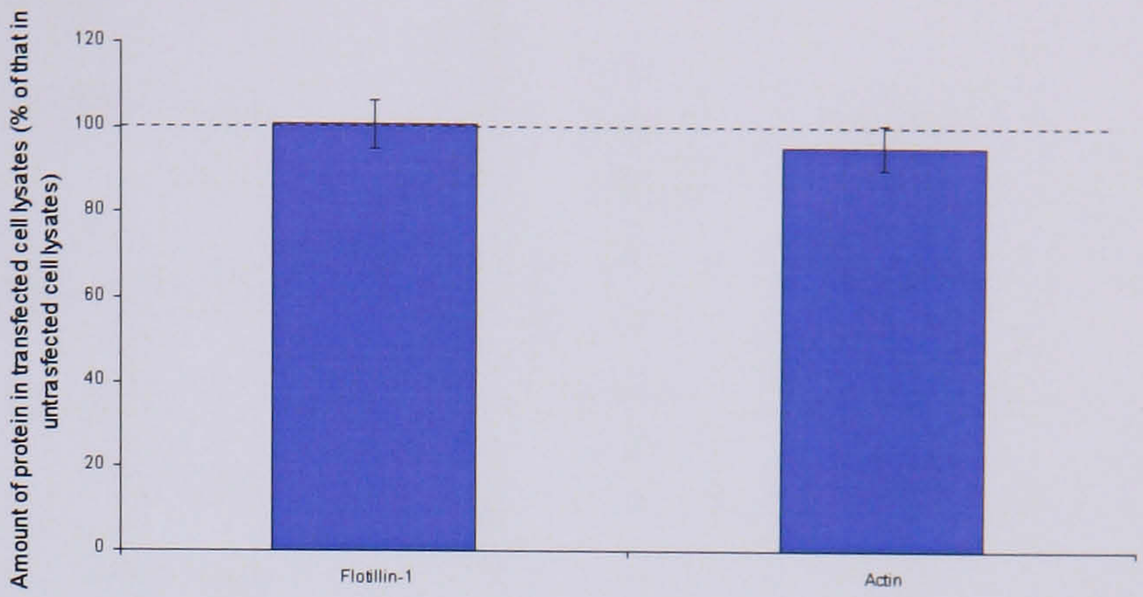

Membranes

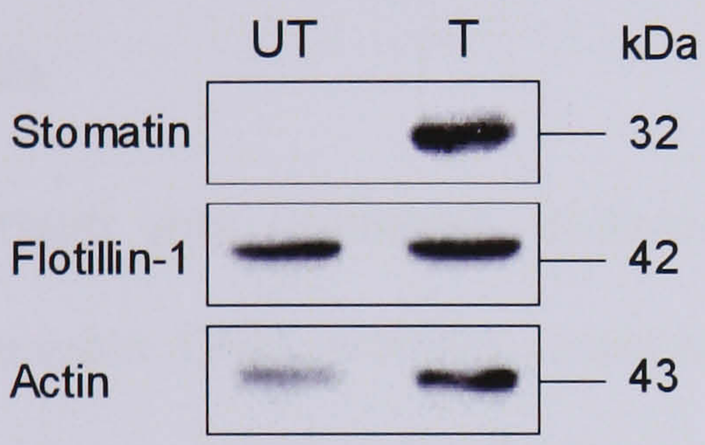

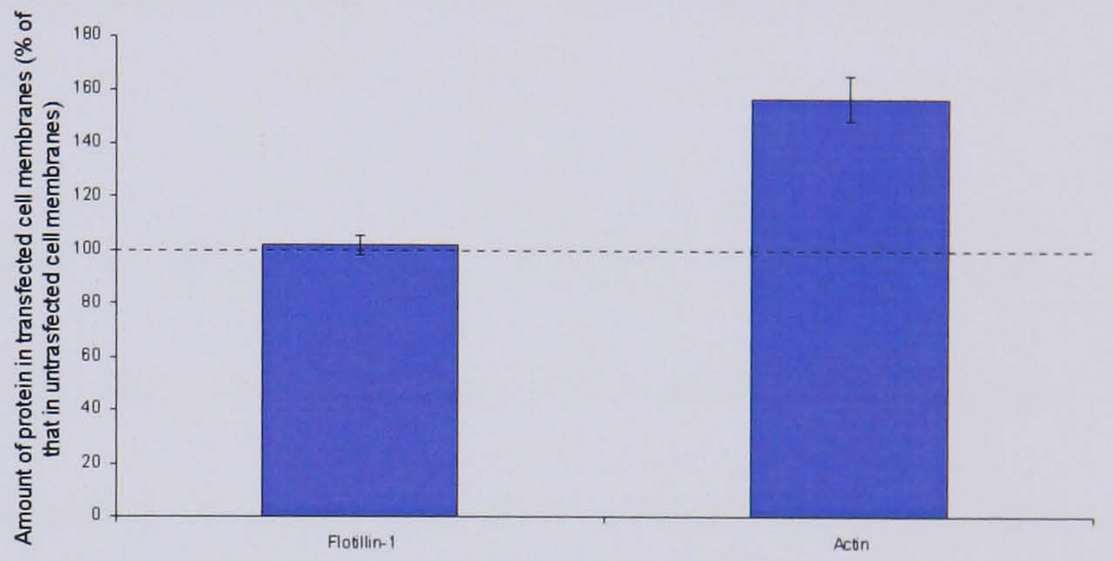

Figure 3.9 Overexpression of stomatin causes increased membrane actin association

Stomatin was transiently overexpressed in MDCK cells (section 2.2.2). Lysate and membrane samples were isolated from untransfected (UT) and transfected (T) cells and subjected to SDS-PAGE (equal protein loading; 5µg) followed by subsequent immunoblot analysis using antibodies against stomatin, flotillin-1 and actin. Immunoblots are representative of two separate experiments.

The density of the bands produced by immunoblot analysis for flotillin-1 and actin content of lysates and membranes was measured using Scion Image software (section 2.5.6). The density measured for UT cells was set to 100%. Results are the mean (± range) of two separate experiments.

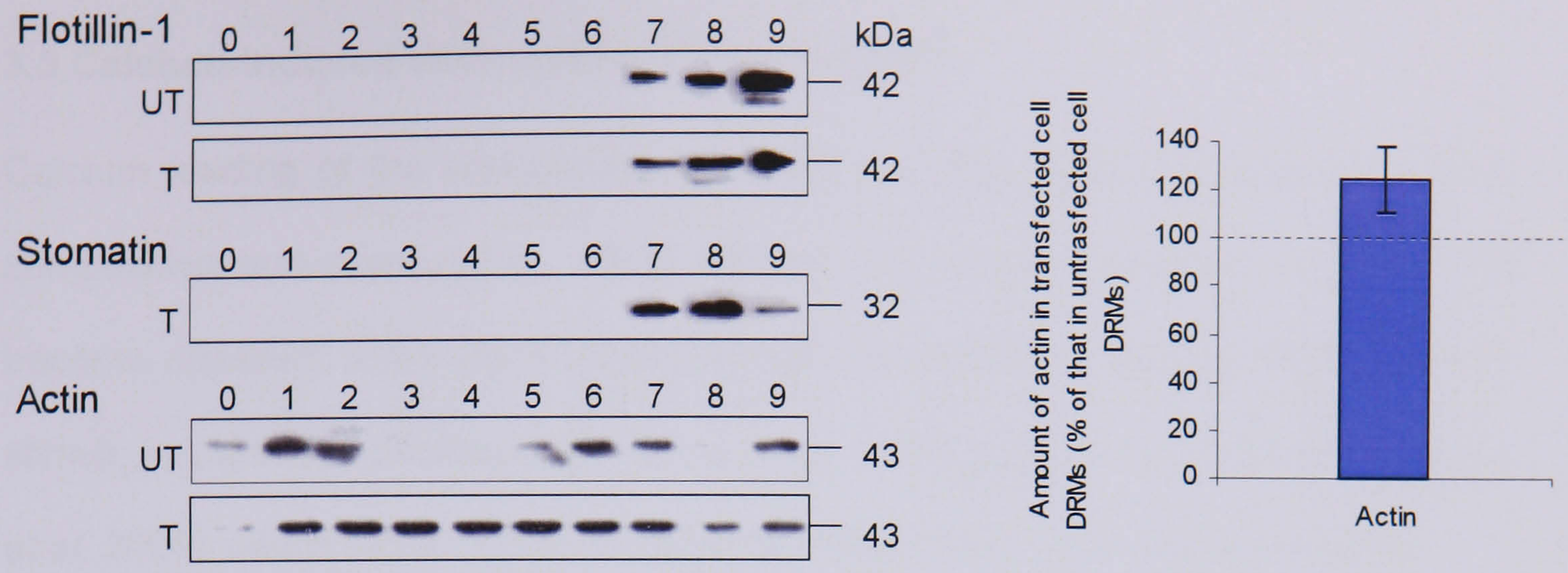

Figure 3.10 Overexpression of stomatin causes increased actin association in DRMs

Stomatin was transiently overexpressed in MDCK cells (section 2.2.2). Cells underwent DRM isolation (section 2.3.5) and the fractionated sucrose gradients were subjected to SDS-PAGE (equal volume of each fraction loaded) followed by subsequent immunoblot analysis using antibodies against stomatin, flotillin-1 and actin. Immunoblots are representative of two separate experiments. UT – untransfected; T – transfected.

The density of bands produced by immunoblot analysis for actin in DRM fractions 7-9 were measured using Scion Image software (section 2.5.6). The density measured for UT cells was set to 100% and the T cells compared to them. Results are the mean (± range) of two separate experiments.

3.3 Calcium-induced vesiculation of erythrocytes

Calcium loading of the erythrocyte has been a useful model to study membrane composition and vesiculation. More recently the clinical relevance of this model became apparent when the erythrocyte was demonstrated to respond to external stimuli, in particular prostaglandin E_2 (Li *et al.* 1996) and lysophosphatidic acid (Fu *et al.* 2004), which induce calcium-dependent processes within the erythrocyte.

Increased cytosolic calcium leads to several intracellular events all thought to contribute to vesiculation of the erythrocyte. Some of these events include:

- Rearrangement of the cytoskeleton – particularly to the spectrin network (Anderson *et al.* 1977)
- Calpain-1 activation – a cysteine protease known to act on the cytoskeletal proteins protein 2.1 and protein 4.1 (Dantas de Medeiros *et al.* 2002) and on stomatin (Salzer *et al.* 2002)
- Loss of lipid asymmetry in the membrane – inhibition of a translocase and activation of a scramblase leads to transbilayer mixing of phospholipids (Zwaal *et al.* 1997)

Treatment of erythrocytes with calcium and ionophore A23187 causes calcium loading and induces the shedding of microvesicles (150 nm diameter) and nanovesicles (60nm diameter) (Allan *et al.* 1980). These haemoglobin-containing exovesicles are devoid of cytoskeletal components (Knowles *et al.* 1997) but enriched in glycosylphosphatidylinositol (GPI)-anchored proteins such as acetylcholinesterase and CD55 (Butikofer *et al.* 1989). This vesiculation is considered to serve as the erythrocyte's defence to complement, rapidly eliminating

the membrane attack complex (MAC) in the exovesicles and is thought to be initiated by calcium influx through the MAC channel (Iida *et al.* 1991). Similar strategies have been described for platelets (Sims *et al.* 1986) and neutrophils (Morgan *et al.* 1987). The process is thought to be raft-based with stomatin concentrating into the microvesicles (Salzer *et al.* 2002). To provide further evidence for this vesiculation being a raft-based process, it was investigated in cholesterol-depleted erythrocytes and stomatocytes.

3.3.1 Methyl-β-Cyclodextrin treatment reduces vesiculation

To provide further evidence for raft involvement with vesiculation, Methyl-β-Cyclodextrin (MβCD) was used to deplete the erythrocyte of cholesterol. Depletion in this manner perturbs lipid rafts functionally and challenges their integrity (Ilangumaran *et al.* 1998). Untreated and cholesterol-depleted erythrocytes were then treated to induce vesiculation and immunoblot analysis was used to assess the process. In this study whole erythrocytes were incubated in 3mM MβCD for 30 min at 37°C (section 2.4.5). This treatment has previously been shown to reduce cholesterol content of the erythrocyte membrane by 40% (Rivas *et al.* 2003). Cholesterol-depleted erythrocytes were then treated with calcium and ionophore to induce vesiculation (section 2.4.4). Membranes were isolated from the post-vesiculation erythrocytes (section 2.4.2). Vesicles and post-vesiculation membranes were subjected to SDS-PAGE (section 2.5.2) followed by subsequent immunoblot analysis (section 2.5.3) using antibodies against the flotillin proteins. All control samples (figure 3.11; - MβCD lane 1-4) were loaded at equal protein concentration. Cholesterol-depleted membranes and vesicles were loaded at equal volume of the equivalent control sample (e.g. lane 1 in each case contained the same volume of sample; lane 2 in each case contained the same volume of sample

etc). Lane 1 represents the post-vesiculation membrane, lanes 2 and 3 represent the microvesicles and lane 3 represents the nanovesicles. The microvesicles in lane 3 represent a smaller subset of microvesicles compared to those in lane 2 due to the longer centrifugation period (Salzer *et al.* 2002).

Under these conditions, the cholesterol-depleted erythrocytes showed reduced vesiculation compared to control erythrocytes (figure 3.11). Densitometric analysis (section 2.5.6) on the immunoblots in figure 3.11 and two other representative immunoblots showed ~ 40% of flotillin-1 and ~ 55% of flotillin-2 vesiculated from the control erythrocytes (figure 3.12). Following cholesterol depletion none of the flotillin-1 and only ~ 10% of flotillin-2 was detected in the vesicles. Longer exposures of the immunoblots to photographic film showed minor amounts of flotillin-1 in the microvesicles (data not shown). It is apparent from this study that the extent to which the erythrocyte is able to vesiculate in response to calcium influx is dramatically reduced following cholesterol depletion. As the process is reportedly raft-based, these results suggest that if raft integrity is perturbed, so too is the ability of the erythrocyte to vesiculate.

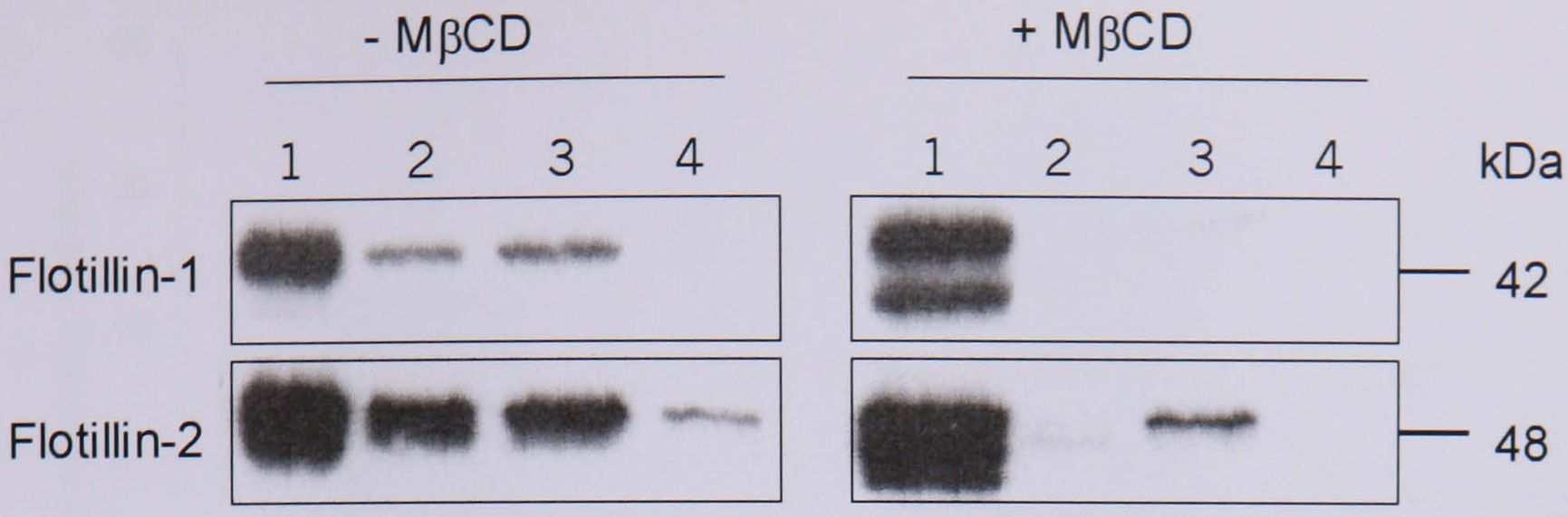

Figure 3.11 Cholesterol depletion reduces calcium-induced vesiculation.

Control (- MβCD) and cholesterol-depleted (+ MβCD) erythrocytes were treated with calcium and the calcium ionophore A23187 to induce shedding of microvesicles and nanovesicles (section 2.4.4). Membranes were then isolated from the treated erythrocytes (section 2.4.2). Erythrocyte membranes and vesicles were subjected to SDS-PAGE and subsequent immunoblot analysis using antibodies against the Flotillin proteins. Lane 1, post-vesiculation membranes. Lane 2, microvesicles isolated following centrifugation for 10 min at 15,000*g*. Lane 3, microvesicles isolated following centrifugation for 20 min at 15,000*g*. Lane 4, nanovesicles. Post-vesiculation membranes and untreated vesicles were loaded at equal protein concentration (5µg). Equivalent volumes of treated membranes and vesicles were loaded. Immunoblots are representative of three separate experiments.

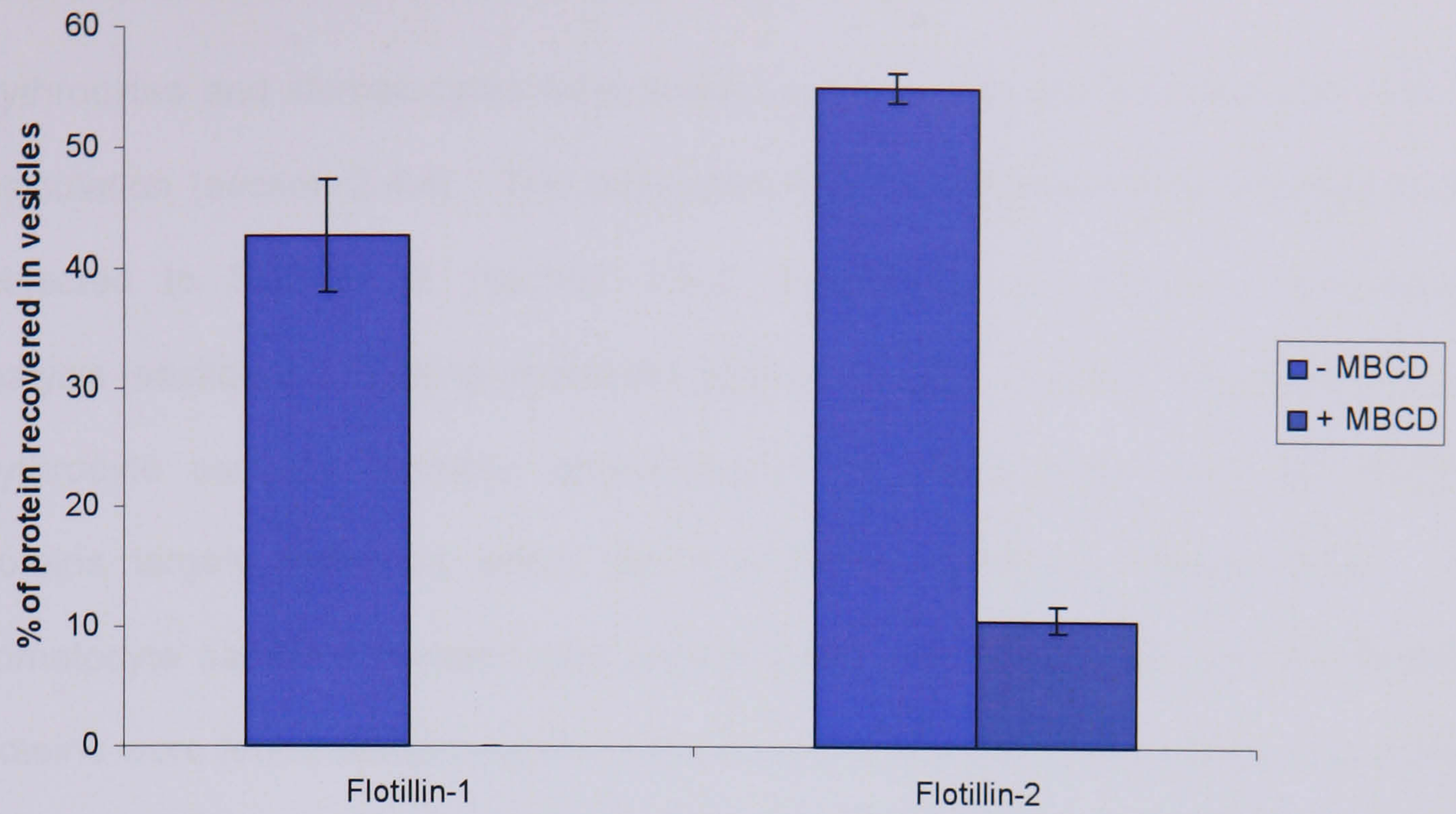

Figure 3.12 Densitometric analysis showing the extent to which the flotillin proteins vesiculate

The density of bands produced by immunoblot analysis for the flotillin content within vesicles (figure 3.11) was measured using Scion Image software (section 2.5.6). Results shown represent the percentage of total flotillin content in all the vesicle fractions (figure 3.11, lanes 2-4) as compared to the post-vesiculation membranes (figure 3.11, lane 1). Control (-MβCD) and cholesterol depleted (+MβCD) are shown. Results are the mean (± SEM) of three separate experiments.

3.3.2 Calcium-induced vesiculation of stomatocytes

Erythrocytes and stomatocytes were treated with calcium and ionophore to induce vesiculation (section 2.4.4). The post-vesiculation membranes and vesicles were subjected to SDS-PAGE (section 2.5.2) followed by subsequent immunoblot analysis (section 2.5.3) using antibodies against stomatin, flotillin-1 and flotillin-2. In erythrocyte samples stomatin concentrated into microvesicles and the flotillin proteins largely remained within the erythrocyte membrane (figure 3.13). In stomatocyte samples stomatin was undetectable (data not shown) and the flotillin proteins were found predominantly in the smaller subset of microvesicles and in the nanovesicles. This left the post-vesiculation stomatocyte membranes almost completely devoid of flotillins. Densitometric analysis (section 2.5.6) on the immunoblots in figure 3.13 and two other representative immunoblots showed in control samples ~ 20% of flotillin-1 and ~30% of flotillin-2 to vesiculate from the erythrocyte (figure 3.14). Vesicles from the stomatocytes contained ~ 100% of the flotillin proteins. These results suggest that stomatin may play an important role in regulating calcium-induced vesiculation. In the absence of stomatin, the vesiculation process appears to be enhanced. To further investigate the possibility that more vesicles are produced from stomatocytes than erythrocytes under similar conditions, vesicle samples were imaged by atomic force microscopy and numbers of vesicles assessed.

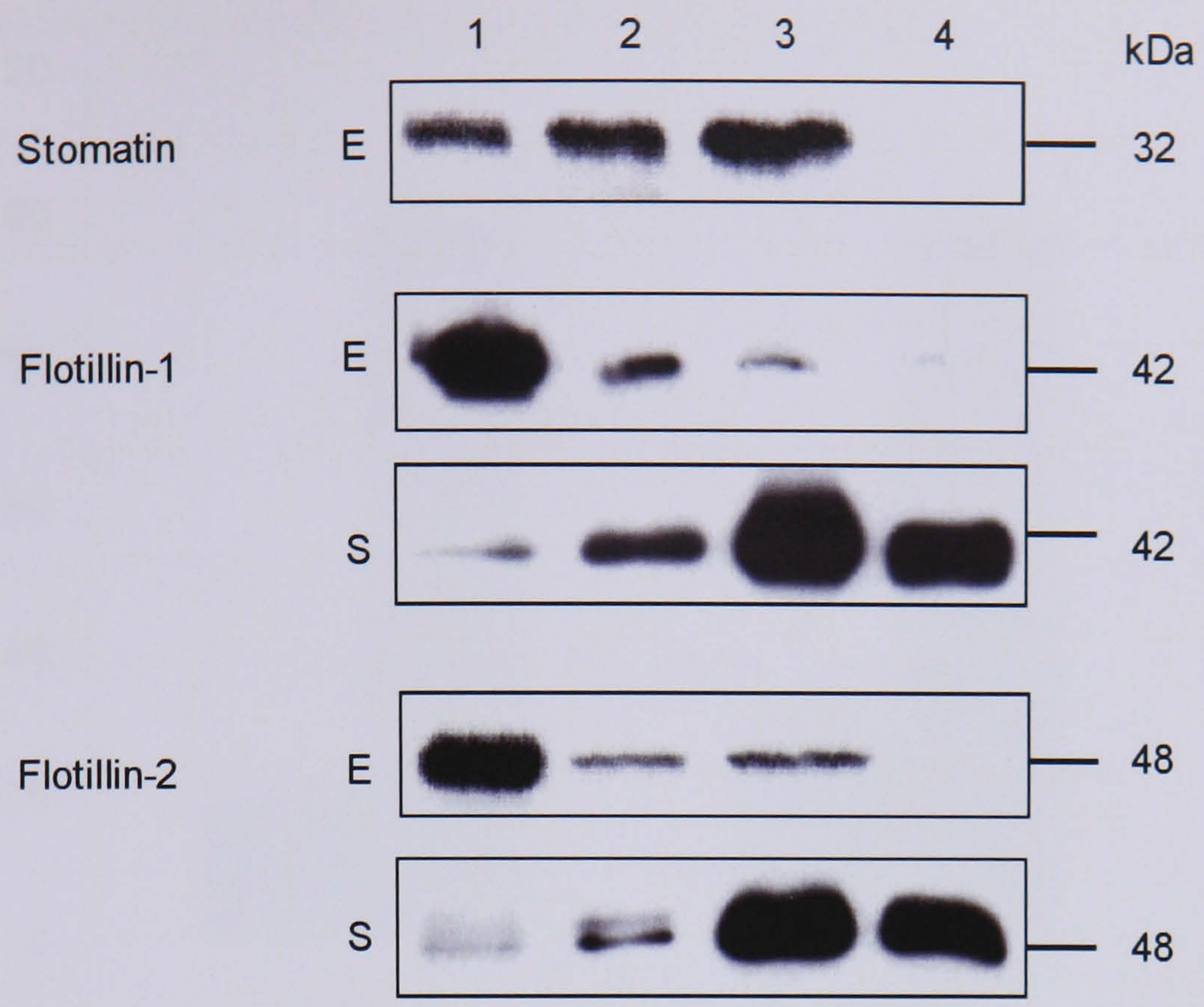

Figure 3.13 Treatment with calcium ionophore induces shedding of microvesicles and nanovesicles from erythrocytes and stomatocytes

Erythrocytes (E) and stomatocytes (S) were treated with calcium and calcium ionophore A23187 to induce shedding of microvesicles and nanovesicles (section 2.4.4). Post-vesiculation membranes and resultant vesicles were subjected to SDS-PAGE followed by subsequent immunoblot analysis using antibodies against the proteins indicated. Lane 1, post-vesiculation membranes. Lane 2, microvesicles isolated following centrifugation for 10 min at 15,000*g*. Lane 3, microvesicles isolated following centrifugation for 20 min at 15,000*g*. Lane 4, nanovesicles. Post-vesiculation membranes and control vesicles were loaded at equal protein concentration (5µg). Equivalent volumes of stomatocyte vesicles were loaded. Immunoblots are representative of three separate experiments.

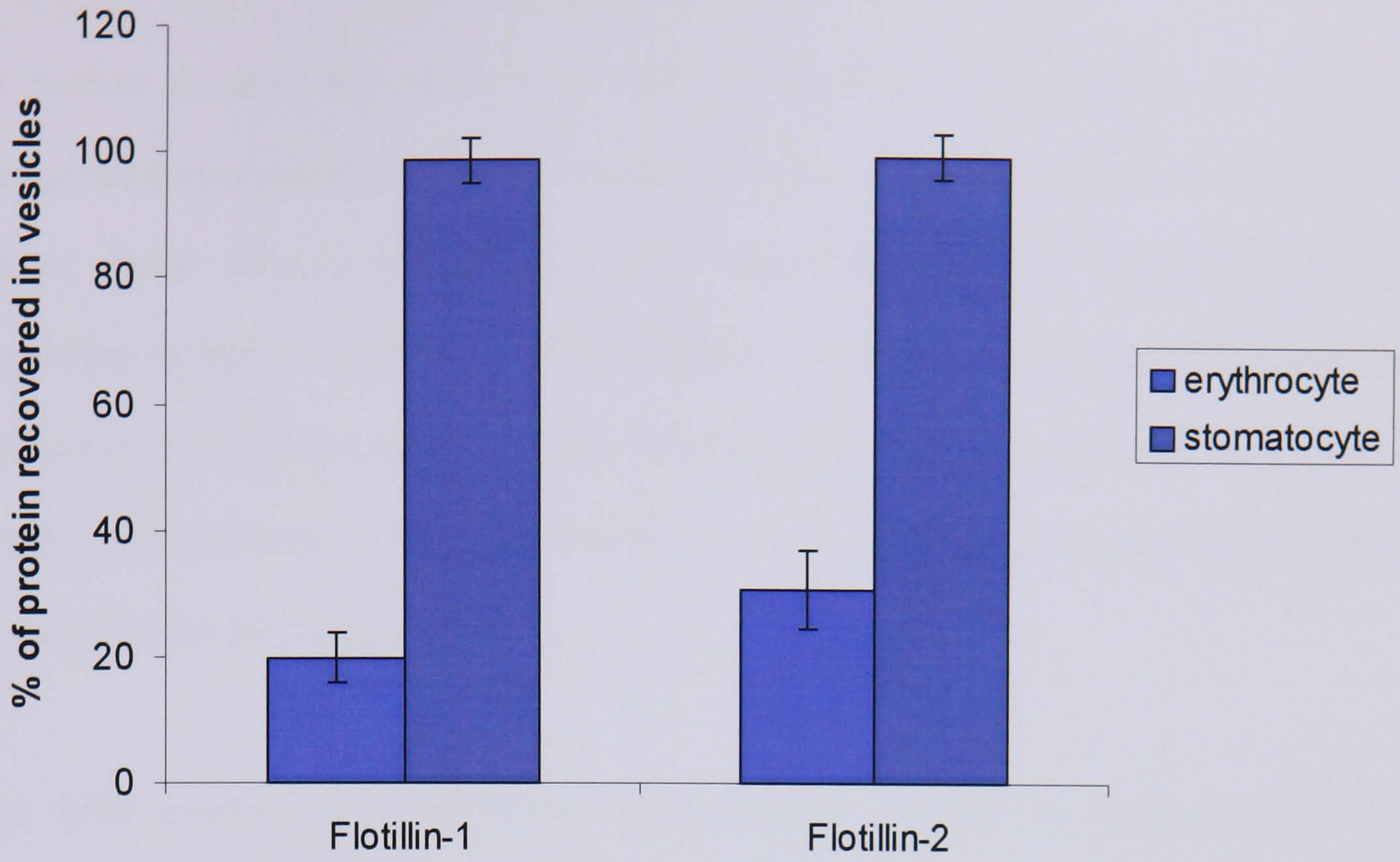

Figure 3.14 Densitometric analysis of vesicles from erythrocytes and stomatocytes

The density of bands produced by immunoblot analysis for the flotillin content within vesicles recovered from erythrocytes and stomatocytes (figure 3.13) were measured using Scion Image software (section 2.5.6). Results shown represent the percentage of total flotillin recovered in all vesicle fractions (figure 3.13, lanes 2-4) as compared to the post-vesiculation membranes (figure 3.13, lane 1). Results are the mean (± SEM) of three separate experiments.

3.3.3 Atomic force microscopy of calcium-induced vesicles

To further confirm the enhanced vesiculation from stomatocytes as seen by immunoblot analysis (figure 3.13), vesicle samples were subjected to analysis using atomic force microscopy (AFM). The technique records height information according to sensor deflection. Erythrocytes and stomatocytes were treated with calcium and ionophore to induce vesiculation. Equivalent volumes of each vesicle sample were placed on a mica-coated surface and kindly imaged using AFM by Miss A.Garner (section 2.4.6).

The AFM images obtained show an increased number of microvesicles and nanovesicles in the stomatocyte samples as compared to erythrocyte samples (figure 3.15). This agrees with immunoblot data suggesting that stomatocytes are more susceptible to calcium-induced vesiculation than erythrocytes. The microvesicles obtained from the stomatocytes appear to be more irregular in shape; the reason for this is unknown. This result agrees with data obtained from immunoblot analysis of vesicle samples from erythrocytes and stomatocytes (figure 3.13). Together these results suggest stomatin may play a regulatory role in calcium-induced vesiculation.

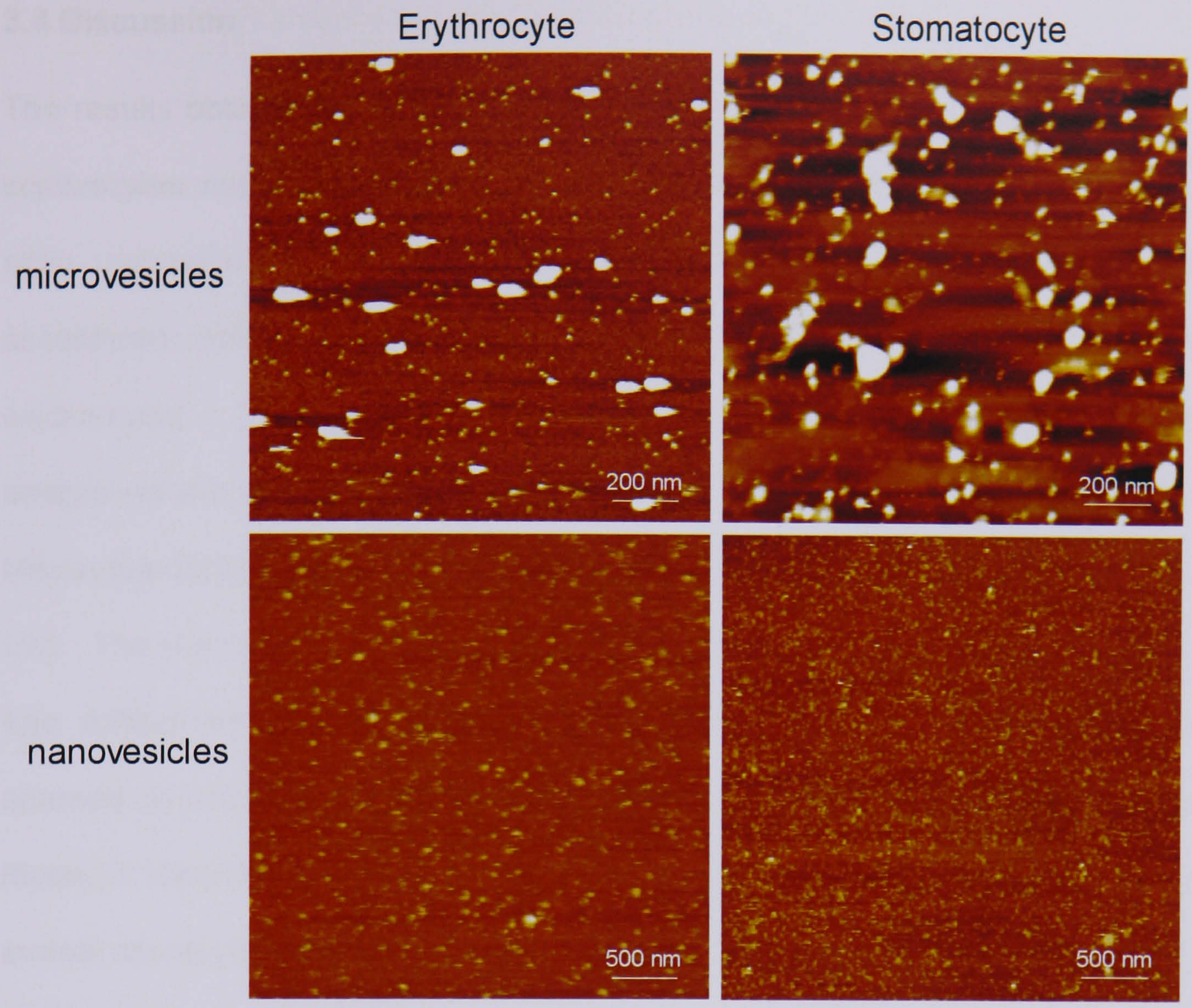

Figure 3.15 AFM images of erythrocyte and stomatocyte microvesicles and nanovesicles.

Erythrocytes and stomatocytes were treated with calcium and ionophore to induce shedding of microvesicles and nanovesicles (section 2.4.4). Microvesicles (upper panels) and nanovesicles (lower panels) were imaged on mica coated surfaces (section 2.4.6). Vesicles formed from erythrocytes are seen on the left, vesicles from stomatocytes are seen on the right.

3.4 Discussion

The results obtained from the analysis of proteins of membranes and DRMs from erythrocytes and stomatocytes indicate an association between stomatin and the actin cytoskeleton. In the stomatin-deficient stomatocytes, reduced actin association was detected in the membranes and DRMs as compared to the erythrocytes. These data are supported by unpublished work in which DRM analysis of stomatocytes showed the same reduction in actin association when an alternative DRM isolation protocol was used (J.Turner, University College London, UK). The possibility of an association between stomatin and the actin cytoskeleton was further investigated in this study through the transient overexpression of stomatin in MDCK cells. Cells overexpressing stomatin showed increased actin levels in membranes and the DRMs. Lysates from the same cells showed no overall increase in cellular actin. This result suggests the overexpression of stomatin had no global effect on the total cell actin level but does indicate a direct involvement with the increased presence of actin detected at the plasma membrane and in DRMs. If stomatin does associate with the actin cytoskeleton, then it is likely in part to have a structural role.

A structural role for stomatin has previously been suggested due to its likeness with the caveolins. Membrane topology, palmitoylation, oligomerisation and raft residence are all features shared. The caveolins form the scaffold for caveolae, flask-shaped invaginations of the membrane. This has led to the suggestion that stomatin may be functioning similarly as a scaffold protein (Umlauf *et al.* 2004).

Several other studies have shown an association between stomatin and the actin cytoskeleton. These have lead to the speculation that stomatin is a structural

protein forming a bridge between the membrane and the actin cytoskeleton. Firstly, stomatin shows an affinity for the cytoskeletal protein β-adducin (Innes *et al.* 1999). Secondly, stomatin has been found concentrated within the actin-rich microvilli of MDCK and UAC cells. This group speculated that this association was perhaps involved in morphogenesis of these cells (Snyers *et al.* 1999a). Thirdly, various members of the SPFH (Stomatins/Prohibitins/Flotillins/HflK/C) domain family of proteins have been found to associate with the actin cytoskeleton. The prohibitins are a group of highly conserved proteins which are responsible for various cellular processes including cell-cycle progression, apoptosis and modulation of epithelial cell migration (Bacher *et al.* 2002; Rajalingam *et al.* 2005). The flotillins, again highly conserved, are involved with cell signalling, trafficking and cytoskeletal rearrangement (Langhorst *et al.* 2005). Podocin is exclusively expressed in podocytes (specialised renal epithelial cells), and linked to the actin cytoskeleton by the adapter protein CD2AP (Schwarz *et al.* 2001). As well as their association with the actin cytoskeleton, these proteins all oligomerise and reside within lipid rafts. This has prompted the suggestion that these proteins, as well as stomatin, form scaffolds for the assembly of multiprotein complexes (Langhorst *et al.* 2005).

Actin association with lipid raft proteins can have functional significance for cells. Studies on T-cell activation have shown that actin controls the coalescence of lipid rafts, in this instance regulating the association of the T cell signalling machinery and the formation of a platform favourable for signalling (Valensin *et al.* 2002). Calcium-induced vesiculation of erythrocytes is raft-based, requires reorganisation of the cytoskeleton and is localised to a given area of membrane according to calcium influx (Salzer 1999). In the erythrocyte the stomatin-actin link may in part assist in the coalescence of proteins and lipids required for localised vesiculation.

Many components which are normally considered raft resident are found enriched in the vesicles e.g. sphingomyelin, cholesterol and GPI-anchored proteins (Civenni *et al.* 1998). In cells lacking GPI-anchored proteins the erythrocytes show an impaired ability to vesiculate (Whitlow *et al.* 1993). In this study, cholesterol-depleted erythrocytes in which the raft structure is perturbed showed significantly reduced vesiculation. This suggests that if components normally associated with erythrocyte rafts are depleted, vesiculation is hindered. This suggests a significant role for rafts in this process.

During calcium-induced vesiculation stomatin concentrates into the microvesicles whilst the flotillins and cytoskeletal proteins remain within the erythrocyte membrane. If stomatin does in part function as a structural protein, it may concentrate into the microvesicles to form part of the scaffold. Vesiculation was significantly enhanced in the stomatocytes, as shown by immunoblot analysis and AFM. This suggests that stomatin may also have a role in the regulation of vesiculation, in its absence there is unrestricted shedding of vesicles. The stomatin-actin link discussed earlier may form part of this regulation, necessitating a cleavage event to allow the release of stomatin from the erythrocyte. Vesiculation is known to require remodelling of the underlying cytoskeleton which is thought in part to be calpain-associated (Iida *et al.* 1991). Calpain is known to cleave the cytoskeletal protein band 4.1 (Dantas de Medeiros *et al.* 2002) and stomatin (Salzer *et al.* 2002) both of which concentrate into microvesicle structures. Stomatin is enriched in the microvesicles themselves and band 4.1 into microvesicle appendages called 'tails'. It has been suggested that the enrichment of band 4.1 into these 'tail' structures is significant in membrane fusion preceding the release of the microvesicle (Allan *et al.* 1980). Preliminary data suggest that calpain activity is increased in stomatocytes

(data not shown). Perhaps the reduction in the stomatin-actin link coupled with the increased calpain activity is responsible for the enhanced vesiculation. Membrane perturbing agents can form stomatocytes from healthy erythrocytes. Studies performed on these stomatocytes have shown reduced vesiculation upon calcium loading. This suggests that the shape of the OHSt stomatocyte could not be responsible for the enhanced vesiculation and further suggests that the absence of stomatin is directly linked (Wolfs *et al.* 2003).

As well as OHSt stomatocytes showing enhanced levels of vesiculation, the protein content of the resultant vesicles is altered. The flotillins are found in the post-vesiculation erythrocyte. Following calcium loading of stomatocytes, the flotillins are found enriched in the smaller subset of microvesicles and in the nanovesicles. The post-vesiculation stomatocyte membrane was left almost devoid of these proteins. As the vesiculation process is thought to be involved in the protection against complement (Iida *et al.* 1991), it can be considered important that this system is maintained. In the stomatocyte it may be critical to replace stomatin in order that vesiculation can continue. The flotillins may form this substitute perhaps due to their SPFH domain or membrane topology, both features they share with stomatin. They may, however, lack the critical regulatory feature contained within stomatin.

Previous studies have not implicated stomatin to be directly involved in the regulation of calcium-induced vesiculation but have linked the protein with various essential features of this process. Firstly, vesiculation is preceded by localised loss of phospholipid asymmetry. This is caused by the inhibition of the phospholipid translocase and activation of a phospholipid scramblase. This scramblase has previously been identified as being an endofacial protein associated with the actin

cytoskeleton (Connor *et al.* 1989); one study has suggested it to be stomatin (Desneves *et al.* 1996). During this redistribution of phospholipids, phosphatidylserine (PS), which is usually confined to the inner leaflet of the membrane, becomes exposed on the outer leaflet (Zwaal *et al.* 1997). The appearance of PS at the surface of the erythrocyte is known to trigger thrombin formation. The OHSt patients who undergo therapeutic splenectomy often suffer problems with thrombosis; this has been attributed to the possible appearance of PS at the surface of the stomatocyte (Stewart 2004). Although stomatocytes show scramblase activity (Stewart *et al.* 1999), thombotic problems post-splenectomy suggest lipid asymmetry may not be correctly regulated. This could be directly due to the deficiency of stomatin or as a result of enhanced vesiculation. Secondly, calcium increase within the erythrocyte results in the binding of the soluble cytoplasmic protein calpromotin to the endoplasmic face of the membrane. This attachment is required for the opening of Ca^{++}-dependent K^+ channels, followed by efflux of K^+ and water and subsequent cell shrinkage. This is known as the Gardos effect; the exact mechanism is not yet fully understood but essential for vesiculation. The erythrocyte holds vast intracellular reserves of calpromotin; only 1% of this reserve is required to bring about the Gardos effect (Moore *et al.* 1991). One proposed binding site on the membrane is stomatin (Moore *et al.* 1997). Intracellular stomatocyte levels of calcium are within the normal range and the Gardos effect is known not to be responsible for the increased permeability to K^+ ions (Stewart 2004). Stomatin had previously been suggested to have an ion channel regulatory role due to stomatocytes showing elevated permeability to Na^+ and K^+ cations, as yet no direct link has been shown (Lande *et al.* 1982). Perhaps this binding of calpromotin to stomatin forms some regulatory feature of calcium-induced vesiculation.

Abnormalities in calcium-induced vesiculation have been noted for other disease states. The erythrocytes from patients with Scott syndrome show diminished membrane vesiculation; this has been attributed to defective reorganisation of the actin cytoskeleton (Bevers *et al.* 1992). Patients with glucose-6-phosphate dehydrogenase (G6PD)-deficient erythrocytes show enhanced vesiculation. Post-vesiculation erythrocytes are more susceptible to hemolysis, a correlation between the extent of vesiculation and sensitivity to complement-mediated hemolysis has been found. This may be due to the selective removal of the GPI-anchored CD55 and CD59 upon vesiculation; both proteins are known to protect the cell from complement attack. Untreated G6PD-deficient erythrocytes are normally more susceptible to hemolysis and it has been suggested that the enhanced vesiculation seen in G6PD-deficient erythrocytes is responsible for this increased sensitivity (Zhu *et al.* 1999). The same may be true for stomatocytes; they too show enhanced vesiculation perhaps they are also more sensitive to hemolysis. This may contribute to the anaemia associated with OHSt which is usually attributed totally to the osmotic fragility of the stomatocyte.

Together, these results suggest stomatin is in part a structural protein tethered to the actin cytoskeleton. The protein plays a multifunctional regulatory role in calcium-induced vesiculation where raft integrity is essential. Further investigation into this vesiculation process is required to form a deeper understanding into the roles of stomatin and may provide a better understanding of the OHSt phenotype.

Chapter 4: Site-directed mutagenesis of stomatin

4.1 Selection of mutants

The addition of palmitate to a protein has varied effects. Palmitoylation of Ras causes the protein to associate with the membrane; depalmitoylation in the membrane causes the protein to leave the membrane. This cycle allows Ras signalling pathways in different subcellular compartments (Meder *et al.* 2005). The palmitoylation of the linker protein LAT in T-cells is essential for its association with lipid rafts; this in turn influences T-cell signalling (Zhang *et al.* 1998). Inhibiting palmitoylation of the ion channel scaffold protein PSD-95 prevents clustering of ion channels in excitatory synapses (El-Husseini *et al.* 2000). Stomatin is palmitoylated at two positions, cysteine-29 and cysteine-86. It is predicted that these lipid modifications could cause the protein to have greater affinity for the membrane, specifically the lipid rafts within the membrane. A series of mutants unable to undergo palmitoylation expressed in the human amniotic cell line UAC showed correct cellular localisation suggesting the lipid modification does not influence the affinity of stomatin for the membrane (Snyers *et al.* 1999b). However, as stomatin is known to homo-oligomerise and UAC cells express stomatin endogenously, this may influence the cellular localisation of the mutants (Snyers *et al.* 1998). In this current study, similar cysteine to serine mutants at positions 29 and 86 in stomatin were investigated; the mutants were expressed in cells which do not express stomatin (figure 4.1). As palmitoylation is known to influence membrane and lipid raft association, the presence of the palmitoylation mutants in the membrane and in detergent-resistant membranes (DRMs) was assessed.

The *Caenorhabditis elegans* (*C.elegans*) proteins MEC-2 and UNC-1 are homologues of stomatin which contain the SPFH (Stomatins, Prohibitins, Flotillins and HflK/C) domain (Tavernarakis *et al.* 1999). MEC-2 is required for mechanosensation through its interaction with the epithelial sodium channels (ENaC); mutations in the *mec-2* gene result in animals unresponsive to touch (Huang *et al.* 1995; Goodman *et al.* 2002). UNC-1 is required for the sinusoidal motion of the nematode, mutations in the *unc-1* gene result in animals with the abnormal motion described as kinked and cause them to be more sensitive to volatile anaesthetics (Rajaram *et al.* 1998). In this study glycines at positions 119, 155 and 185, arginine at position 151 and leucine at position 255 were also selected for investigation. Mutations in glycine 119 and 185, and leucine 255 disrupt the function of MEC-2 (figure 4.1). Mutations in arginine 151 and glycine 155 disrupt the function of UNC-1. Glycine 185 in stomatin is conserved in all SPFH domain proteins (Tavernarakis *et al.* 1999). This residue, as well as disrupting the function of UNC-1, exists centrally within the plasma membrane targeting domain of flotillin-1 (Liu *et al.* 2005). If the same domain exists in stomatin, disruption of glycine 185 may hinder stomatin's ability to associate with the membrane. As with the palmitoylation mutants, membrane and DRM association of the mutants was investigated.

Stomatin is a known to localise to the nucleus; its role there has not been defined (Fricke *et al.* 2005). The SPFH domain protein flotillin-1 is also known to translocate to the nucleus. For unknown reasons it is present in the organelle at highest levels during S-phase (Langhorst *et al.* 2005). Band 4.1 is a major cytoskeletal protein within the erythrocyte (Takakuwa 2000). However, in nucleated cells it can also be found in the nucleus; its role here is yet to be defined (Gascard *et al.* 1999). There

is increasing evidence for the presence of cytoskeletal proteins in the nucleus forming a nucleoskeleton. These proteins include actin, spectrin and various actin-binding proteins (Parfenov *et al.* 1995; Padmakumar *et al.* 2005). Localisation to the nucleus was assessed for both the palmitoylation and SPFH domain mutants.

Palmitoylation mutants		
Mutant	Mutation	Base change
Cys 29 Ser	Cysteine → Serine	TGC → AGC
Cys 86 Ser	Cysteine → Serine	TGC → AGC

SPFH domain mutants		
Mutant	Mutation	Base change
Arg 151 Leu	Arginine → Leucine	AGG → CTA
Arg 151 Lys	Arginine → Lysine	AGG → AAG
Gly 119 Ala	Glycine → Alanine	GGT → GCT
Gly 155 Ala	Glycine → Alanine	GGC → GCC
Gly 185 Ala	Glycine → Alanine	GGA → GCA
Leu 255 Ala	Leucine → Alanine	CTG → GCG
Leu 255 Ile	Leucine → Isoleucine	CTG → ATA
Leu 255 Lys	Leucine → Lysine	CTG → AAG

Figure 4.1 Details of the stomatin mutants investigated

The palmitoylation mutants at positions 29 and 86 in stomatin are both missense mutations. The base change results in the native cysteine residue being substituted for a serine residue. The mutants are unable to unable to be palmitoylated at these residues.

The SPFH domain mutants at positions 119, 151, 155, 185 and 255 in stomatin are all missense mutations. The glycine residues at positions 119 and 185, and leucine 255 are critical for MEC-2 function and arginine 151 and glycine 155 are critical for UNC-1function.

4.2 Site-Directed Mutagenesis

The dsDNA template used in this investigation was the pcDNA3.1/V5-His TOPO®TA vector (Invitrogen Ltd, Paisley, UK) containing wild type (Wt) stomatin (section 3.2.1). Mutagenic primers were designed using the on-line Stratagene QuikChange® primer design program (http://labtools.stratagene.com). The QuikChange® Site-Directed Mutagenesis kit was purchased from Stratagene (Amsterdam, Netherlands) and used according to the manufacturer's instructions. Briefly, mutant strand synthesis reactions using 10ng of dsDNA template and the desired mutagenic primers (figures 4.2 and 4.3) were subjected to the cycling parameters detailed in figure 4.4. Following cycling, samples were incubated on ice for 2 min. The methylated parental DNA was digested using 1 μl of *Dpn* I (10 U/μl); each sample was incubated at 37°C for 1 hr. The entire digested sample was transformed into XL1-Blue competent cells and plated on selective medium containing ampicillin (section 2.6.6). Plasmid DNA was isolated from selected colonies (section 2.6.3) and sequenced.

The mutant samples were transiently transfected (section 2.2.2) into HEK cells. This cell line was selected as it does not express endogenous stomatin which could associate with the mutants and influence cellular localisation (figure 3.8). Lysates (section 2.3.1), membranes (section 2.3.2), lysed nuclei (section 2.3.3) (section 2.3.4) and detergent-resistant membranes (DRMs) (section 2.3.5) were prepared from the cells 48 hours post-transfection.

Mutant	Primers
Cys 29 Ser	Forward 5'-GGGCCTTGGACCTAGCGGATGGATTTTGGTG-3' Reverse 5'-CACCAAAATCCATCCGCTAGGTCCAAGGCCC-3'
Cys 86 Ser	Forward 5'-GGTTTGTTTTTTATTCTGCCAAGCACTGACAGCTTCATCAAAG-3' Reverse 5'-CTTTGATGAAGCTGTCAGTGCTTGGCAGAATAAAAAACAAACC-3'

Figure 4.2 Primers used to produce palmitoylation mutants

The primers used to create the palmitoylation mutants of stomatin. Cysteines at positions 29 and 86 were mutated into serine residues. The altered base is shown in red. Mutagenic primers were designed using the on-line Stratagene QuikChange® primer design program (http://labtools.stratagene.com).

Mutant	Primers
Arg 151 Leu	Forward 5'-TCTTTTGGCACAAACTACTCTGCTAAATGTTCTGGGCACCAAGAATC-3' Reverse 5'-GATTCTTGGTGCCCAGAACATTTAGCAGAGTAGTTTGTGCCAAAAGA-3'
Arg 151 Lys	Forward 5'-GGCACAAACTACTCTGAAGAATGTTCTGGGCACCA-3' Reverse 5'-TGGTGCCCAGAACATTCTTCAGAGTAGTTTGTGCC-3'
Gly 119 Ala	Forward 5'-TGACAATTAGCGTGGATGCTGTGGTCTATTACCGC-3' Reverse 5'-GCGGTAATAGACCACAGCATCCACGCTAATTGTCA-3'
Gly 155 Ala	Forward 5'-TCTGAGGAATGTTCTGGCCACCAAGAATCTTTCTC-3' Reverse 5'-GAGAAAGATTCTTGGTGGCCAGAACATTCCTCAGA-3'
Gly 185 Ala	Forward 5'-CCACTGATGCCTGGGCAATAAAGGTGGAGCG-3' Reverse 5'-CGCTCCACCTTTATTGCCCAGGCATCAGTGG-3'
Leu 255 Ala	Forward 5'-CGATACCTGCAGACAGCGACCACCATTGCTTGCT-3' Reverse 5'-AGCAGCAATGGTGGTCGCTGTCTGCAGGTATCG-3'
Leu 255 Ile	Forward 5'-CTCCGATACCTGCAGACAATAACCACCATTGCTGCTGAG-3' Reverse 5'-CTCAGCAGCAATGGTGGTTATTGTCTGCAGGTATCGGAG-3'
Leu 255 Lys	Forward 5'-CCGATACCTGCAGACAAAGACCACCATTGCTGCTG-3' Reverse 5'-CAGCAGCAATGGTGGTCTTTGTCTGCAGGTATCGG-3'

Figure 4.3 Primers used to produce the SPFH domain mutants

The primers used to create the SPFH domain mutants of stomatin. Arginine at position 151 was mutated into a leucine or a lysine; glycines at positions 119, 155 and 185 were mutated into alanines and the leucine at position 255 was mutated into an alanine, isoleucine or a lysine. In this study specific residues were selected for mutation based on the proteins palmitoylation and SPFH domain. Mutagenic primers were designed using the on-line Stratagene QuikChange® primer design program (http://labtools.stratagene.com).

Segment	Cycles	Temperature	Time
1	1	95°C	30 sec
2	16	95°C	30 sec
		55°C	1 min
		68°C	10 min

Figure 4.4 PCR cycling parameters used for site-directed mutagenesis

Mutant strand synthesis reactions using 10ng of pcDNA3.1/V5-His©TOPO®TA vector containing Wt stomatin and the desired mutagenic primers were subjected to the above cycling parameters. Times and temperatures used were as recommended by the manufacturer Stratagene (Amsterdam, Netherlands).

4.2.1 Analysis of palmitoylation mutants

Lysate, membrane, DRM gradients and nuclei were isolated from HEK cells expressing Wt stomatin and the palmitoylation mutants. Samples were subjected to SDS-PAGE (section 2.5.2) followed by subsequent immunoblot analysis (section 2.5.3). Flotillin-1, actin and stomatin content were all investigated. The presence of flotillin-1 should be unaffected by the transfection of the mutant forms of stomatin. The overexpression of Wt stomatin is known to increase the levels of actin associated with the membrane and DRMs (section 3.2). It was investigated if the mutant forms of stomatin altered the presence of actin in the membrane, DRMs or nucleus.

All the lysate samples showed expression of stomatin at varying degrees (figure 4.5). The palmitoylation mutant at position 29 (Cys 29 Ser) was expressed at similar levels to Wt stomatin. The palmitoylation mutant at position 86 (Cys 86 Ser) was expressed at much lower levels compared to Wt stomatin. Why this should be the case is unknown but agrees with a previous study in which a mutation at position 86 in stomatin was only expressed at low levels (Snyers *et al.* 1999b).

Analysis of the membrane samples showed that the little Cys 86 Ser that was being expressed assumed correct cellular localisation and resided in the membrane. Densitometric analysis (section 2.5.6) on the immunoblot in figure 4.5 and one other representative immunoblot showed approximately 30% of Cys 29 Ser was localised in the membrane compared to Wt stomatin (figure 4.6). Palmitoylation is known to affect membrane localisation of some proteins (Meder *et al.* 2005). This result suggests palmitoylation at position 29 in stomatin may influence the proteins affinity for the membrane.

The overall level of stomatin, actin and flotillin-1 detected was less in the nuclei than the levels detected in lysates or membranes. The mutant Cys 86 Ser was barely detectable in the nuclei of transfected HEK cells, most likely due to its low expression. Densitometric analysis on the immunoblot in figure 4.5 and one other representative immunoblot showed a 2-fold increase in levels of Cys 29 Ser associated with the nuclei compared to Wt stomatin (figure 4.6). Palmitoylation of certain proteins is known to influence the distribution between the nucleus and plasma membrane. For example, upon palmitoylation, phospholipid scramblase 1 is trafficked to the plasma membrane. Inhibition of this palmitoylation prevents membrane association and traffics the protein to the nucleus (Wiedmer *et al.* 2003). Taken together these results suggest a similar mechanism may be true for stomatin. The decreased levels of Cys 29 Ser compared to Wt stomatin in the membrane coupled with the increased levels found in the nucleus may be due to an inefficient affinity of this mutant for the membrane. The depalmitoylated form of stomatin may be targeted to the nucleus instead of the membrane, hence the increased presence. Levels of flotillin-1 were constant between cells expressing Wt stomatin compared with cells expressing mutant stomatin throughout. The mutant forms of stomatin would not be expected to exert any influence on the level of expression or cellular location of flotillin-1 as no association with stomatin has ever been reported. As actin associates with stomatin it was possible that a mutant form of stomatin may show reduced affinity for actin and influence the levels of actin in the various cellular compartments investigated. This was not the case and actin was present at the same level in the cellular compartments of cells expressing mutant stomatin as compared to cells expressing Wt stomatin.

The DRM distribution of stomatin did not vary between the cells expressing Wt stomatin as compared to cells expressing mutant stomatin; the protein was found mainly in the DRM fractions 7-9 (figure 4.7). Densitometric analysis on the immunoblot in figure 4.7 and one other representative immunoblot showed there was a decrease to roughly 30% in the level of actin associated with the DRM fractions for the mutant Cys 86 Ser (figure 4.8). As stomatin associates with the actin cytoskeleton (chapter 3), the decreased presence of Cys 86 Ser in the DRMs would be consistent with reduced actin association also seen with these structures. This may be due to the overall lower expression of this mutant, thus attracting less actin association in the DRMs.

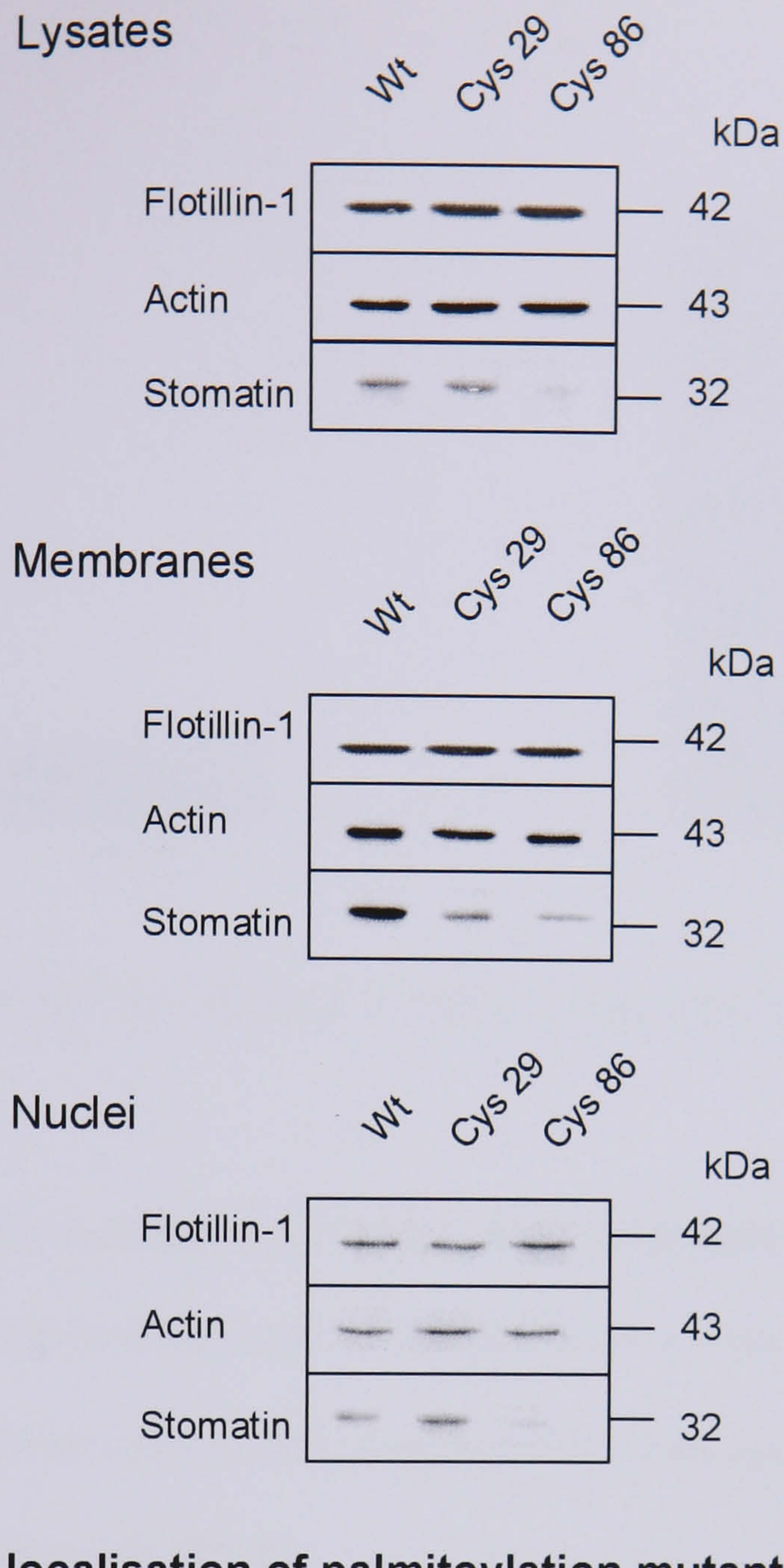

Figure 4.5 Cellular localisation of palmitoylation mutants

Lysates (section 2.3.1), membranes (section 2.3.2) and nuclei (section 2.3.3) were isolated from HEK cells transiently overexpressing Wt stomatin and the palmitoylation mutant's Cys 29 (Cys 29 Ser) and Cys 86 (Cys 86 Ser). Samples were subjected to SDS-PAGE (equal protein loading; lysates 20µg; membranes 10µg; nuclei 10µg) followed by subsequent immunoblot analysis using antibodies against flotillin-1, actin and stomatin. Blots are representative of two separate experiments. Molecular weights are shown to the right of each immunoblot (kDa).

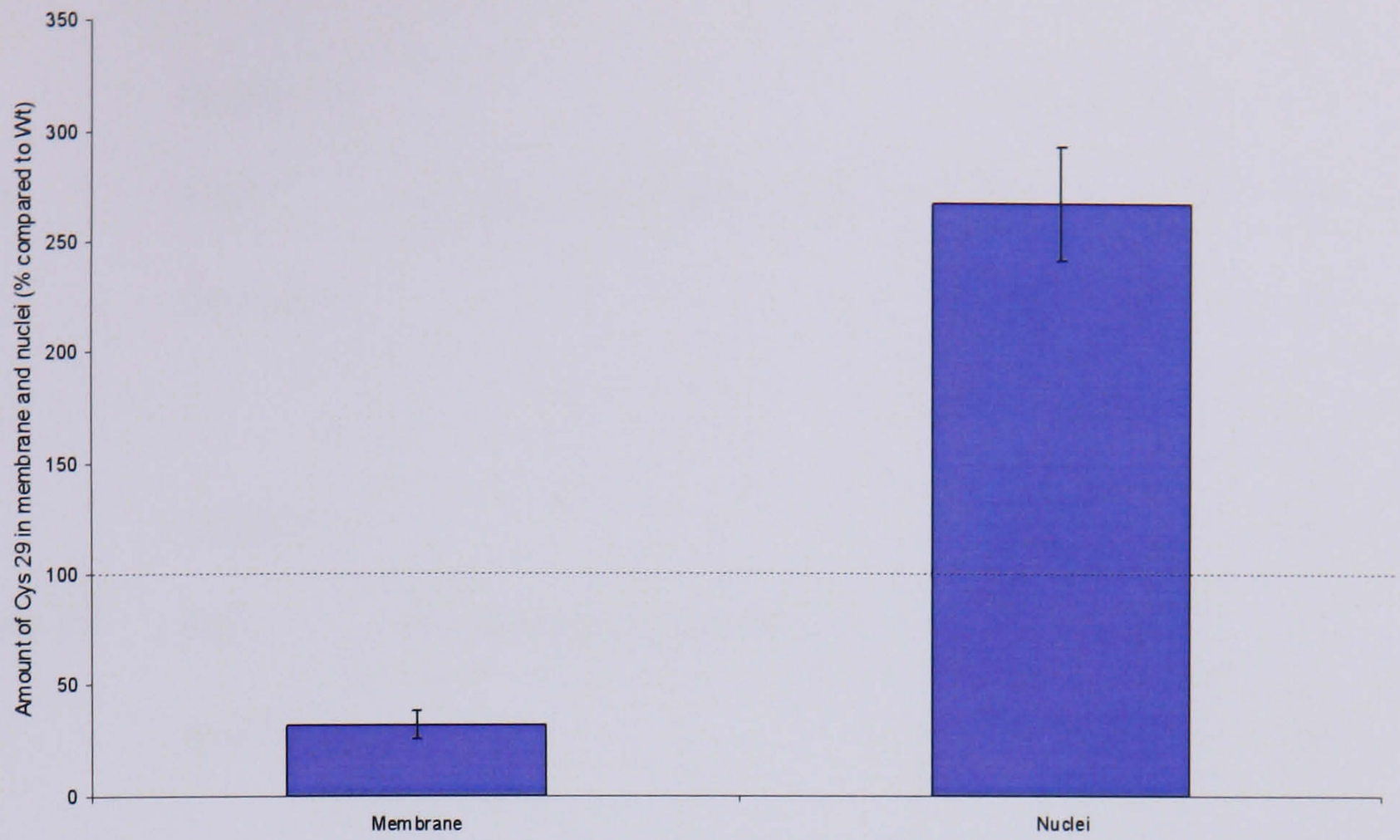

Figure 4.6 Amount of Cys 29 Ser in membrane and nuclei compared to Wt stomatin

Densitometric analysis (section 2.5.6) was used to compare the Cys 29 Ser and Wt stomatin content of membranes and nuclei (as seen in figure 4.5). The Wt sample was set to 100% and the Cys 29 Ser compared to. Results shown are the mean (± range) of two separate experiments.

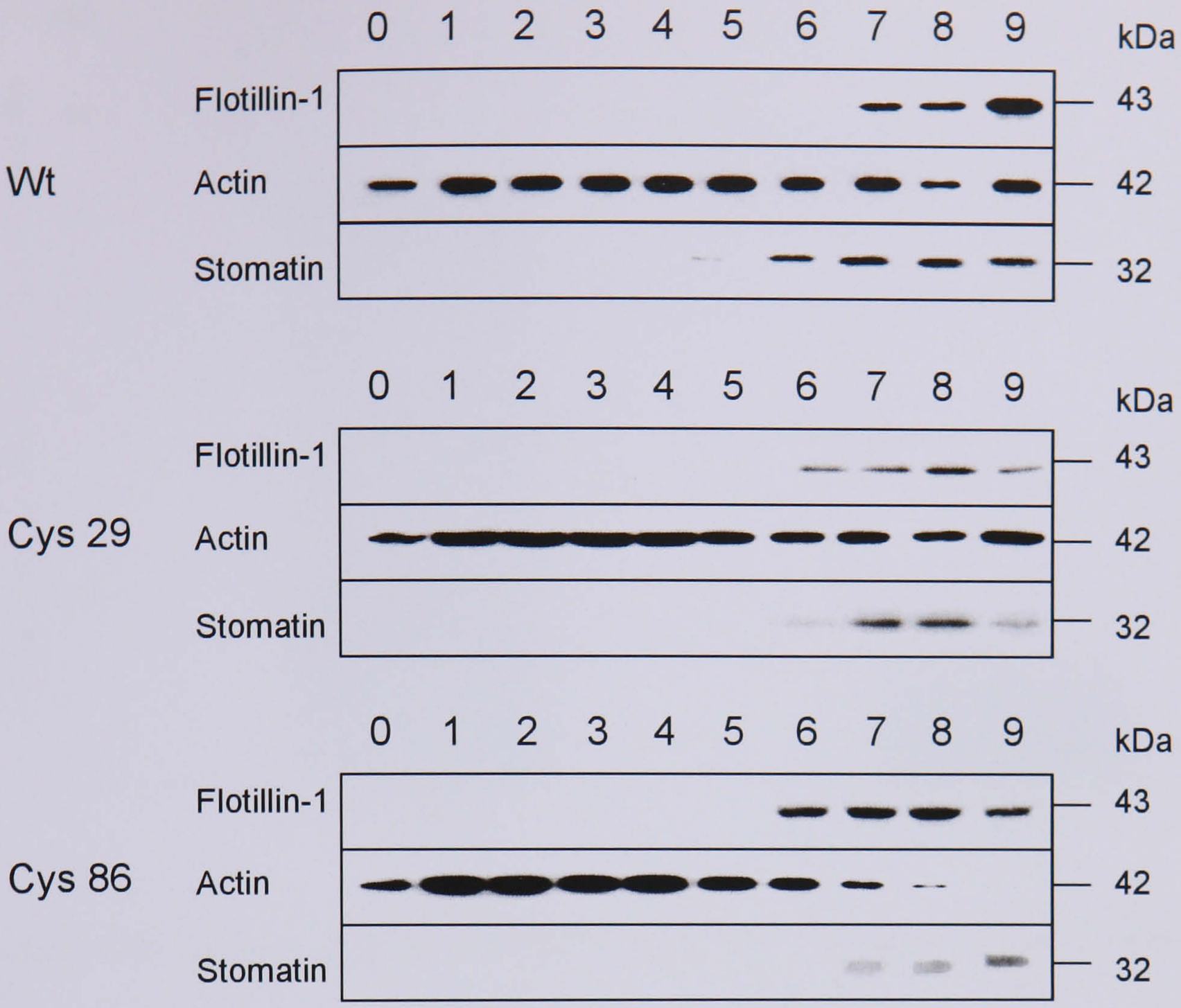

Figure 4.7 DRM analysis of the palmitoylation mutants

DRMs were isolated (section 2.3.5) from HEK cells transiently overexpressing Wt stomatin (Wt) and the palmitoylation mutant's Cys 29 Ser (Cys 29) and Cys 86 Ser (Cys 86). Samples were subjected to SDS-PAGE (equal volume of each fraction loaded) followed by subsequent immunoblot analysis using antibodies against flotillin-1, actin and stomatin. Blots are representative of two separate experiments.

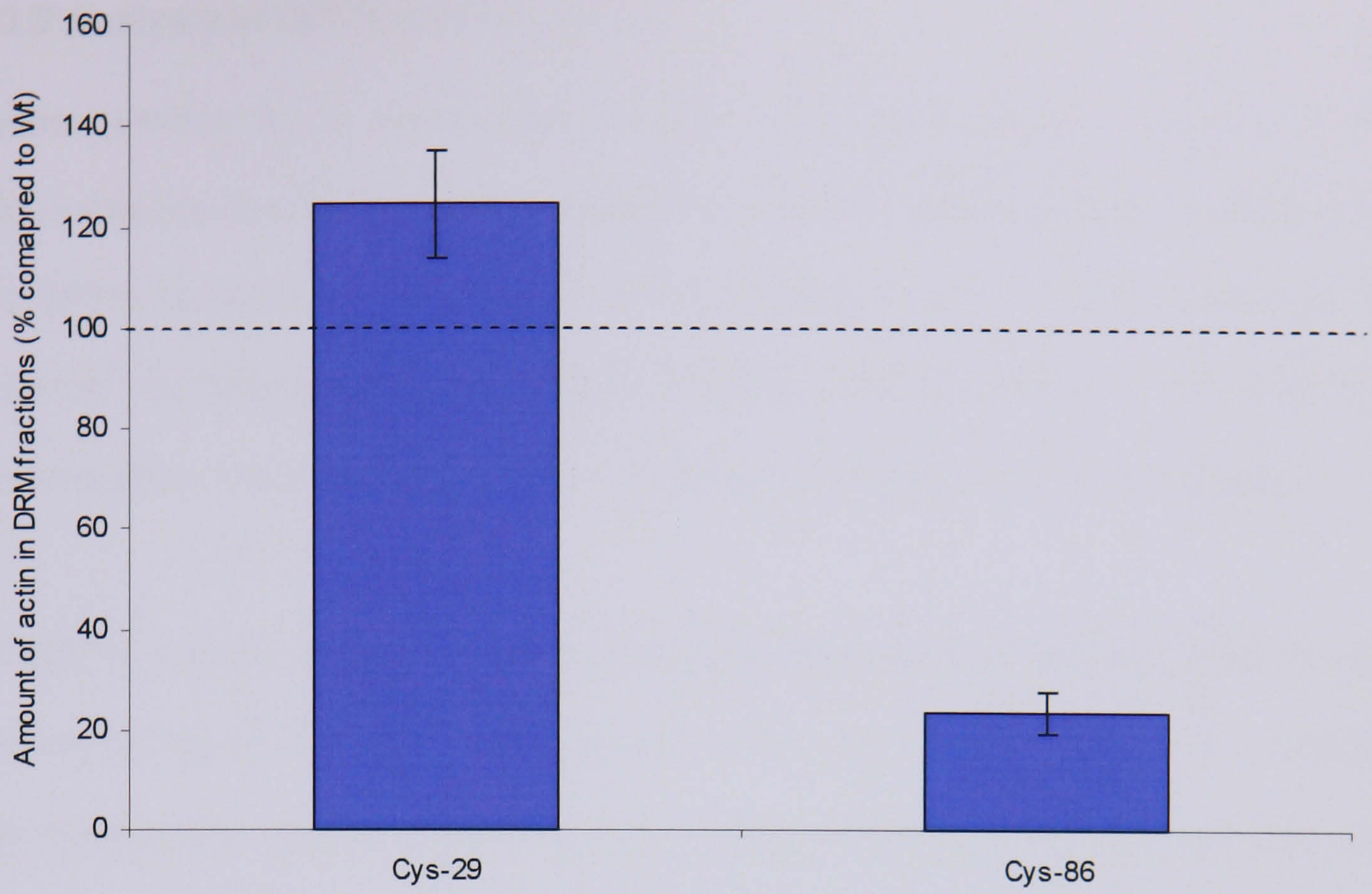

Figure 4.8 Amount of actin present in the DRM factions of Cys 29 Ser and Cys 86 Ser as compared to Wt stomatin

The DRM fractions 7-9 (as seen in figure 4.7) were analysed by densitometric analysis (section 2.5.6) for actin content. Wt stomatin was set to 100% and Cys 29 Ser (Cys 29) and Cys 86 Ser (Cys 86) compared to. Results shown are the mean (± range) of two separate experiments.

4.2.2 Analysis of SPFH domain mutants

Lysate (section 2.3.1), membrane (section 2.3.2), DRM gradients (section 2.3.5) and nuclei (section 2.3.4) were isolated from HEK cells expressing Wt stomatin and the SPFH domain mutants. Samples were subjected to SDS-PAGE (section 2.5.2) followed by subsequent immunoblot analysis (section 2.5.3). As with the palmitoylation mutants; flotillin-1, actin and stomatin levels were all investigated.

All SPFH domain mutants were successfully expressed at various levels in the transiently transfected HEK cells, as seen in the cell lysates (figure 4.9). Notably the mutants Gly 155 Ala and Leu 255 Lys were expressed at higher levels than the Wt stomatin. Why theses two mutant forms showed increased levels of expression is unknown. One possibility is that they show decreased levels of cellular degradation, perhaps due to the disruption of protease cleavage site within stomatin.

All mutants successfully located to the membrane where they were present at levels reflecting that of their cellular expression as see in the lysates. As with the lysate samples, increased levels of Gly 155 Ala and Leu 255 Lys were detected in the membrane compared to level of Wt stomatin.

All mutants were present in the nucleus at roughly the same level. Gly 155 Ala and Leu 255 Lys were present in the nucleus at higher levels reflecting their higher overall expression in the cell.

All mutants successfully located to the DRM fractions of the gradients, 7-9 (figure 4.10). Less actin was found associated with the DRM fractions of the Arg 151 Lys

and Leu 255 Ile gradients. Why this is the case is unknown but suggests these residues may be involved in the association of stomatin with actin.

Whilst specific base changes in the *C.elegans* proteins MEC-2 and UNC-1 disrupted their function, the results from this study do not suggest the same is true for stomatin. The residues mutated in the SPFH domain of stomatin do not show a dominant role in membrane, DRM or nuclear localisation.

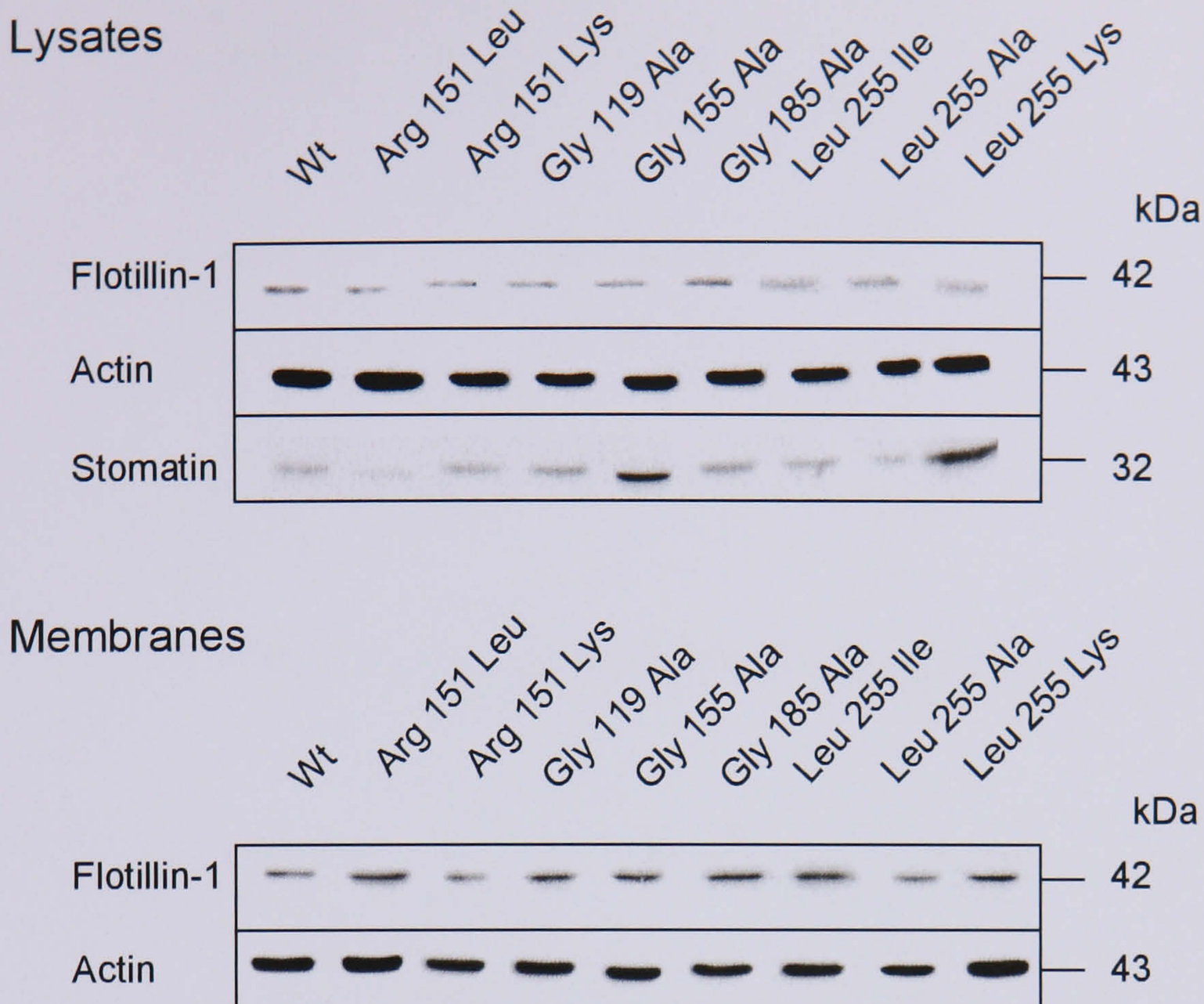

Figure 4.9 Cellular localisation of SPFH domain mutants

Lysates (section 2.3.1), membranes (section 2.3.2) and nuclei (2.3.3) were isolated from HEK cells transiently overexpressing Wt stomatin and the SPFH mutants. Samples were subjected to SDS-PAGE (equal protein loading; lysates 20µg; membranes 10µg; nuclei 10µg) followed by subsequent immunoblot analysis using antibodies against flotillin-1, actin and stomatin. Blots are representative of two separate experiments.

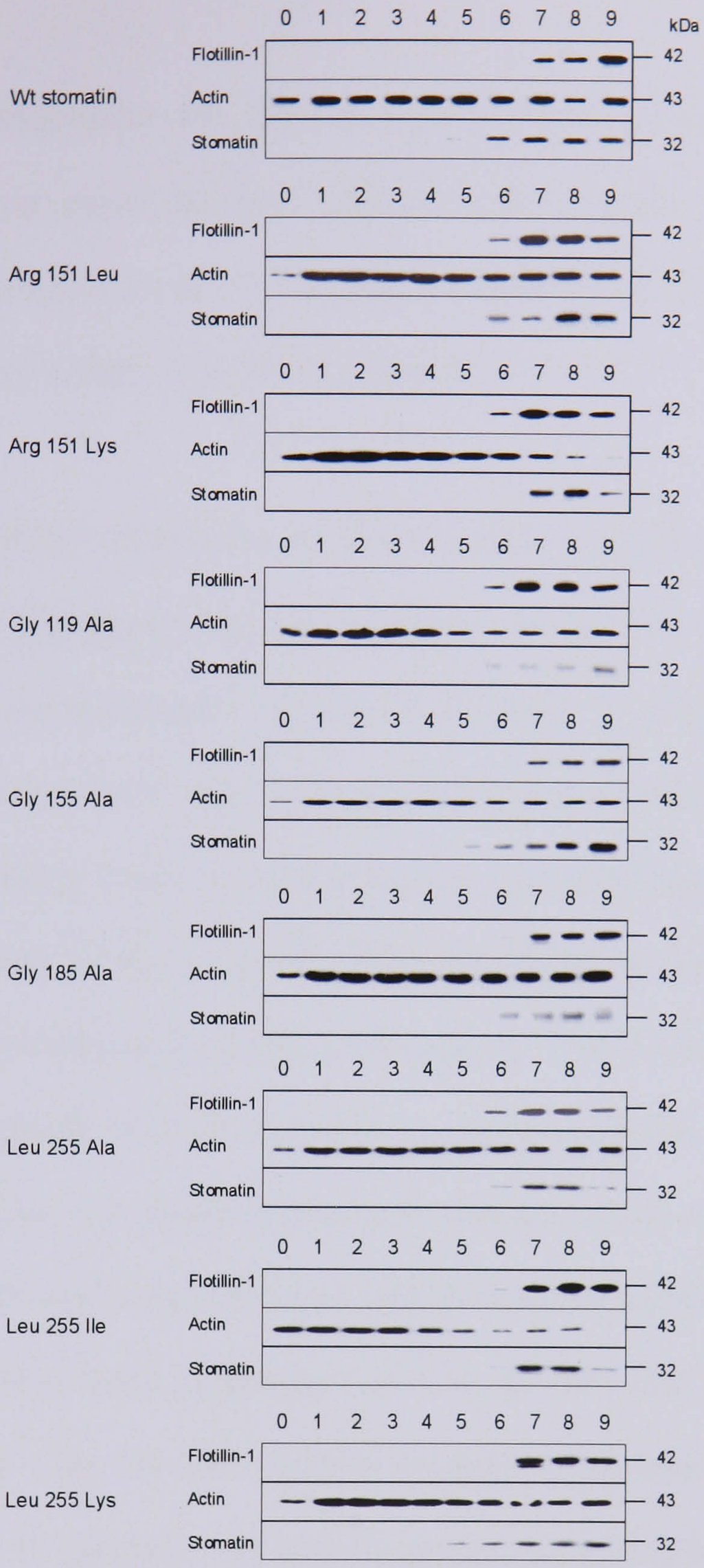

Figure 4.10 DRM analysis for SPFH domain mutants

DRMs were isolated (section 2.3.5) from HEK cells transiently overexpressing Wt stomatin and the SPFH mutants Arg 151 Leu, Arg 151 Lys, Gly 119 Ala, Gly 155 Ala, Gly 185 Ala, Leu 255 Ala, Leu 255 Ile, Leu 255 Lys. Samples were subjected to SDS-PAGE (equal volume of each fraction loaded) followed by subsequent immunoblot analysis using antibodies against flotillin-1, actin and stomatin. Blots are representative of two separate experiments.

4.3 Discussion

Site-directed mutagenesis was used to assess if the palmitoylation of stomatin or conserved residues within its SPFH domain influence the protein's affinity for the membrane or detergent-resistant membranes (DRMs). The ability of the mutants to gain access to the nucleus was also investigated.

Protein palmitoylation contributes to many cellular processes including membrane association and signalling (Neumann-Giesen *et al.* 2004; Zhang *et al.* 1998). Studies with the palmitoylation mutants of stomatin, Cys 29 Ser and Cys 86 Ser, suggest that palmitoylation may increase the protein's affinity for the membrane. For unknown reasons the Cys 86 Ser mutant was expressed at lower levels than either Wt stomatin or Cys 29 Ser but appeared to assume correct cellular localisation in the membrane, DRMs and nucleus. The Cys 29 Ser mutant lacks the major site of palmitoylation within stomatin, substituting the cysteine at position 29 for a serine reduced the levels of stomatin present in the membrane compared to the Wt protein. As this mutant showed similar levels of expression in the cell lysates to Wt stomatin, this result suggests that Cys 29 Ser has a lower affinity for the membrane. The Cys 29 Ser mutant showed increased levels in the nucleus compared to the Wt protein. As palmitoylation is reversible, in some instances it can control the distribution of a protein between the plasma membrane and the nucleus. Phospholipid scramblase 1, estrogen receptor α and a regulator in GPCR signal transduction all exist in the membrane when palmitoylated and in the nucleus when not (Wiedmer *et al.* 2003; Acconcia *et al.* 2005; Drenan *et al.* 2005). As Cys 29 Ser shows decreased presence within the membrane and increased presence within the nucleus, it may be that palmitoylation at residue 29 has a role in the cellular distribution of stomatin. Whilst palmitoylated the protein resides within the

membrane, upon depalmitoylation the protein is trafficked to the nucleus. Two proteins have been isolated from the lysates of erythrocytes, ECP-51 and ECP-54, that are predicted to chaperone stomatin (Salzer *et al.* 1999). They are both found in the cytosol and in the nucleus and so could potentially be involved in the shuttling of stomatin between the plasma membrane and the nucleus. It is as yet unclear what role stomatin may have in the nucleus (Fricke *et al.* 2005). There is increasing evidence to support the existence of a network of cytoskeletal proteins within the nucleus, the nucleoskeleton (Padmakumar *et al.* 2005). Stomatin in the plasma membrane is known to associate with the actin cytoskeleton (Snyers *et al.* 1997) (chapter 3). It has been suggested that stomatin may form an anchorage site in the plasma membrane with the actin cytoskeleton; a similar scenario may be envisaged in the nucleus. It could be that stomatin plays a role in the structural support of this organelle. As well as providing structural support in the nucleus it could be that stomatin has additional roles. The SPFH domain proteins, flotillin-1 and prohibitin, are also found in the nucleus. The presence of flotillin-1 in the nucleus is pronounced at the beginning of S-phase, it is as yet unknown what purpose this serves (Langhorst *et al.* 2005). Prohibitin is known to function in cell-cycle regulation through its interaction with the E2F family of proteins. Prohibitin inhibits E2F activity; this results in transcriptional regulation of genes which have E2F sites in their promoters, many of which are responsible for the progression of S phase (Wang *et al.* 2002). The stomatin-like protein-2 (hSLP-2) is known to be essential for cell growth and progression of the cell-cycle through S phase (Zhang *et al.* 2005). There is as yet no direct evidence that stomatin can exert an influence on the progression of the cell cycle but given stomatins presence in the nucleus, observations with hSLP-2 and similarity to prohibitin, it seems only a matter of time before its role here is investigated in more depth.

The second set of stomatin mutants investigated in this study were concerned with the SPFH domain of stomatin. The SPFH domain is found in a variety of proteins in eukaryotes and prokaryotes (Tavernarakis *et al.* 1999). As yet a clear role for this domain has not been defined. The emerging theme for the SPFH domain proteins seems to suggest that they are a set of scaffold proteins involved in membrane proteolysis (Langhorst *et al.* 2005). It was hoped that mutations introduced into this domain may have revealed more about this domain. The residues selected for investigation in the SPFH domain are known to disrupt the function of either MEC-2 or UNC-1, stomatin homologues in the nematode *C.elegans* (Huang *et al.* 1995; Rajaram *et al.* 1998).

All the mutants were successfully expressed at varying levels in HEK cells. Two mutants, Gly 155 Ala and Leu 255 Lys, were expressed at higher levels than the Wt protein. Why this should be the case is unknown. It may be that glycine 155 and leucine 255 are located within proteolysis sites of stomatin. If these sites were concerned with the degradation of stomatin, then disruption would hinder cellular clearance. This could prolong the life time of stomatin and account for the higher levels of expression for these two mutants seen in the lysates, membranes and nuclei.

As all the mutants were found in the membrane at levels reflecting their overall cellular expression, it suggests that the residues mutated are not essential for the localisation of stomatin to the membrane. Correct cellular localisation of the mutants into the nucleus was also seen, suggesting the investigated residues are not critical in the localisation of stomatin to the nucleus. All the mutants localised to the DRM fractions on their respective sucrose gradients. Less actin was found

associated with the DRM fractions isolated from HEK cells expressing Arg 151 Lys and Leu 255 Ile. Why less actin was found in the DRM fractions of these gradients is unknown but suggests arginine 151 and leucine 255 perhaps reside within domains responsible for the association of stomatin with the actin cytoskeleton.

The SPFH domain mutants of stomatin investigated in this study revealed no individual residue involved in the location of stomatin in the membrane, DRMs or nucleus. In a separate investigation, a series of truncation mutants of flotillin-1 isolated the domains responsible for membrane and DRM targeting, both of which are in the SPFH domain (Liu *et al.* 2005). In hindsight, this approach may have been more suitable in the identification of similar domains in stomatin.

Essentially all the mutants investigated in this study behaved similarly to Wt stomatin. Palmitoylation at cysteine 29 increased the protein's affinity for the membrane and may also provide the mechanism behind the shuttling of stomatin between the plasma membrane and the nucleus. There are indications in this study, as with chapter 3, that stomatin interacts with the actin cytoskeleton. The Cys 86 Ser mutant was poorly expressed; in the DRM fractions, where little of this protein resided, there was less actin association. Arginine 151 and leucine 255 may be involved in the association of stomatin with the actin cytoskeleton as mutations at these positions also reduced the level of actin associated with DRMs.

Chapter 5: Proteolytic cleavage of stomatin

5.1 Stomatin and its proteolysis

Stomatin is known to associate with lipid rafts, discrete microdomains involved in many cellular processes, including proteolysis. It is considered possible that as a direct result of their concentrated presence within rafts, the closer association of crucial proteins increases the likelihood of a proteolytic event (Vetrivel *et al.* 2005). Lipid rafts are also concentrated in cholesterol, another factor known to influence proteolysis (Wolfe *et al.* 2004). Recently a proteolytic cleavage site has been proposed within stomatin (Yokoyama *et al.* 2005). The prokaryotic homologue of stomatin PH1511 is cleaved by the serine protease PH1510 at this site. It is thought likely PH1151 and PH1510 share the same operon and their interaction forms the basis of an ion channel regulatory role. C-terminal sequence alignment with PH1151 reveals the corresponding protease cleavage site in stomatin (figure 5.1). The site is flanked by hydrophobic residues in both cases and is proposed to interact with the membrane. However, the adjacent proline residue in stomatin makes this an unlikely position for proteolysis. If cleavage were to occur at this position in stomatin, a cytosolic C-terminal fragment of 19 amino acids would be released from the parent protein (figure 5.2).

Stomatin is known to be cleaved by calpain, a predominantly cytosolic protease that has been reported to be raft-associated and is involved in a variety of calcium-regulated cellular processes (Mairhofer *et al.* 2002; Suzuki *et al.* 2004; Goll *et al.* 2003). The reason for calpain cleavage of stomatin is as yet unknown.

Stomatin contains an SPFH (Stomatins, Prohibitins, Flotillins and HflK/C) domain (Tavernarakis *et al.* 1999) that spans the entire C-terminal section of the protein. The function of this domain is unclear but has been implicated in membrane targeting and the degradation of membrane-associated proteins (Suzuki *et al.* 2003; Tavernarakis *et al.* 1999). More recently, the group of SPFH proteins have been suggested to function as raft-based scaffolds of multiprotein complexes (Langhorst *et al.* 2005). The prohibitins are found mainly in the mitochondria where they regulate membrane protein degradation by chaperoning the mAAA proteases (Tatsuta *et al.* 2005). The bacterial members, HflK and HflC, are known to function similarly. They chaperone the AAA protease FtsH, which regulates protein turnover in the membrane (Saikawa *et al.* 2004). The significant sequence similarity that the SPFH proteins share, suggests stomatin may too form part of membrane-associated proteolytic complex (Kaser *et al.* 2000).

Given that the prokaryotic homologues of stomatin exist in an operon with a serine protease, the proven cleavage of PH1151 by PH1510 and the association of the SPFH proteins with proteases, the possibility that stomatin is proteolytically processed was investigated.

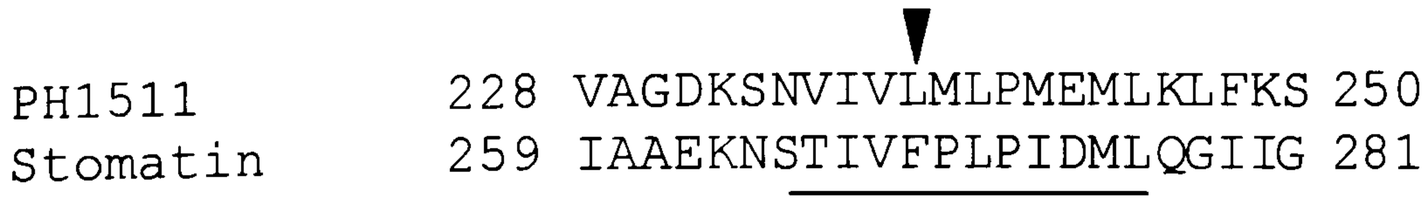

Figure 5.1 Sequence alignment of C-terminal regions of PH1151 and stomatin

The blue arrow indicates the cleavage site in the stomatin homologue PH1151. The underlined sequence highlights a stretch of hydrophobic residues which is proposed to interact with the membrane allowing interaction with the membrane-bound serine protease (Yokoyama *et al.* 2005). The residues highlighted in red are conserved between PH1151 and stomatin. Cleavage of PH1151 by PH1510 is thought to be involved in ion channel regulation.

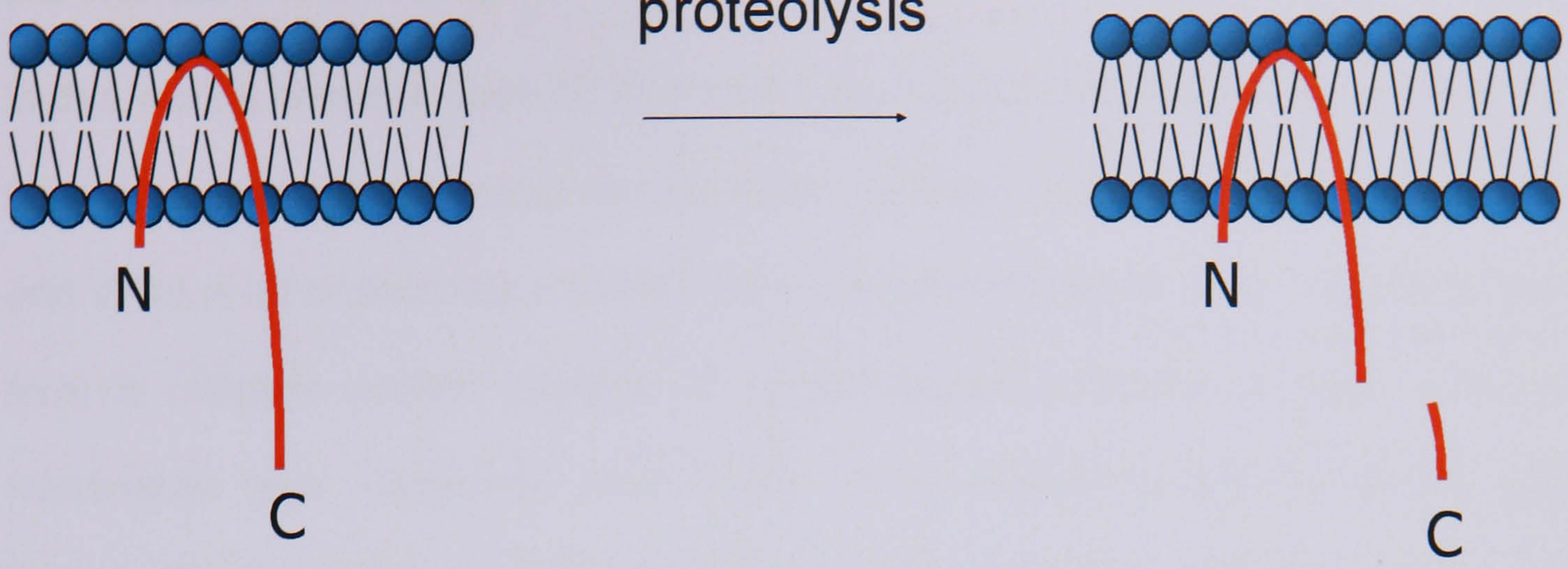

Figure 5.2 Schematic showing the proposed cytoplasmic proteolysis of stomatin

The proteolytic processing of stomatin in the membrane may result in the release of a cytoplasmic C-terminal fragment. A serine protease site has been proposed for stomatin.

5.2 The Gal4-VP16 assay

In this work a chimeric Gal4-VP16 protein was fused to the C-terminus of stomatin. Gal4 is a yeast DNA-binding domain which contains a nuclear localisation signal and VP16 is a transactivation domain from the herpes simplex virus. Together, they form a chimeric protein capable of transcriptional activation at high levels in mammalian cells (Sadowski *et al.* 1988). If the chimeric protein is able to gain access to the nucleus, Gal4-VP16-dependent luciferase expression from the experimental reporter will be observed. The experimental reporter contains multiple Gal4-binding motifs upstream of a firefly luciferase gene. The Gal4-VP16 assay has previously been used to demonstrate the intracellular processing of the amyloid precursor protein (APP), the low density lipoprotein receptor and notch (Karlstrom *et al.* 2002; May *et al.* 2002; Struhl *et al.* 1998).

The proteins to be used in this assay are wild type (Wt) stomatin and a mutant form which lacks the N-terminal and transmembrane regions (ΔTMN) (residues 59-289). The soluble ΔTMN stomatin should be unimpeded (except for cellular degradation) in gaining access to the nucleus and thus show an uninhibited luciferase expression from the experimental reporter. If a C-terminal fragment of Wt stomatin is to gain access to the nucleus, some proteolytic processing in order to release the Gal4-VP16 from the membrane would be required.

The pMstGV vector encoding the Gal4-VP16 protein was kindly gifted by X. Cao and T. Sudhof, University of Texas Southwestern Medical Centre, Dallas. The vector was generated from the pM vector (Clontech, Nottingham, UK) by mutagenesis of the termination codon in the Gal4 BD (Sadowski *et al.* 1992) and insertion of VP16 into the *Eco*R I/*Bam*H I (figure 5.3). The protein of interest, in this

case Wt or ΔTMN stomatin, can be cloned into the *Bgl* II or the *Nhe* I site of pMstGV. Consequently, the protein of interest will be expressed with Gal4-VP16 attached to the C-terminus. The pMstGV vector containing APP (pMstAPP-GV) was kindly gifted by X. Cao and T. Sudhof, University of Texas, Southwestern Medical Centre, Dallas. APP had been cloned into the *Nhe* I site of the pMstGV vector (Cao *et al.* 2001). This test construct will be used as a positive control.

The pRL-TK vector (Promega, Southampton, UK) which encodes *Renilla* luciferase was used as a control reporter in order to standardise transfection efficiency (figure 5.4). The herpes simplex virus thymidine kinase promoter provides low-level, constitutive expression of *Renilla* luciferase in transfected mammalian cells. This is distinguishable from the firefly luciferase encoded by the experimental reporter (Sherf *et al.* 1996). Both the Firefly and *Renilla* luciferase readings were taken using the Dual-Luciferase® Reporter Assay System Kit (Promega).

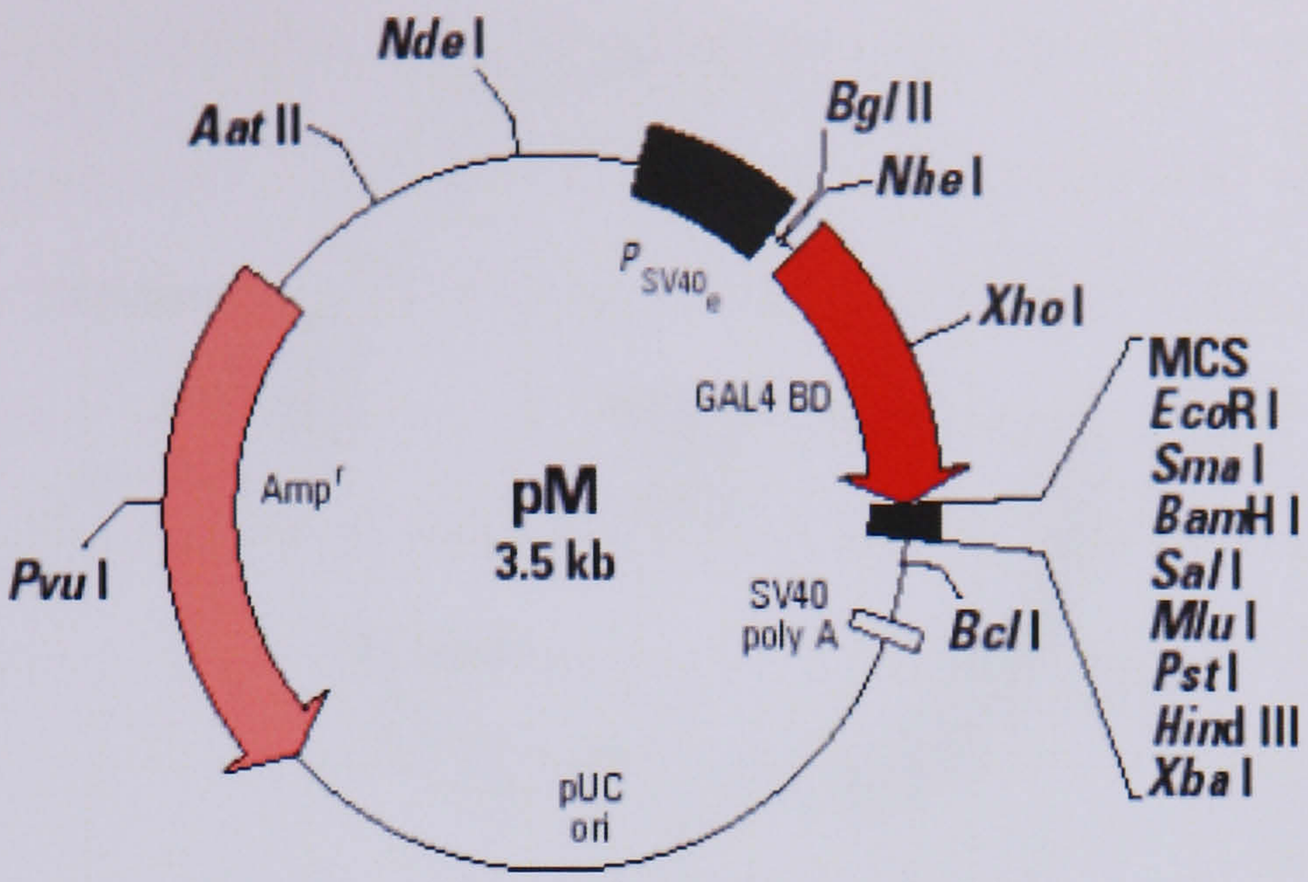

Figure 5.3 Vector map of the pM vector (Clontech)

The vector was used by X. Cao and T. Sudhof, University of Texas, Southwestern Medical Centre, Dallas to generate pMstGV. The termination codon in the Gal4 binding domain was removed by site directed mutagenesis and the transactivation domain VP16 inserted into the *Eco*R I/*Bam*H I site. The protein of interest can be cloned into either the *Bgl* II or the *Nhe* I site.

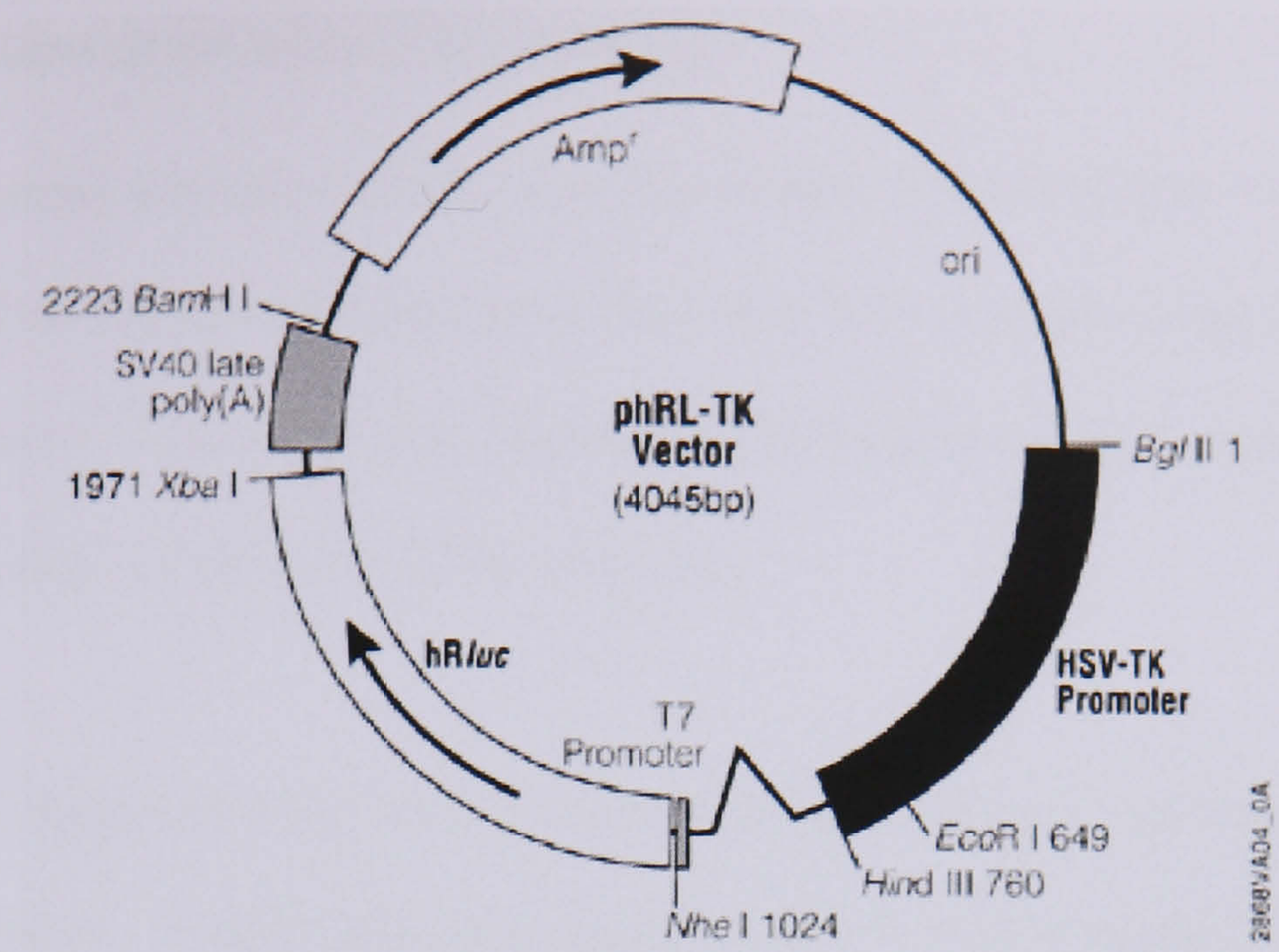

Figure 5.4 Vector map of pRL-TK (Promega)

The low level of constitutive *Renilla* luciferase expression from pRL-TK was used as an internal transfection efficiency control. *Renilla* luciferase is distinguishable from the firefly luciferase encoded by the experimental reporter.

5.2.1 Generation of Wt and ΔTMN stomatin

Full length human stomatin cDNA was purchased from OriGene Technologies Inc. (MD, USA). The clone was supplied as plasmid DNA and retrieved as suggested by the manufacturer. The DNA was sequenced and subsequently used as a template in the amplification of Wt and ΔTMN stomatin.

Primers were designed such that the products could be cloned into pMstGV in the correct orientation. A *Bgl* II site was placed at the 5' end of each cDNA and a *Nhe* I site at the 3' end. The termination codon in each case was omitted from the final sequence in order that the chimeric Gal4-VP16 protein would form the C-terminal end of each protein upon expression. Wt stomatin retained all other original features (figure 5.5). The 5' end primer of ΔTMN stomatin was designed to attach immediately downstream of the transmembrane region. The primer included a start codon as the original would be omitted along with the entire N-terminal and membrane domain (figure 5.6).

Wt and ΔTMN stomatin were generated by PCR using the Accutaq LA DNA Polymerase mix (Sigma-Aldrich Ltd., Poole, UK) which was selected for use due to the proofreading system attached to the enzyme. The enzyme and reagents supplied were used as suggested by the manufacturer. Strand synthesis reactions using 200ng of dsDNA template (full length stomatin cDNA purchased from OriGene Technologies Inc) and the desired primers were subject to the cycling parameters detailed in figure 5.7. Both reactions were successful as seen by agarose gel electrophoresis (section 2.6.7) (figure 5.8).

Forward primer (Wt *Bgl* II)

Bgl II

5'- GGAAGATCTTCCATGGCCGAGAAGCGCGACACA – 3'

Reverse primer (C-ter *Nhe* I)

Nhe I

5'- CTAGCTAGCTAGGCCTAGATGGCTGTGTTTTGC – 3'

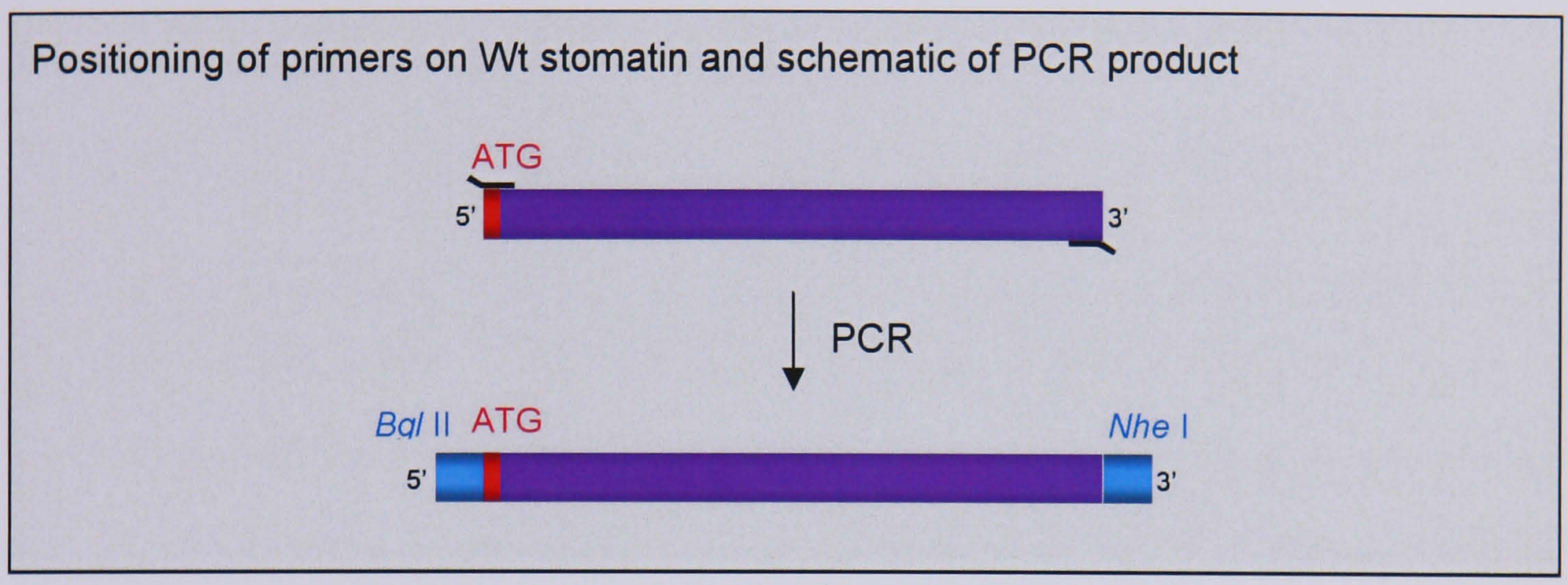

Figure 5.5 Primers used to amplify Wt stomatin

The Wt construct had a *Bgl* II site introduced preceding the native start codon and a *Nhe* I site following the final codon, the termination codon was omitted.

Forward primer (ΔTMN *Bgl* II)

Bgl II

5'- GGAAGATCTTCCATGGAGTATGAAAGAGCCATCATC – 3'

Reverse primer (C-ter *Nhe* I)

Nhe I

5'- CTAGCTAGCTAGGCCTAGATGGCTGTGTTTTGC – 3'

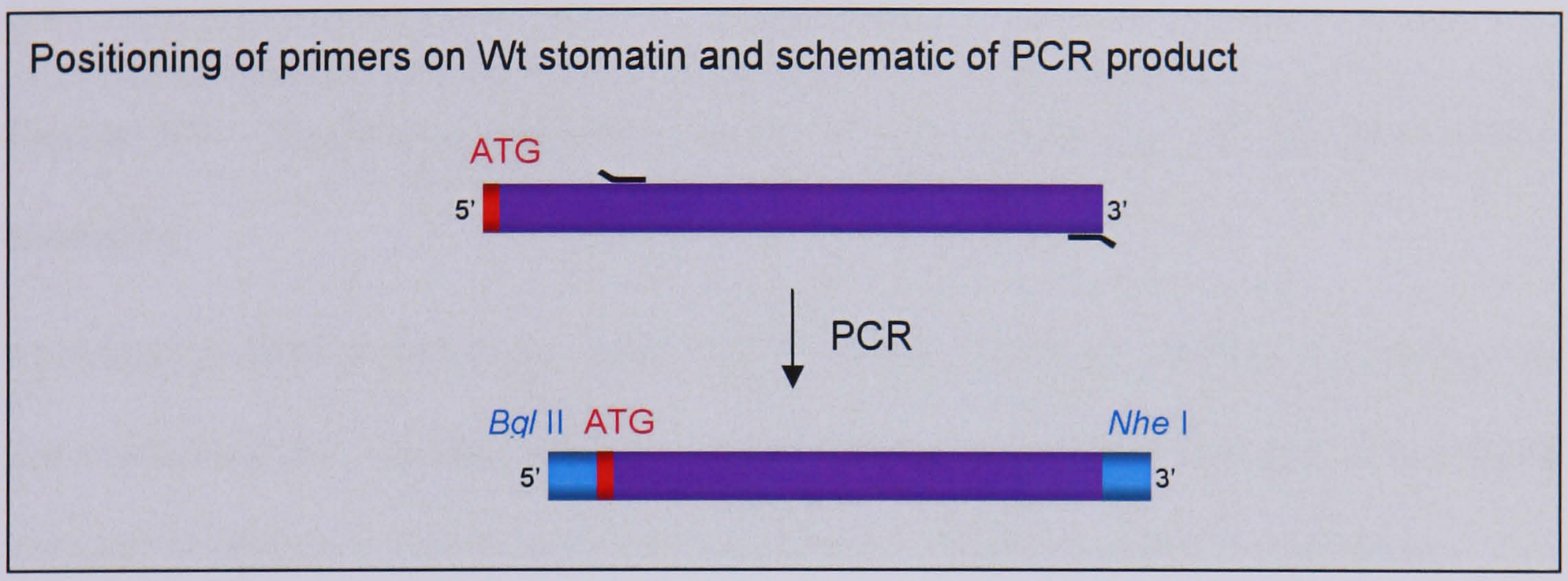

Figure 5.6 Primers used to amplify ΔTMN stomatin

The ΔTMN construct (residues 59-289) had a *Bgl* II site introduced following the sequence encoding the transmembrane domain and a *Nhe* I site following the final codon, the termination codon was omitted. A start codon was introduced immediately following the *Bgl* II site.

Segment	Cycles	Temperature	Time
1	1	98°C	30 sec
2	16	94°C	15 sec
		68°C	20 sec
		68°C	2 min
3	1	68°C	10 min

Figure 5.7 Cycling parameters used in the generation of Wt and ΔTMN stomatin

Accutaq LA DNA Polymerase mix (Sigma-Aldrich Ltd.) was used as suggested by the manufacturer. Human stomatin cDNA (200ng) was amplified using the primers detailed in figures 5.5 and 5.6 to produce Wt and ΔTMN stomatin respectively.

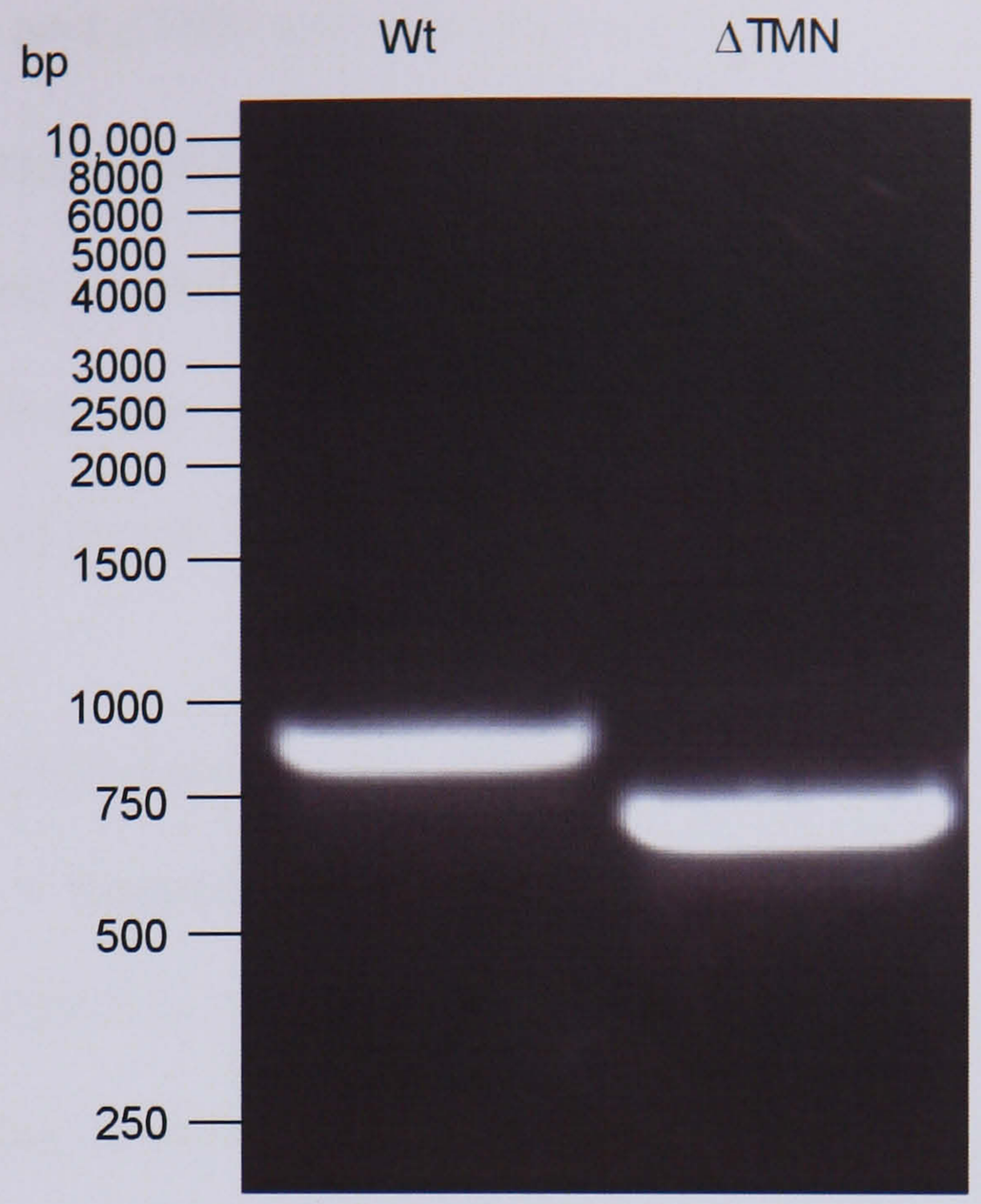

Figure 5.8 PCR products of Wt and ΔTMN stomatin

Human stomatin cDNA was amplified using the relevant primers to produce Wt and ΔTMN stomatin. Loading buffer containing ethidium bromide was added to the samples and subjected to electrophoresis on an agarose gel (section 2.6.7). The gel was imaged under ultraviolet light. Markers are shown to the left of the image (base pairs).

5.2.2 Cloning of Wt and ΔTMN stomatin into pMstGV

Fusion of Wt and ΔTMN stomatin to the chimeric Gal4-VP16 protein was achieved by cloning the proteins into the pMstGV vector. Cloning into this vector, upstream of Gal4VP16, would form the fusion proteins Wt-Gal4VP16 (Wt-GV) and ΔTMN-Gal4VP16 (ΔTMN-GV) (figure 5.9).

Direct cloning of the PCR products into pMstGV following restriction digest failed on several occasions. Instead the PCR products were cloned directly into pcDNA3.1/V5-His©TOPO®TA (TOPO). The vector was supplied as a component of the pcDNA3.1/V5-His©TOPO®TA Expression Kit (Invitrogen Ltd., Paisley, UK). The kit was used as suggested by the manufacturer (section 2.6.8). The single deoxyadenosine added to the 3' end of the PCR product by Accutaq LA DNA Polymerase, is easily ligated into the linearised TOPO vector due to the overhanging 3' deoxythymidine residues (figure 5.10).

The TOPO vector containing Wt or ΔTMN stomatin and pMstGV were digested using the restriction enzymes *Bgl* II and *Nhe* I. In each case, 10 μg of DNA were incubated with both restriction enzymes at 37°C for 1 hr (section 2.6.4). The digested samples were electrophoresed on agarose gels (section 2.6.7) and the relevant bands excised. The DNA was isolated from the gel sections using a Qiagen gel isolation kit (section 2.6.3). Wt and ΔTMN stomatin were ligated into the linearised pMstGV vector overnight at 14°C (section 2.6.5). The ligation reactions were transformed into XL1-Blue competent cells (section 2.6.6) and following incubation in LB media (section 2.6.1) for 1 hr at 37°C, the cells were plated on

selective media containing ampicillin (section 2.6.2). Colonies were selected, the plasmid DNA isolated and sequenced (section 2.6.3).

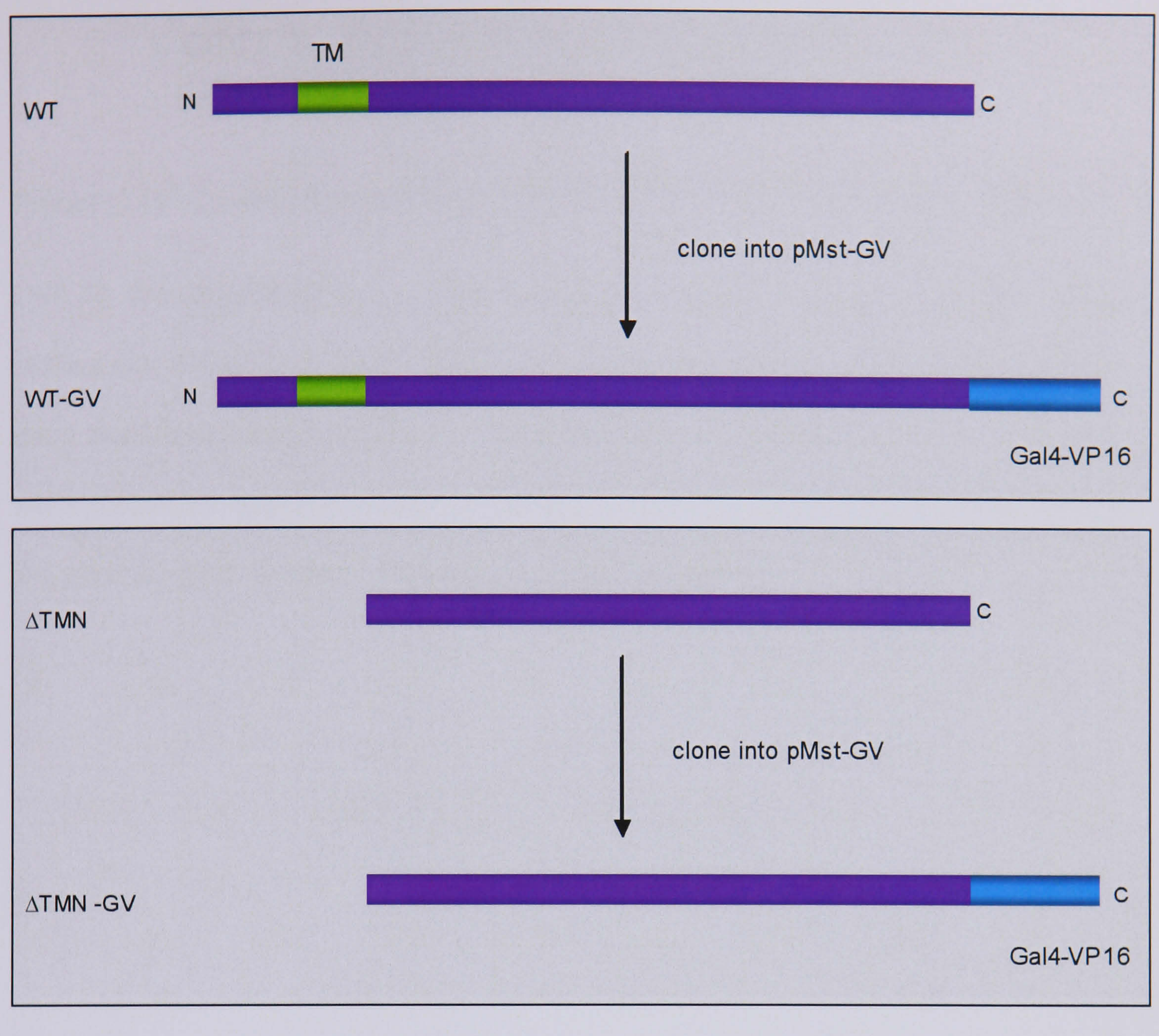

Figure 5.9 Fusion of Wt and ΔTMN to the chimeric Gal4-VP16 protein

Wt and ΔTMN stomatin were cloned into pMstGV in frame with the chimeric protein Gal4-VP16. The resultant fusion proteins were Wt-GV and ΔTMN-GV.

Figure 5.10 Cloning into pcDNA3.1/V5-His©TOPO®TA (TOPO) (Invitrogen Ltd)

Due to the overhanging 3' deoxythymidine residues, PCR products are easily cloned into pcDNA3.1/V5-His©TOPO®TA. Following overnight ligation, the reactions were then transformed into the TOP10 competent cells supplied in the kit. The cells were plated on selective media containing ampicillin. Colonies were selected and the plasmid DNA isolated. Plasmid DNA was sequenced.

5.2.3 Transient expression of the Gal4-VP16 fusion proteins

Madin-Darby canine kidney (MDCK) cells were selected for use in this study due to endogenous expression of stomatin (section 3.2). They are therefore more likely to contain the relevant cellular machinery required for the proteolytic processing of stomatin.

In all cases the MDCK cells were cultured to 50% confluency and then transiently transfected with the relevant vectors. In some instances the cells were treated with various compounds; all were dissolved in DMSO and used as suggested by the manufacturer (figure 5.11). Cell lysates were made and then assayed for luciferase activity. The format is detailed below.

Day one - a suspension of MDCK cells was counted and plated in 6-well plates (35mm x 18mm; Fisher) at a density of 2.5 x 10^5 cells per well. This density was selected as it would provide cells at 50% confluency the following day. The cells were cultured using standard cell culture techniques (section 2.2.1).

Day two - DNA was transiently transfected using Lipofectamine reagent (section 2.2.2). The cells were simultaneously transfected with three vectors, the test construct (1μg of DNA), the experimental reporter (1.5μg) and the control reporter (0.15μg). The test construct was either pMstGV, pMstWt-GV, pMstΔTMN-GV, pMstAPP-GV (positive control) or Wt (TOPO) (Wt stomatin without Gal4-VP16 in pcDNA3.1/V5-His©TOPO®TA).

Day three - medium was changed and if desired the cells were treated with and without various compounds (detailed below). Where relevant, DMSO levels were maintained at a minimum and kept at an equal concentration in all wells. All solutions were made up immediately prior to use.

Day four - cells were harvested using the passive lysis buffer supplied in the Dual-Luciferase® Reporter Assay System Kit (Promega). The lysates were assayed for both firefly and *Renilla* luciferase expression (section 2.6.9).

All assays were done in triplicate and repeated on at least two separate occasions. Experimental reporter gene activity was calculated taking into consideration transfection efficiency.

Compound	Concentration	Action
1, 10-Phenanthroline	5mM	Metallo-protease inhibitor
3,4-dichloroisocoumarin	100μM	Serine protease inhibitor
Calpastatin (Calbiochem®)	10μM	Calpain I and calpain II inhibitor
Calphostin C (Calbiochem®)	1μM	Protein kinase C inhibitor
Lactacystin	10μM	Proteasome inhibitor
Pepstatin A	1μM	Aspartyl protease inhibitor
Phenylmethylsulphonyl Fluoride	1μM	Serine protease inhibitor
Phorbol 12-myristate 13-acetate	100nM	Protein kinase C activator
Trans-Epoxysuccinyl-L-Leucylamido-(4-Guanidino) Butane	10μM	Cysteine protease inhibitor

Figure 5.1 The various compounds used in the Gal4-VP16 assay

All compounds were purchased from Sigma-Aldrich Ltd. (Poole, UK) unless otherwise stated.

5.3 Stomatin is cleaved to release a cytosolic C-terminal fragment

To assess if Wt stomatin is proteolytically processed releasing a cytoplasmic C-terminal fragment, the test constructs pMstGV, pMstWt-GV, pMstΔTMN-GV, pMstAPP-GV and Wt (TOPO) were transiently transfected into MDCK cells (section 5.2.3). Cell lysates were assayed for luciferase activity.

All samples showed reporter gene activity, with the exception of Wt (TOPO) (figure 5.12). This form of Wt stomatin does not contain the Gal4-VP16 chimeric protein and thus should not produce reporter gene activity. This test was set up to ensure that there was no expression from the experimental reporter when unstimulated. This also proves the *Renilla* luciferase expressed from the control reporter does not produce false positives. Normal levels of *Renilla* luciferase activity were recorded for this sample (data not shown). It can therefore be assumed that the experimental reporter is not expressed without the interaction of Gal4-VP16 and that the firefly and *Renilla* luciferase readings are distinct. Upon transfection of pMstGV, the soluble Gal4-VP16 protein was expressed. Gal4-VP16 has no membrane anchorage system and owing to its nuclear localisation signal (NLS), should be directly targeted to the nucleus. This vector caused the greatest reporter gene expression. Allowing for possible degradation of Gal4-VP16, this reading represents unimpeded access to the nucleus and thus a constitutive expression of the reporter gene. APP-GV was used as the positive control in this investigation. The same assay has been used to show this protein undergoes proteolytic processing by γ-secretase activity, resulting in the release of a cytoplasmic fragment (Karlstrom *et al.* 2002). As previously found, APP-GV caused reporter gene activity. Like Gal4-VP16, ΔTMN-GV is a soluble protein; one may expect them to behave

similarly under these assay conditions. The ΔTMN-GV sample recorded only 10% of the reporter gene activity in comparison. One possible explanation for this observation could be the degradation of ΔTMN-GV to maintain correct cellular balance of stomatin. It is also possible that ΔTMN-GV may still contain a membrane localisation signal; this would cause it to be trafficked differently to Gal4-VP16. Finally, ΔTMN-GV although soluble may have to be processed before access to the nucleus is possible. The Wt-GV sample recorded reporter gene activity. The inclusion of the transmembrane region to anchor the protein to the membrane reduced the reporter gene activity to 70% compared to its soluble counterpart ΔTMN-GV. Wt-GV would require some proteolytic event in order that the Gal4-VP16 protein attached to the C-terminus of stomatin is released from the membrane and is able to traffic to the nucleus.

These results suggest that a C-terminal fragment of stomatin is released from the membrane. Further investigation into the nature of this release is necessary to assess if the process can be regulated and the protease which may be involved.

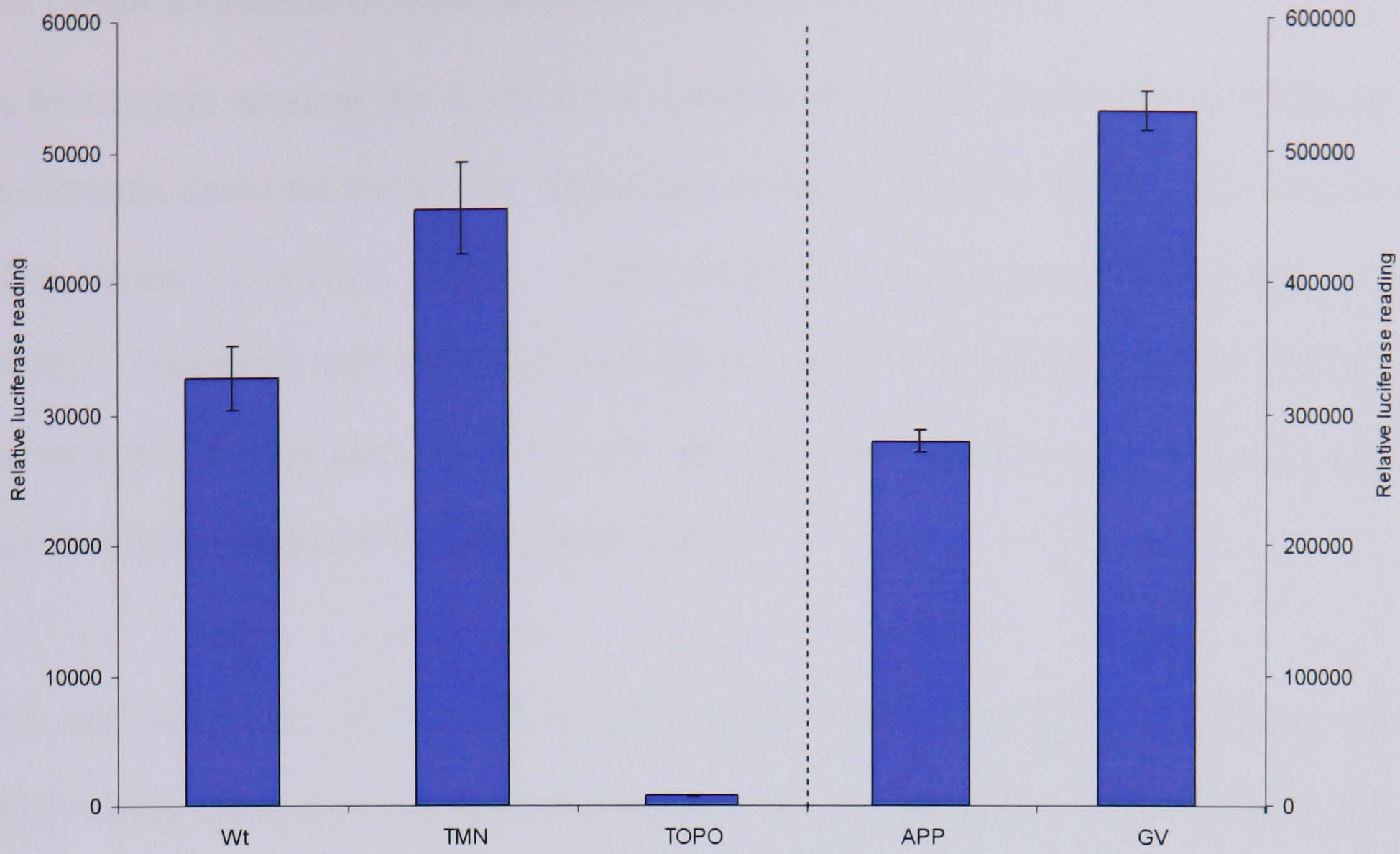

Figure 5.12 Luciferase activity in cells expressing the Gal4-VP16 fusion proteins

MDCK cells were transfected with 1μg of the indicated test construct, 1.5μg of the experimental reporter and 0.15μg of the control reporter. After 48 hours the cells were lysed and readings for both firefly and *Renilla* luciferase recorded. Wt (pMstWt-GV); TMN (pMstΔTMN-GV); TOPO (Wt stomatin without the Gal4-VP16 protein attached); APP (pMstAPP-GV); GV (pMstGV). Results are the mean (±SEM) of three separate experiments. Relative luciferase reading (firefly luciferase expression from experimental reporter).

5.3.1 PMA treatment of cells expressing Wt-GV and APP-GV

To investigate whether the event leading to the release of the C-terminal fragment of stomatin could be modulated, cells were treated with the phorbol ester, phorbol 12-myristate 13-acetate (PMA). PMA functions by activating protein kinase C (PKC). Treatment with PMA and has been used previously in a similar study to demonstrate the processing of the low density lipoprotein receptor-related protein (LRP) is modulated by PKC (May *et al.* 2002).

The test constructs pMstWt-GV or pMstAPP-GV were transiently transfected into MDCK cells along with the experimental and control reporters. Cells were treated with or without 100nM PMA 24 hours post-transfection (section 5.2.3). Cell lysates were assayed for luciferase activity.

Treatment with PMA had little effect on luciferase levels in cells expressing APP-GV (figure 5.13). This agrees with a previous study (May *et al.* 2002). Cells expressing Wt-GV showed a 6-fold increase in reporter gene activity upon treatment with PMA compared to those left untreated. This may be as a result of increased processing to stomatin and indicates the involvement of PKC in this process. Enhanced processing of stomatin would increase the availability of the C-terminal fragment to the experimental reporter and cause the higher levels of reporter gene activity.

To further investigate the possibility of the involvement of PKC in the processing of stomatin, treatment with the PKC inhibitor calphostin C was tested. If PKC does enhance the processing to stomatin, the inhibitor should decrease the reporter gene activity. The test construct pMstWt-GV was transiently transfected into MDCK cells along with the experimental and control reporters. Cells were treated with or without

100nM PMA and 1μM calphostin C 24 hours post-transfection (section 5.2.3). Cell lysates were assayed for luciferase activity.

Cells treated with PMA and calphostin C showed a 40% reduction in reporter gene activity compared to those cells treated with PMA alone (figure 5.14). This indicates the inhibition of PKC reduces the processing of stomatin. Treatment with calphostin C alone stimulated reporter gene activity compared to those cells that received no treatment. This should not be the case. Analysis of *Renilla* luciferase expression from the control reporter showed that calphostin C has an inhibitory affect on its expression from the pRL-TK vector. The reason for this is unknown. The expression of *Renilla* luciferase is under the control of thymidine kinase in the pRL-TK vector, it may be that calphostin C has an inhibitory effect on this kinase as well as PKC. Taking this into account, the *Renilla* luciferase readings for samples containing calphostin C were excluded and an average reading from the remaining values calculated. This set of data showed that the processing of stomatin is not stimulated following calphostin C treatment alone. It also showed a much greater reduction in reporter gene activity following the combined treatment compared to those cells treated with PMA alone.

These results suggest that the cytosolic processing of stomatin can be modulated by PKC.

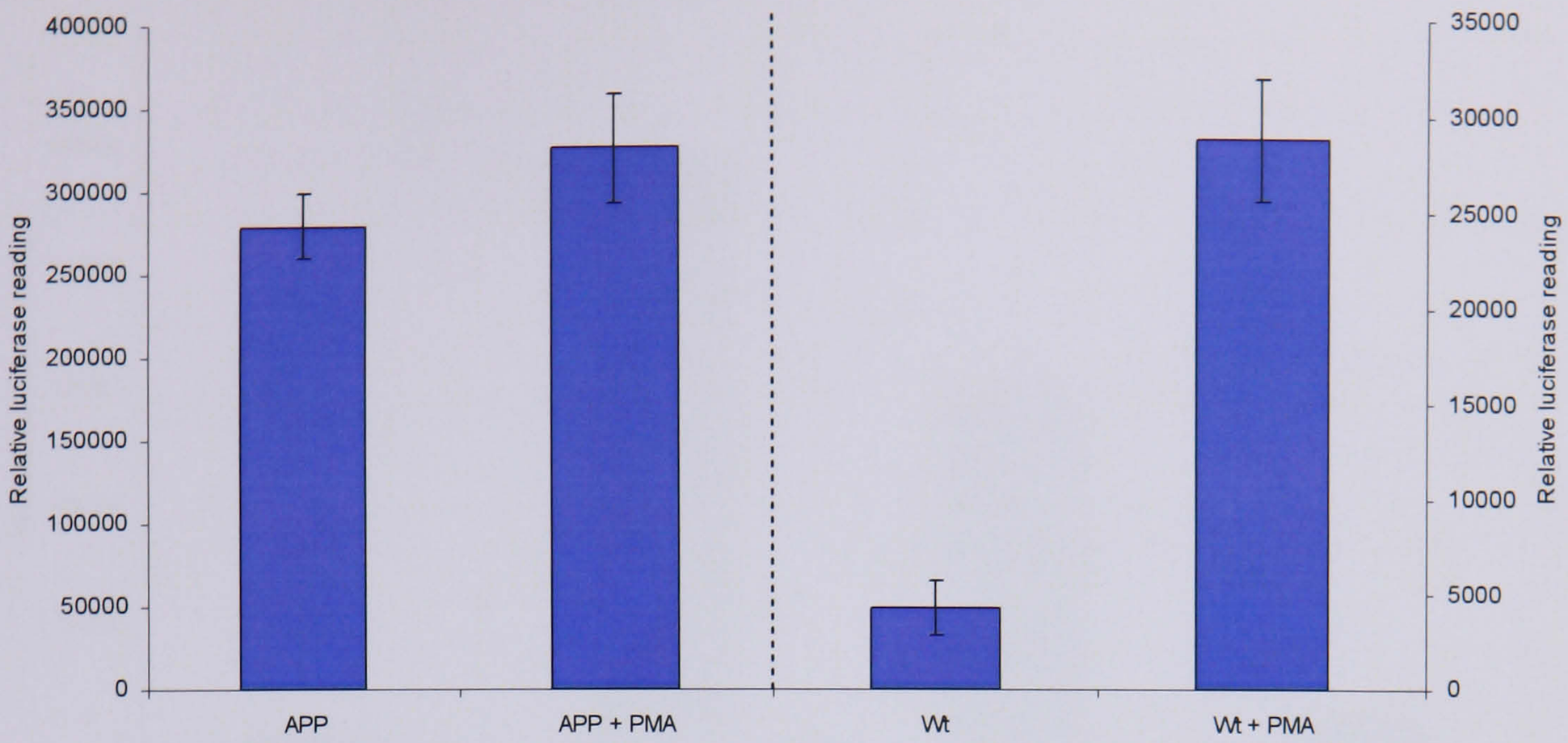

Figure 5.13 PMA enhances reporter gene activity

MDCK cells were transfected with 1μg of either pMstAPP-GV or pMstWt-GV, 1.5μg of the experimental reporter and 0.15μg of the control reporter. After 24 hours cells were treated with or without 100nM PMA. After a further 24 hours, the cells were lysed and readings for both *Renilla* and firefly luciferase recorded. APP (pMstAPP-GV without PMA); APP + PMA (pMstAPP-GV with 100nM PMA); Wt (pMstWt-GV without PMA); Wt + PMA (pMstWt-GV with 100nM PMA). Results are the mean (±SEM) of three separate experiments. Relative luciferase reading (firefly luciferase expression from experimental reporter).

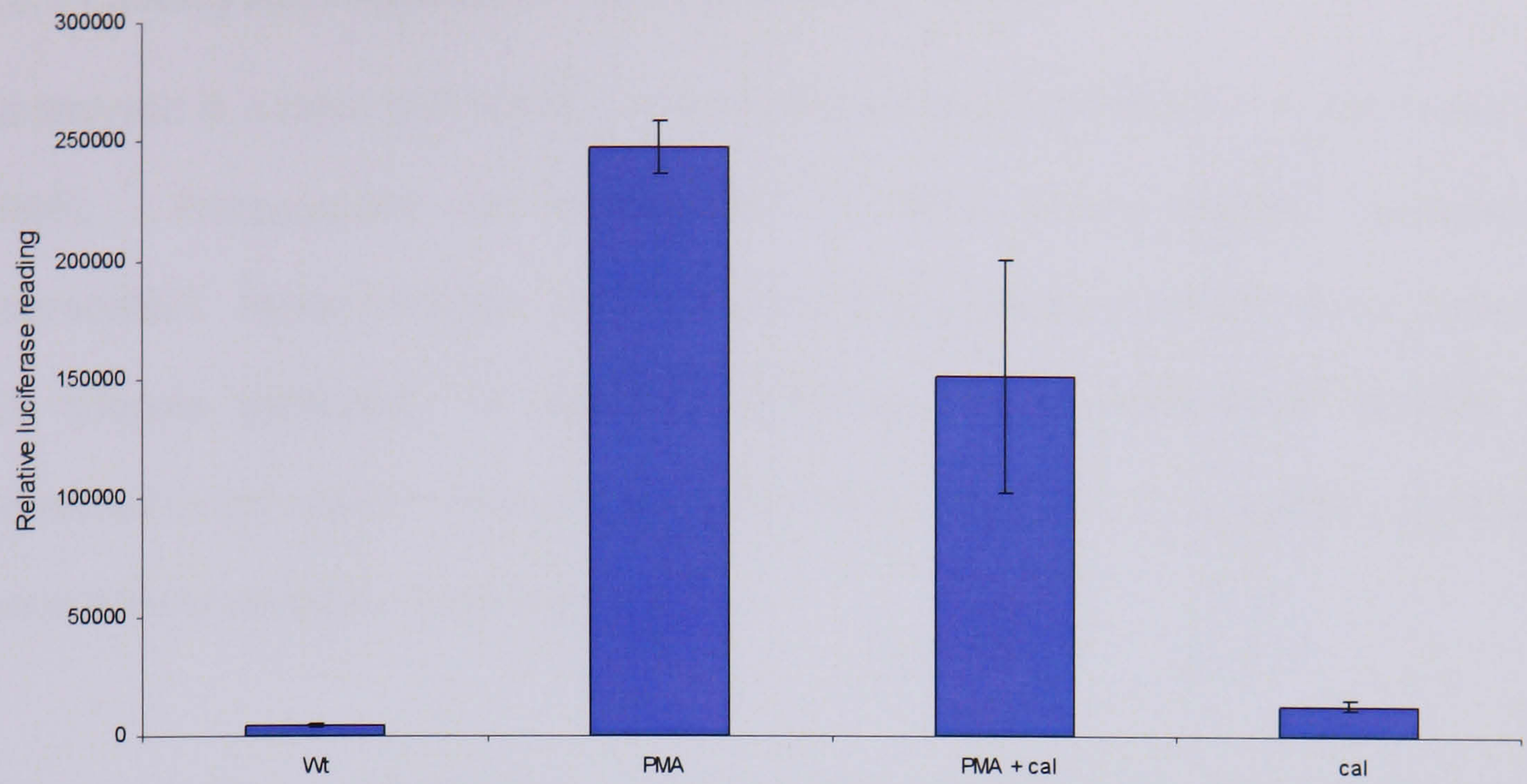

Figure 5.14 Calphostin C reduces reporter gene activity in PMA-treated cells

MDCK cells were transfected with 1μg pMstWt-GV, 1.5μg of the experimental reporter and 0.15μg of the control reporter. After 24 hours cells were treated with or without 100nM PMA and 1μM calphostin C. After a further 24 hours, the cells were lysed and readings for both *Renilla* and firefly luciferase recorded. Wt (pMstWt-GV without PMA); PMA (pMstWt-GV with 100nM PMA); PMA + cal (pMstWt-GV with 100nM PMA and 1μM calphostin C); cal (pMstWt-GV with 1μM calphostin). Results are the mean (±SEM) of three separate experiments. Relative luciferase reading (firefly luciferase expression from experimental reporter).

5.3.2 Lactacystin treatment of cells expressing Wt-GV

Lactacystin is a rapid and specific, irreversible proteasome inhibitor (Fenteany *et al.* 1998). Proteasomes are responsible for most non-lysosomal intracellular degradation. When inhibited, proteins which are normally degraded in this fashion will become protected. If the C-terminal fragment released from stomatin is protected in this manner following treatment with lactacystin, an increase in reporter gene activity would be expected.

The test construct pMstWt-GV was transiently transfected into MDCK cells along with the experimental and control reporters. Cells were treated with or without 10 μM lactacystin 24 hours post-transfection (section 5.2.3). Cell lysates were assayed for luciferase activity.

Reporter gene activity increased approximately 10-fold following lactacystin treatment suggesting that the proteasome is responsible for the degradation of the C-terminal fragment of stomatin (figure 5.15).

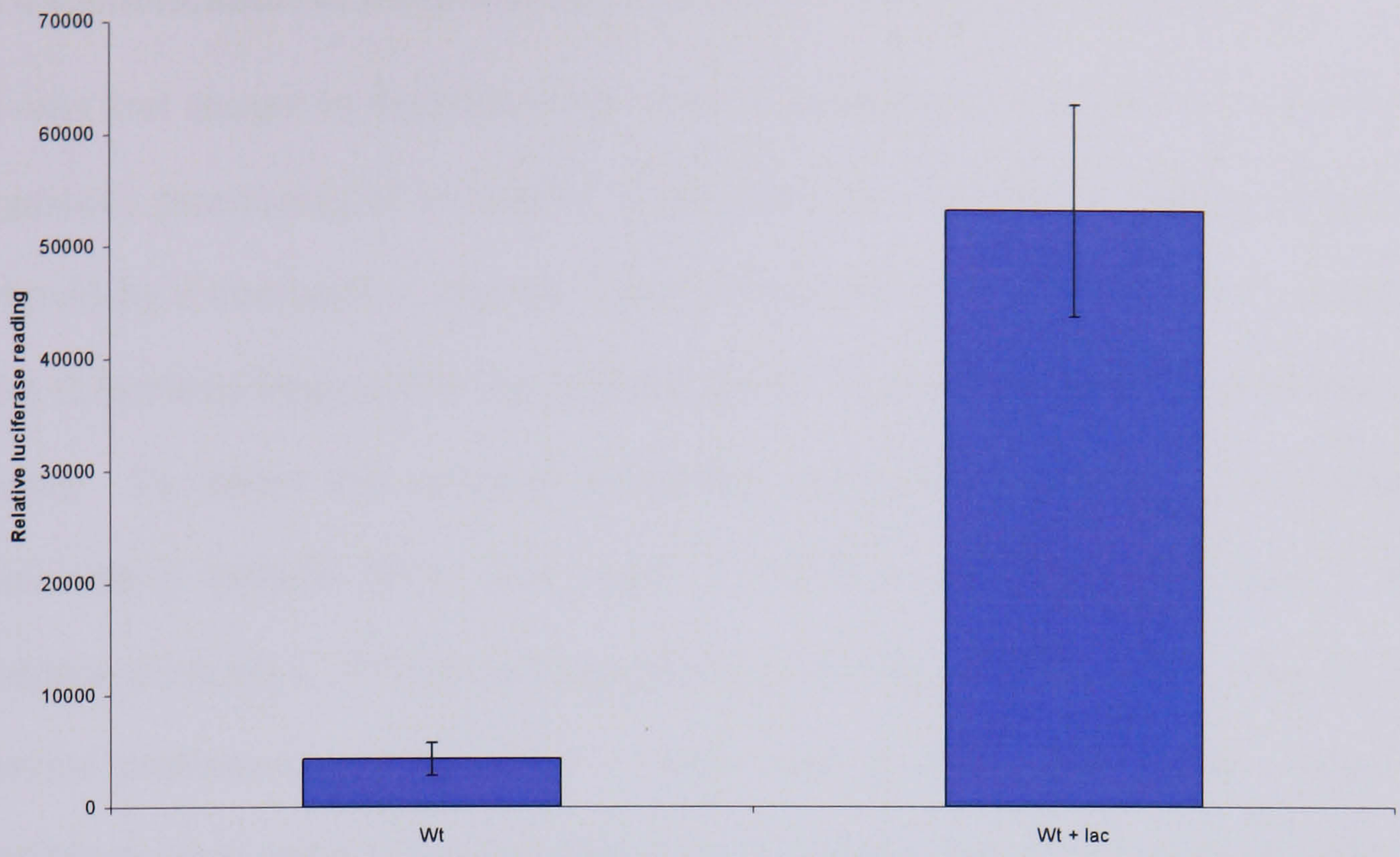

Figure 5.15 Lactacystin enhances reporter gene activity

MDCK cells were transfected with 1μg pMstWt-GV, 1.5μg of the experimental reporter and 0.15μg of the control reporter. After 24 hours cells were treated with or without 10μM lactacystin. After a further 24 hours, the cells were lysed and readings for both *Renilla* and firefly luciferase recorded. Wt (pMstWt-GV without lactacystin); Wt + lac (pMstWt-GV with 10μM lactacystin). Results are the mean (±SEM) of three separate experiments. Relative luciferase reading (firefly luciferase expression from experimental reporter).

5.4 Identification of the protease involved the proteolysis of stomatin

It was first sought to determine the class of protease which may be involved in the cytosolic processing of stomatin. If the protease responsible was inhibited, there should be a decrease in reporter gene activity due to the decrease in availability of the C-terminal fragment to the reporter gene. Various inhibitors of proteases were used. To inhibit the cysteine proteases Trans-Epoxysuccinyl-L-Leucylamido-(4-Guanidino) Butane (E64) was used, 1, 10-Phenanthroline was used to inhibit metallo-proteases, Phenylmethylsulphonyl Fluoride (PMSF) was used to inhibit serine proteases and Pepstatin A was used to inhibit aspartyl proteases. All inhibitors were used at a concentration as recommended by the manufacturer.

The test construct pMstWt-GV was transiently transfected into MDCK cells along with the experimental and control reporters. Cells were treated with or without the protease inhibitor 24 hours post-transfection (section 5.2.3). Cell lysates were assayed for luciferase activity.

Cells treated with the cysteine protease inhibitor E64 produced the same level of reporter gene activity as untreated cells (figure 5.16). This result suggests that a cysteine protease is not responsible for the processing of stomatin in the membrane with the subsequent release of a C-terminal fragment. The metallo-protease inhibitor 1, 10-Phenanthroline completely abolished reporter gene activity, suggesting the processing of stomatin is due to the activity of a metallo-protease and should be further investigated. Reporter gene activity was reduced to 65% in cells treated with PMSF compared to those cells left untreated. This suggests a serine protease could be involved in the processing of stomatin. Again, this result should be further investigated. The aspartyl protease inhibitor Pepstatin A caused a

marginal increase in reporter gene activity. This could be due to inhibition of proteases involved in the degradation pathway of stomatin. By inhibiting degradation the half-life of stomatin and/or the C-terminal fragment is increased. This enhances availability of the C-terminal fragment to the experimental reporter.

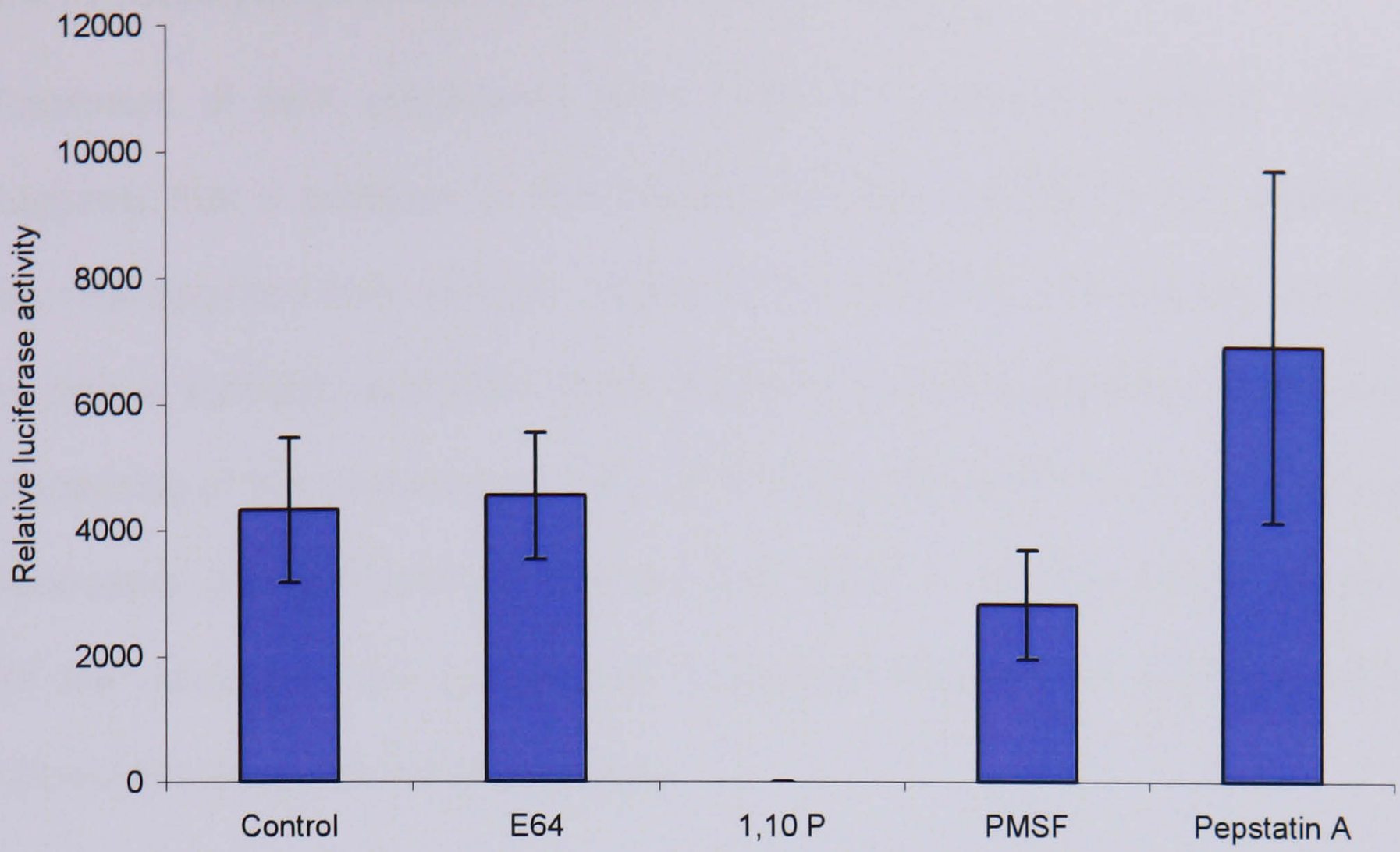

Figure 5.16 The effect of various protease inhibitors on reporter gene activity

MDCK cells were transfected with 1μg pMstWt-GV, 1.5μg of the experimental reporter and 0.15μg of the control reporter. After 24 hours cells were treated with or without the indicated protease inhibitor. After a further 24 hours, the cells were lysed and readings for both *Renilla* and firefly luciferase recorded. Control (pMstWt-GV without treatment); E64 (pMstWt-GV with 10μM E64); 1, 10 P (pMstWt-GV with 5mM 1, 10-Phenanthroline); PMSF (pMstWt-GV with 1μM PMSF); Pepstatin A (pMstWt-GV with 1μM Pepstatin A). Results are the mean (±SEM) of three separate experiments. Relative luciferase reading (firefly luciferase expression from experimental reporter).

5.4.1 Proteolytic processing of stomatin by calpain

Treatment of cells expressing Wt-GV with the cysteine protease inhibitor E64 suggests that a protease in this class is not responsible for the release of a C-terminal fragment from stomatin (figure 5.16). However, calpain has been reported to cleave stomatin and thus forms the only known candidate for the proteolytic processing of this protein (Mairhofer *et al.* 2002) (figure 5.17). Calpastatin is a cell-permeable, potent inhibitor of calpain I and calpain II. If either calpain is responsible for the release of the cytoplasmic C-terminal fragment of stomatin, addition of calpastatin should inhibit the process.

The test construct pMstWt-GV was transiently transfected into MDCK cells along with the experimental and control reporters. Cells were treated with or without 10μM calpastatin 24 hours post-transfection (section 5.2.3). Cell lysates were assayed for luciferase activity.

Reporter gene activity increased by 50% following treatment with calpastatin (figure 5.18). This suggests the calpains are involved in the degradation of stomatin rather than the release of the C-terminal fragment. By inhibiting the calpains, stomatin and/or its C-terminal fragment become protected from degradation and cause the increased reporter gene expression.

Figure 5.17 Calpain-2 cleavage of stomatin

Whole HEK cell lysates overexpressing stomatin were incubated at room temperature for 2hrs with calpain-2 and various inhibitors of calpain-2 as shown. The uncleaved sample received no calpain-2 or inhibitor treatment. The samples were subjected to SDS-PAGE (10μg) (section 2.5.2) followed by subsequent immunoblot analysis (section 2.5.3) using an antibody against stomatin. Thanks to Dr D.Thomas (GSK, Harlow, UK) for advice on appropriate concentrations and kind donation of the calpastatin and Z-LLY-fmk.

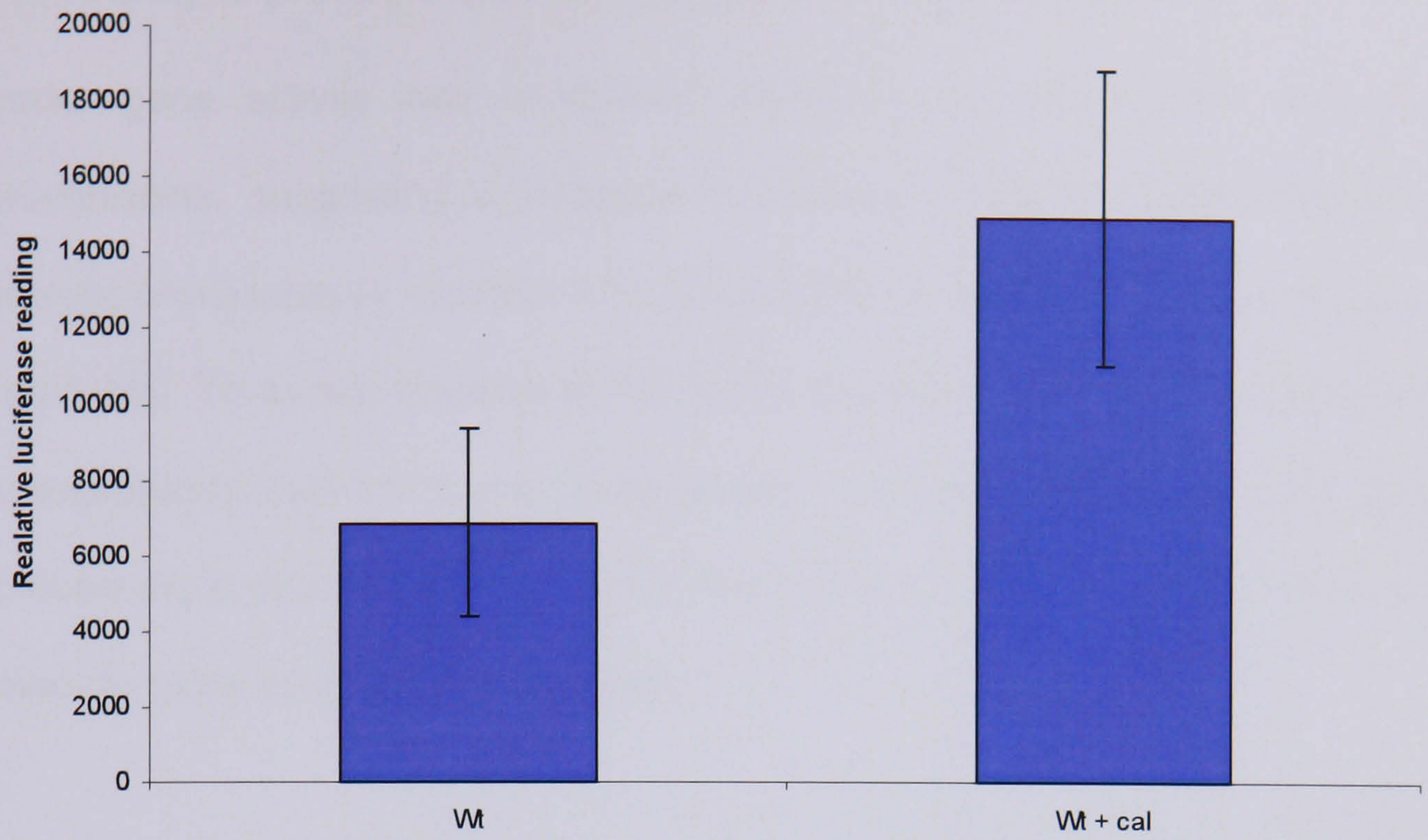

Figure 5.18 The use of calpastatin to inhibit Calpain I and Calpain II

MDCK cells were transfected with 1μg pMstWt-GV, 1.5μg of the experimental reporter and 0.15μg of control reporter. After 24 hours cells were treated with or without 10μM calpastatin. After a further 24 hours, the cells were lysed and readings for both *Renilla* and firefly luciferase recorded. Wt (pMstWt-GV without calpastatin), Wt + cal (pMstWt-GV with 10μM calpastatin). Results are the mean (±range) of two separate experiments. Relative luciferase reading (firefly luciferase expression from experimental reporter). Thanks to Dr D.Thomas (GSK, Harlow, UK) for advice on appropriate concentration and kind donation of the calpastatin.

5.4.2 Proteolytic processing of stomatin by a metallo-protease

Reporter gene activity was completely abolished in cells treated with 1, 10-Phenanthroline, suggesting a protease in this class may be responsible for the proteolytic processing to stomatin with subsequent release of a C-terminal fragment (figure 5.16). To further investigate this result, the effect of 1, 10-Phenanthroline on cells expressing Gal4-VP16 was investigated. As Gal4-VP16 is a soluble protein, no processing is required for it to access the reporter construct. Therefore no effect on reporter gene activity should be seen.

The test constructs pMstWt-GV and pMstGV were transiently transfected into MDCK cells along with the experimental and control reporters. Cells were treated with or without 5mM 1, 10-Phenanthroline 24 hours post-transfection (section 5.2.3). Cell lysates were assayed for luciferase activity.

As previously shown, treatment with 1, 10-Phenanthroline significantly reduced reporter gene activity in cells transfected with pMstWt-GV (figure 5.19). However, the same treatment also reduced reporter gene activity in the cells expressing Gal4-VP16. As reporter gene activity in cells expressing the soluble Gal4-VP16 is not dependent on proteolytic activity, the luciferase levels should not be affected by the inhibition of any protease. The most likely cause of the reduced activity seen in cells treated with 1, 10-Phenanthroline is the inhibition of the luciferase reaction resulting in photon emission. Upon further investigation of the firefly luciferase reaction, it was realised that Mg^{++} is crucial for photon emission. 1, 10-Phenanthroline functions by chelating metal ions and thus is almost certain to inhibit this reaction. This however cannot explain the inhibition of the *Renilla* luciferase also seen (data not shown). Why the *Renilla* luciferase was inhibited is unknown.

The possible involvement of a metallo-protease in the release of a C-terminal fragment of stomatin cannot be ruled out by this study. Alternative methodology would have to be used in order to assess further the possible involvement of a metallo-protease in the release of a C-terminal fragment from stomatin.

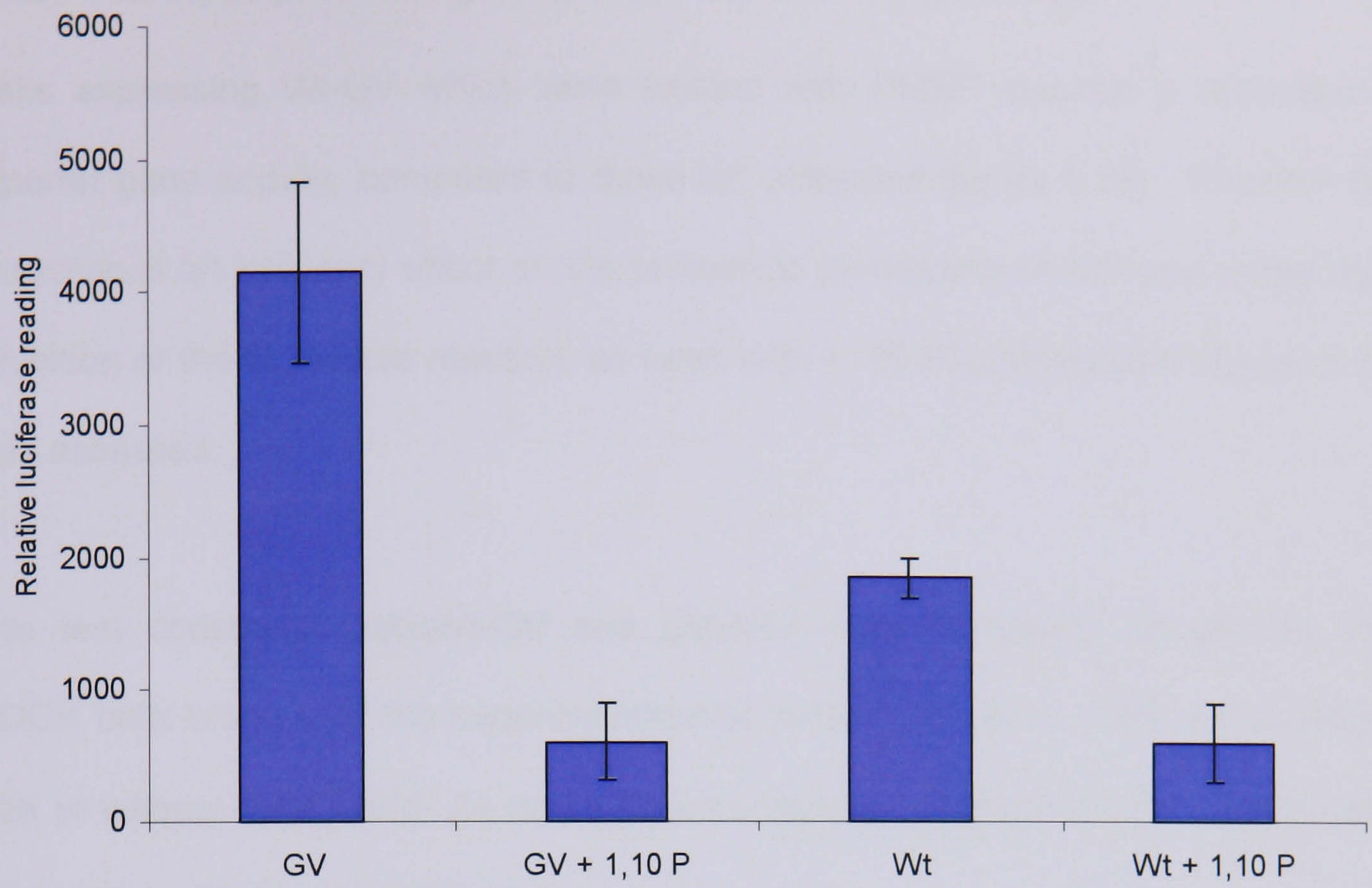

Figure 5.19 The effect of 1, 10-Phenanthroline on reporter gene activity

MDCK cells were transfected with 1μg pMstWt-GV, 1.5μg of the experimental reporter and 0.15μg of the control reporter. After 24 hours cells were treated with or without 5mM 1, 10 Phenanthroline. After a further 24 hours, the cells were lysed and readings for both *Renilla* and firefly luciferase recorded. GV (Gal4-VP16 without 11, 10-Phenanthroline); GV + 1,10P (Gal4-VP16 with 5mM 1, 10-Phenanthroline); Wt (Wt-GV without 1, 10-Phenanthroline); Wt + 1, 10 P (Wt-GV with 5mM 1, 10-Phenanthroline). Results are the mean (±range) of two separate experiments. Relative luciferase reading (firefly luciferase expression from experimental reporter).

5.4.3 Proteolytic processing of stomatin by a serine protease

Cells expressing Wt-GV which were treated with PMSF showed a reduction in reporter gene activity, compared to those left untreated (figure 5.16). Whether this reduction is an inhibitory effect on the proteolytic processing of stomatin rather than inhibition of the luciferase reaction, as seen with 1, 10-Phenanthroline (figure 5.19) was assessed.

The test constructs pMstWt-GV and pMstGV were transiently transfected into MDCK cells along with the experimental and control reporters. Cells were treated with or without 1μM PMSF 24 hours post-transfection (section 5.2.3). Cell lysates were assayed for luciferase activity.

Cells expressing Gal4-VP16 treated with PMSF showed increased reporter gene activity compared to those left untreated (figure 5.20). As previously seen (figure 5.16), cells expressing Wt-GV which were treated with PMSF showed decreased reporter gene activity compared to untreated cells. This suggests the observed reduction in reporter gene activity in cells expressing Wt-GV cannot be as a result of inhibition of luciferase activity (as seen with 1, 10 Phenanthroline). It is therefore possible that PMSF causes inhibition of a serine protease responsible for processing stomatin, reducing the availability of the C-terminal fragment to the reporter gene. Given the enhanced reporter gene activity seen in the treated cells expressing Gal4-VP16, it is likely that the inhibition observed in the Wt-GV sample is underestimated. Insufficient levels of PMSF could explain why the reporter gene activity was not completely abolished. Also, the remaining reporter gene activity could be due to other processing events by enzymes not identified in this study. This result agrees with data to suggest stomatin is cleaved by a membrane-bound

serine protease. It has been suggested the cleavage event forms the basis of an ion channel regulatory feature for stomatin (Yokoyama *et al.* 2005). To further investigate the possibility that a serine protease is responsible for the processing to stomatin, a second serine protease inhibitor 3,4-dichloroisocoumarin (dci) was used.

The test constructs pMstWt-GV and pMstGV were transiently transfected into MDCK cells along with the experimental and control reporters. Cells were treated with or without 100μM dci 24 hours post-transfection (section 5.2.3). Cell lysates were assayed for luciferase activity.

As seen with 1, 10-Phenanthroline, reporter gene activity was completely abolished in treated samples transfected with pMstGV. This suggests that the luciferase reaction was inhibited, it is unclear why (figure 5.21).

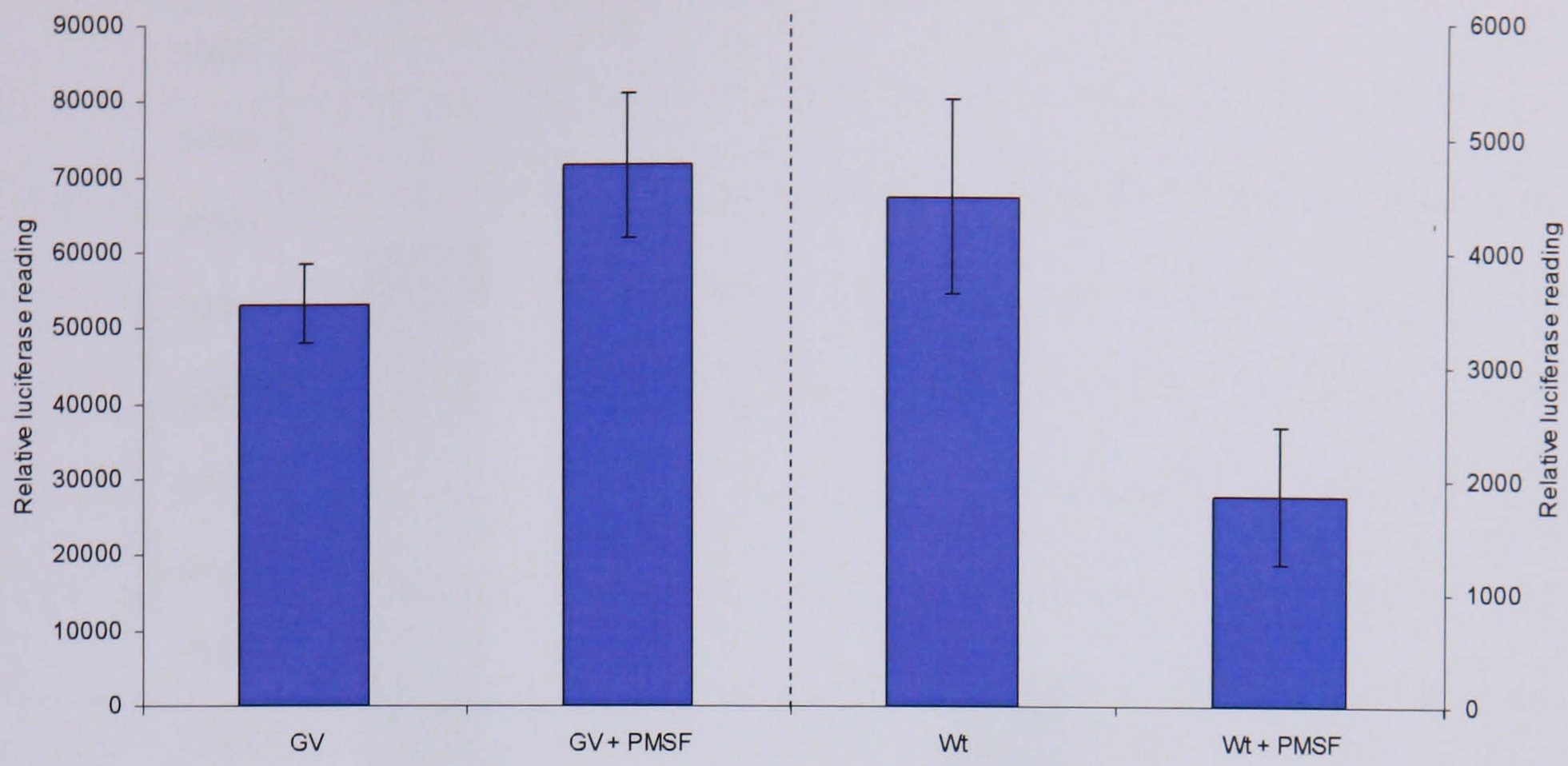

Figure 5.20 PMSF reduces reporter gene activity

MDCK cells were transfected with 1μg pMstWt-GV or pMstGV, 1.5μg of the experimental reporter and 0.15μg of the control reporter. After 24 hours cells were treated with or without 1μM PMSF. After a further 24 hours, the cells were lysed and readings for both *Renilla* and firefly luciferase recorded. GV (pMstWt-GV without PMSF); GV + PMSF (pMstWt-GV with 1μM PMSF); Wt (pMstWt-GV without PMSF); Wt + PMSF (pMstWt-GV with 1μM PMSF). Results are the mean (±SEM) of three readings from separate experiments. Relative luciferase reading (firefly luciferase expression from experimental reporter).

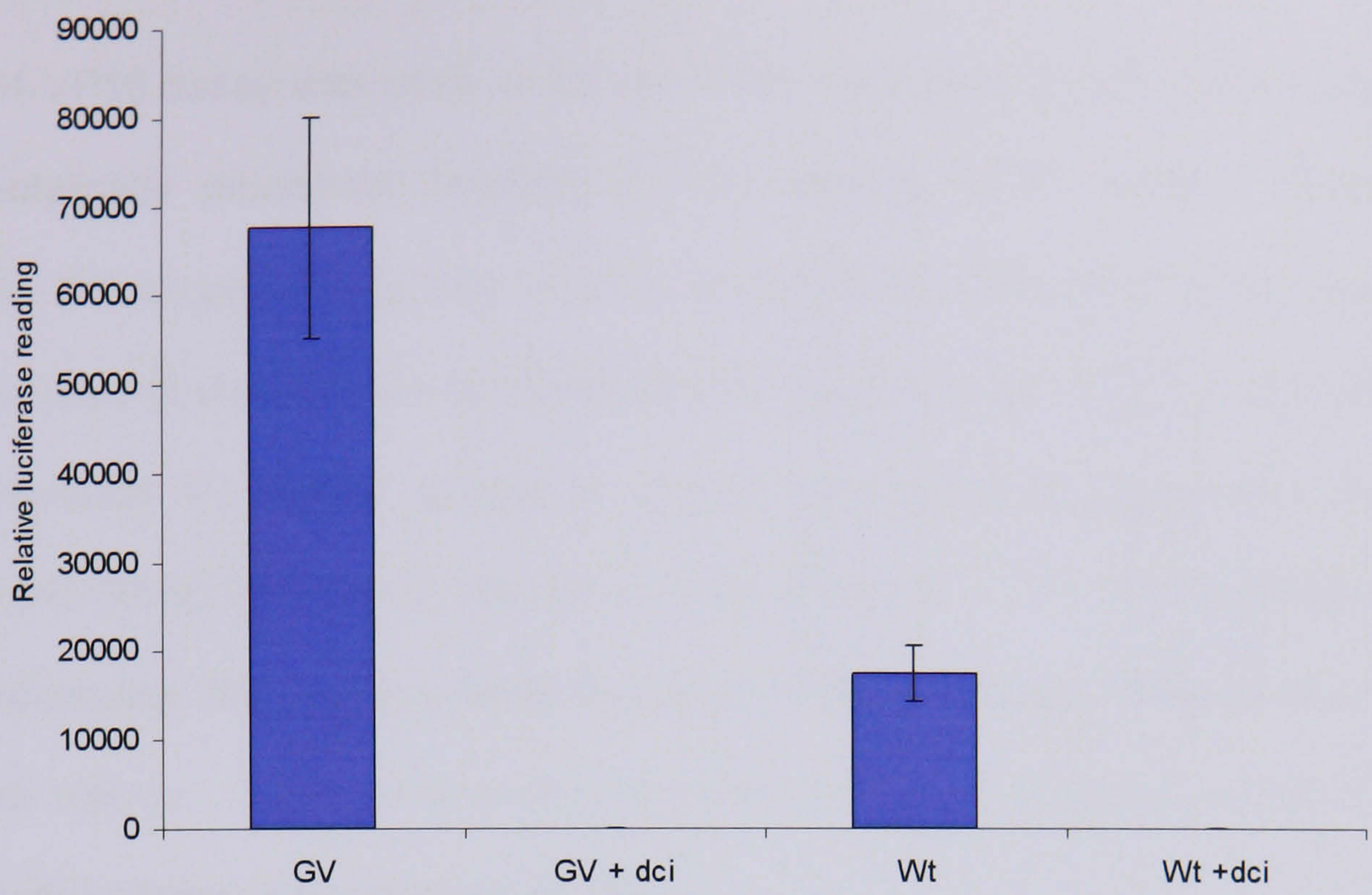

Figure 5.21 The effect of 3,4-dichloroisocoumarin on reporter gene activity

MDCK cells were transfected with 1μg pMstWt-GV or pMstGV, 1.5μg of the experimental reporter and 0.15μg of the control reporter. After 24 hours cells were treated with or without 100μM 3,4-dichloroisocoumarin (dci). After a further 24 hours, the cells were lysed and readings for both *Renilla* and firefly luciferase recorded. GV (pMstGV without dci); GV + dci (pMstGV with 100μM dci); Wt (pMstWt-GV without dci), Wt + dci (pMstWt-GV with 100μM dci). Results are the mean (±range) of two separate experiments. Relative luciferase reading (firefly luciferase expression from experimental reporter).

5.5 Discussion

The Gal4-VP16 assay was used to assess if the membrane-bound protein stomatin is proteolytically processed resulting in the release of a cytosolic C-terminal fragment. If such processing was to occur, the chimeric Gal4-VP16 protein fused to the C-terminus of stomatin would cause reporter gene activity. This assay has been used previously by several groups to assess the proteolytic processing in other proteins (Karlstrom *et al.* 2002; May *et al.* 2002; Struhl *et al.* 1998). If stomatin were to be processed, the event is likely to occur in the C-terminal domain due to its extensive nature. There is a predicted serine protease cleavage site in the C-terminal of stomatin (Yokoyama *et al.* 2005).

It was first assessed if the C-terminal domain of stomatin could gain access to the nucleus and cause reporter gene activity. Studies with the soluble protein ΔTMN-GV showed that the C-terminal domain of stomatin lacking a membrane anchorage system could access the experimental reporter in the nucleus. It is unknown if the protein did this as a whole or was first processed in order to gain access to the nucleus. Significantly higher levels of reporter gene activity were recorded in cells expressing the soluble Gal4-VP16; this suggests that the C-terminal fragment of stomatin is hindered in its access to the nucleus in some way. Studies with Wt-GV showed that membrane-bound form of stomatin could also cause reporter gene activity. As expected, the level of reporter gene activity was less than that in the cells expressing ΔTMN-GV. In order that the reporter gene was expressed in cells expressing Wt-GV, some processing event of stomatin would have to occur. This would release the C-terminally fused Gal4-VP16 protein from the membrane and allow it to gain access to the nucleus. Together these results suggest that stomatin is proteolytically processed in the membrane, resulting in the release of a C-terminal

fragment. The size of this fragment is yet to be determined. The processing of proteins in the membrane sometimes results in the release of a functional fragment (Struhl *et al.* 1998). Whether this is the case for stomatin would require further investigation.

The processing that leads to the release of the cytosolic fragment of stomatin can be modulated by protein kinase C (PKC). The activator of PKC, phorbol 12-myristate 13-acetate (PMA), has previously been used to demonstrate the processing of the low density lipoprotein receptor-related protein (LRP) is modulated by PKC (May *et al.* 2002). As with the LRP study, PMA significantly increased reporter gene activity in cells expressing Wt-GV. This suggests the processing of stomatin was enhanced following activation of PKC. Combined treatment of PMA and calphostin C (a PKC inhibitor) reduced the level of reporter gene activity in cells expressing Wt-GV; this suggests that the processing of stomatin in the membrane was reduced. Together these data suggest that the event leading to the release of a C-terminal fragment from stomatin can be modulated by PKC.

Treatment of cells with the proteasome inhibitor lactacystin has been used previously to demonstrate the fragment released from LRP is degraded by the proteasome (May *et al.* 2002). Reporter gene activity in cells expressing Wt-GV was increased 10-fold following treatment with lactacystin. This suggests that the C-terminal fragment of stomatin may be degraded by the proteasome.

In order to assess which protease may be responsible for the processing of the C-terminus of stomatin, compounds that inhibit a class of protease (e.g. cysteine proteases) were applied to cells transfected with Wt-GV. This study suggests that

cysteine and aspartyl proteases are not involved in the processing of stomatin in the membrane; the involvement of metallo-proteases could not be ruled out. Inhibiting the serine proteases caused a decrease in reporter gene activity, suggesting a protease in this class is responsible for the release of the C-terminal fragment from stomatin. This is in line with previous studies that suggested stomatin is the partner to a membrane-bound protease, most likely a serine protease. The prokaryotic stomatins have been proposed to form an operon with a membrane-bound serine protease in at least 19 organisms; the catalytic serine is 100% conserved (Green *et al.* 2004). This relationship has been speculated to represent a role for stomatin as a binding partner to the serine protease, possibly as a substrate, chaperone or as a regulator. The data in this study suggest stomatin partners this serine protease as its substrate. More recently this serine protease in *Pyrococcus horikoshii* PH1510 has been shown to cleave PH1511, the stomatin homologue (Yokoyama *et al.* 2005). Sequence alignment highlighted a stretch of hydrophobic residues as being the proposed cleavage site in stomatin, a hydrophobic region speculated to interact with the membrane. It has been proposed that cleavage of stomatin at this position causes the opening of an ion channel and forms the basis of its regulation. Since the realisation that stomatin is deficient in erythrocyte membranes of patients with Over-hydrated Hereditary Stomatocytosis (OHSt), it has been considered possible that stomatin has an ion channel regulatory function (Fricke *et al.* 2003). OHSt patients suffer increased monovalent cation permeability across the erythrocyte membrane; as a result the cell accumulates sodium and water which in turn increases the fragility of the cell which leads to anaemia. No direct evidence to show the stomatin deficiency causes the cation leak has ever been shown.

To date the only protease reported to cleave stomatin is calpain; the functional significance of this is unknown (Mairhofer *et al.* 2002). Cleavage of stomatin by calpain was confirmed in this study. The data presented in this study suggest calpain processing of stomatin may function as part of the protein's degradation pathway rather than in the release of a C-terminal fragment. The inhibition of calpain with calpastatin increased reporter gene activity in cells expressing Wt-GV. If calpain were responsible for the release of a C-terminal fragment of stomatin, a decrease in reporter gene activity would have been expected. The increase suggests that higher levels of the C-terminal fragment are made available to the reporter gene construct. This may be as a result of inhibiting a degradation pathway of stomatin and/or the C-terminal fragment.

The data presented in this study suggest that the membrane protein stomatin is proteolytically processed by a serine protease in its C-terminal domain. This agrees with data from prokaryotes showing prokaryotic stomatin shares an operon with a serine protease. This relationship in prokaryotes has been shown to regulate an ion channel; whether the same is true in mammals requires further investigation.

Chapter 6: General Discussion

This study set out to characterise the integral membrane protein stomatin and to further understand its role within the cell. Stomatin is found predominantly in the plasma membrane (Wang *et al.* 1991) but has also been reported in the nucleus (Fricke *et al.* 2005) and mitochondria (Argent *et al.* 2004). This study focused on the role of stomatin in the plasma membrane but also considered characteristics which may contribute to intracellular trafficking of the protein. As stomatin is known to partition into detergent-resistant membranes, the protein is thought to reside within lipid rafts (Salzer *et al.* 2001). It is becoming increasingly apparent that many cellular processes take advantage of the localised organisation these microdomains can offer. For this reason lipid rafts were of particular interest in this study.

Stomatin is deficient in the erythrocyte membrane of patients suffering Over-hydrated Hereditary Stomatocytosis (OHSt). The protein composition of membranes from OHSt erythrocytes, known as stomatocytes due to their altered morphology, were compared to membranes of control erythrocytes. When this investigation was undertaken it was unclear as to why the stomatocyte membrane was deficient in stomatin. The absence of a binding partner in the membrane and trafficking problems were both considered possible (Stewart 1997). This study aimed to find other differences between the membranes of erythrocytes and stomatocytes which may provide some indication towards a role for stomatin and why it is deficient in the stomatocyte membrane. Results showed a decreased level of actin associated with the stomatocyte membrane as compared to the erythrocyte membrane. The lipid rafts isolated from stomatocytes also showed reduced levels of actin. This suggests that stomatin is associated with actin and its reduced

presence in the stomatocyte membrane causes the reduced levels of actin. This is consistent with as yet unpublished data showing similar diminished actin levels associated with the stomatocyte membrane particularly in the lipid rafts (J.Turner, University College London, UK). A recent study has suggested that it is most likely that stomatin is trafficked wrongly in the maturing stomatocyte (Fricke *et al.* 2005). This therefore means any altered protein composition in the stomatocyte membrane is most likely due to the initial deficiency of stomatin rather than being the cause of the deficiency. These data agree with previous observations that stomatin associates with the actin cytoskeleton possibly forming a cytoskeletal anchor in the membrane and that it is involved in the control of cell morphology (Snyers *et al.* 1997; Snyers *et al.* 1999a). Previous to this a structural role for stomatin had been considered due to its similarities to the scaffold protein caveolin (Snyers *et al.* 1999b). The link between stomatin and actin may be considered similar to that seen with spectrin. The spectrin network in the erythrocyte is considered essential for the stability, and in the deformability, of the cell; it is anchored to the membrane in two positions through its association with the integral membrane proteins band 3 and glycophorin (Bennett 1989). Stomatin may form the integral membrane part of a complex responsible for tethering the under-lying actin cytoskeleton to the membrane. To further investigate a possible interaction between stomatin and actin, stomatin was overexpressed in MDCK cells. The overexpression of stomatin did not affect the actin content of cell lysates. However, actin levels were increased in the membrane and lipid rafts of cells overexpressing stomatin. This suggests the increased level of stomatin in the membrane and lipid rafts enhances actin association with these structures. This further suggests that stomatin associates with actin and that this association has a functional relevance.

A possible role for stomatin in the raft-based process of calcium-induced vesiculation was investigated by comparing the process in erythrocytes and stomatocytes. It had previously been shown that stomatocytes showed defective ATP-dependent vesiculation (Turner *et al.* 2003). In erythrocytes, during calcium-induced vesiculation, the flotillins remain within the post-vesiculation membrane and stomatin vesiculates in the microvesicles. In stomatocytes, the flotillins were found to vesiculate in both the microvesicles and nanovesicles leaving the post-vesiculation membrane almost devoid of flotillin content. If the vesiculation process does serve as a protection strategy against complement (Iida *et al.* 1991) then it may be considered essential that this process is maintained, even in the absence of stomatin. As the flotillins contain the SPFH domain and assume a hair-pin loop in the lipid bilayer, they may form substitutes for stomatin to maintain vesiculation within the stomatocyte. Compared to erythrocytes, stomatocytes showed significantly increased levels of vesiculation. This suggests stomatin may be acting as a negative regulator in this process. Enhanced vesiculation is also seen with glucose-6-phosphate dehydrogenase (G6PD)-deficient erythrocytes (Tsai *et al.* 1996). It therefore seems unlikely that the deficiency in stomatin is solely responsible for the enhanced vesiculation seen from stomatocytes.

Calpain activity is involved in the remodelling of the underlying actin cytoskeleton during calcium-induced vesiculation (Zwaal *et al.* 1997). The enzyme is known to cleave band 2.1, band 4.1 and stomatin (Dantas de Medeiros *et al.* 2002; Salzer *et al.* 2002). Preliminary investigations suggest that the level of calpain activity is elevated in stomatocytes compared to erythrocytes. It is possible that elevated levels of calpain activity may contribute to the enhanced vesiculation seen from stomatocytes by increasing the processing of cytoskeletal proteins normally

associated with rate-limiting steps in vesiculation. Elevated calpain activity may also be, in part, responsible for the degradation and thus the deficiency of stomatin within the stomatocyte membrane. If the remodelling of the cytoskeleton is rate-limiting in calcium-induced vesiculation, stomatin deficiency would reduce the level of rate-limiting elements in the membrane and may cause enhanced vesiculation. This is supported by results which show that the inhibition of calpain in MDCK cells protects stomatin from degradation. Elevated calpain activity was recorded in the single OHSt pedigree tested and the study should be extended to include more pedigrees. The involvement of lipid rafts in this vesiculation process was further confirmed in this current study through cholesterol depletion of erythrocytes which inhibited vesiculation. Actin is known to be crucial for the coalescence of rafts during T-cell signalling (Valensin *et al.* 2002). A similar scenario may be envisaged for lipid rafts during calcium-induced vesiculation. If actin association with the plasma membrane is involved in the localised positioning of lipid rafts which contain critical proteins for controlled vesiculation, a diminished actin association with the membrane due to stomatin deficiency may hinder this process. Erythrocytes are more susceptible to hemolysis following vesiculation; G6PD-deficient erythrocytes are even more susceptible due to the enhanced vesiculation (Tsai *et al.* 1996). If the same is true for stomatocytes, this may contribute to the anaemia seen in OHSt patients, the primary cause being the osmotic fragility of the stomatocyte. The post-vesiculation erythrocyte has to quickly restore lipid asymmetry moving the phosphatidylserine (PS) from the outer leaflet back to the inner leaflet of the bilayer. The enhanced vesiculation in stomatocytes could cause an increased presence of PS at the cell surface; this may explain the thrombotic problems experienced by OHSt patients who have undergone therapeutic splenectomy.

Characterisation of the SPFH (Stomatins, Prohibitins, Flotillins and HflK/C) domain within stomatin was also considered in this investigation. The SPFH domain proteins are considered to function in the regulation of membrane protein proteolysis or as scaffold proteins in the membrane for the formation of multiprotein complexes (Kaser *et al.* 2000; Langhorst *et al.* 2005). Conserved residues within this domain were investigated due to mutations at these positions causing defects in *C.elegans*. The residues when mutated in stomatin caused no difference to membrane targeting or lipid raft partitioning. They were also not essential in the trafficking of stomatin to the nucleus. This is likely due to these residues being of little importance in targeting stomatin to these structures. Interaction between the mutant forms of stomatin investigated and the stomatin like protein-2 cannot be ruled out. It may be that this interaction contributes to membrane, lipid raft and nuclear localisation of the mutant forms.

The major palmitoylation site in stomatin is Cysteine 29 (Snyers *et al.* 1999b); the effect this may have on stomatin was investigated. A Cysteine – Serine mutation at position 29 caused less stomatin to locate to the membrane and lipid rafts; with increased levels found in the nucleus. Palmitoylation is known to increase the affinity of certain proteins for the membrane and/or lipid rafts (Zhang *et al.* 1998), this could possibly explain why the mutant form of stomatin failed to partition into membranes and lipid rafts as well as the wild type protein. Some proteins, e.g. phospholipid scramblase 1, use reversible palmitoylation as a means of influencing their distribution within different compartments of the cell (Wiedmer *et al.* 2003). When palmitoylated they localise to the membrane and when depalmitoylated they localise to the nucleus. Given that a mutation at position 29 causes less stomatin to localise to the membrane and more to the nucleus, this could indicate a defect in the

shuttling process of stomatin between the plasma membrane and the nucleus. Coupled with the reversible depalmitoylation of stomatin, it is possible that two chaperones of stomatin found in the cytosol and nucleus may be responsible for the transit of stomatin between cellular compartments (Salzer *et al.* 1999). As yet, the role of stomatin in the nucleus has not been investigated. As stomatin functions as a structural protein in the plasma membrane through its interaction with the actin cytoskeleton, it may assume a similar role in the nucleoskeleton.

A reporter gene assay was used to assess if a proteolytic event caused the release of a C-terminal fragment of stomatin from the membrane. Recent studies have shown that prokaryotic stomatin exists in an operon with a serine protease, suggesting a functional link between the two (Green *et al.* 2004). In *Pyrococcus horikoshii* the serine protease PH1510 has been demonstrated to cleave PH1511, the stomatin homologue (Yokoyama *et al.* 2005). Cleavage occurs in a domain rich in hydrophobic residues which is thought to interact with the membrane. Cleavage at this site is proposed to disassociate the domain from the membrane and allow the opening of an ion channel. If this is true for stomatin, it may partially explain the cation leak in the stomatocytes of OHSt patients. An ion channel regulatory role for stomatin has been considered likely since its deficiency in the stomatocyte membrane was found (Lande *et al.* 1982). Results in this current study suggest that the C-terminus of stomatin is subject to proteolytic processing with the subsequent release of a C-terminal fragment from the membrane. With the use of various protease inhibitors it was found that a serine protease is most likely responsible for this processing of stomatin. However, the action of a metallo-protease could not be ruled out and further investigation should be carried out to assess this. The proposed serine protease cleavage site in stomatin (Yokoyama *et al.* 2005) cannot

be confirmed or ruled out in this study as the size of the fragment was not investigated. It is however an unlikely site of cleavage due to an adjacent proline residue. The possibility of calpain being responsible for the release of a C-terminal fragment of stomatin was ruled out. Inhibition of calpain increased reporter gene activity, suggesting the enzyme may be involved in a degradation pathway of stomatin. The processing event was stimulated following treatment with phorbol 12-myrisate 13-acetate. This suggests that protein kinase C modulates this processing of stomatin. Inhibition of the proteasome protected the C-terminal fragment from degradation.

In conclusion this study has further confirmed the role of stomatin as a structural protein, most likely forming an anchor between the membrane and the actin cytoskeleton particularly in lipid rafts. Palmitoylation of stomatin on cysteine 29 increases the affinity of the protein for the membrane and may also regulate the distribution of stomatin between the membrane and the nucleus. Stomatin is the substrate for a serine protease; whether this forms the basis of ion channel regulation requires further investigation.

Chapter 7: References

Abriel, H., J. Loffing, J. F. Rebhun, J. H. Pratt, L. Schild, J. D. Horisberger, D. Rotin and O. Staub (1999). "Defective regulation of the epithelial Na+ channel by Nedd4 in Liddle's syndrome." J Clin Invest **103**(5): 667-73.

Acconcia, F., P. Ascenzi, A. Bocedi, E. Spisni, V. Tomasi, A. Trentalance, P. Visca and M. Marino (2005). "Palmitoylation-dependent estrogen receptor alpha membrane localization: regulation by 17beta-estradiol." Mol Biol Cell **16**(1): 231-7.

Ahmed, S. N., D. A. Brown and E. London (1997). "On the origin of sphingolipid/cholesterol-rich detergent-insoluble cell membranes: physiological concentrations of cholesterol and sphingolipid induce formation of a detergent-insoluble, liquid-ordered lipid phase in model membranes." Biochemistry **36**(36): 10944-53.

Allan, D., P. Thomas and A. R. Limbrick (1980). "The isolation and characterization of 60 nm vesicles ('nanovesicles') produced during ionophore A23187-induced budding of human erythrocytes." Biochem J **188**(3): 881-7.

Allende, D., A. Vidal and T. J. McIntosh (2004). "Jumping to rafts: gatekeeper role of bilayer elasticity." Trends Biochem Sci **29**(6): 325-30.

Almeida, P. F., W. L. Vaz and T. E. Thompson (1992). "Lateral diffusion and percolation in two-phase, two-component lipid bilayers. Topology of the solid-phase domains in-plane and across the lipid bilayer." Biochemistry **31**(31): 7198-210.

Anderson, D. R., J. L. Davis and K. L. Carraway (1977). "Calcium-promoted changes of the human erythrocyte membrane. Involvement of spectrin, transglutaminase, and a membrane-bound protease." J Biol Chem **252**(19): 6617-23.

Anderson, R. G. and K. Jacobson (2002). "A role for lipid shells in targeting proteins to caveolae, rafts, and other lipid domains." Science **296**(5574): 1821-5.

Argent, A. C., M. C. Chetty, B. Fricke, Y. Bertrand, N. Philippe, S. Khogali, M. von During, J. Delaunay and G. W. Stewart (2004). "A family showing recessively inherited multisystem pathology with aberrant splicing of the erythrocyte Band 7.2b ('stomatin') gene." J Inherit Metab Dis **27**(1): 29-46.

Bacher, S., G. Achatz, M. L. Schmitz and M. C. Lamers (2002). "Prohibitin and prohibitone are contained in high-molecular weight complexes and interact with alpha-actinin and annexin A2." Biochimie **84**(12): 1207-20.

Banuett, F. and I. Herskowitz (1987). "Identification of polypeptides encoded by an Escherichia coli locus (hflA) that governs the lysis-lysogeny decision of bacteriophage lambda." J Bacteriol **169**(9): 4076-85.

Barnes, T. M., Y. Jin, H. R. Horvitz, G. Ruvkun and S. Hekimi (1996). "The Caenorhabditis elegans behavioral gene unc-24 encodes a novel bipartite protein similar to both erythrocyte band 7.2 (stomatin) and nonspecific lipid transfer protein." J Neurochem **67**(1): 46-57.

Bennett, V. (1989). "The spectrin-actin junction of erythrocyte membrane skeletons." Biochim Biophys Acta **988**(1): 107-21.

Bennett, V. and A. J. Baines (2001). "Spectrin and ankyrin-based pathways: metazoan inventions for integrating cells into tissues." Physiol Rev **81**(3): 1353-92.

Bevers, E. M., T. Wiedmer, P. Comfurius, S. J. Shattil, H. J. Weiss, R. F. Zwaal and P. J. Sims (1992). "Defective Ca(2+)-induced microvesiculation and deficient expression of procoagulant activity in erythrocytes from a patient with a bleeding disorder: a study of the red blood cells of Scott syndrome." Blood **79**(2): 380-8.

Bhat, R. A. and R. Panstruga (2005). "Lipid rafts in plants." Planta: 1-15.

Bickel, P. E. (2002). "Lipid rafts and insulin signaling." Am J Physiol Endocrinol Metab **282**(1): E1-E10.

Brown, D. A. (2001). "Seeing is believing: visualization of rafts in model membranes." Proc Natl Acad Sci U S A **98**(19): 10517-8.

Brown, D. A. and J. K. Rose (1992). "Sorting of GPI-anchored proteins to glycolipid-enriched membrane subdomains during transport to the apical cell surface." Cell **68**(3): 533-44.

Butikofer, P., F. A. Kuypers, C. M. Xu, D. T. Chiu and B. Lubin (1989). "Enrichment of two glycosyl-phosphatidylinositol-anchored proteins, acetylcholinesterase and decay accelerating factor, in vesicles released from human red blood cells." Blood **74**(5): 1481-5.

Cao, X. and T. C. Sudhof (2001). "A transcriptionally [correction of transcriptively] active complex of APP with Fe65 and histone acetyltransferase Tip60." Science **293**(5527): 115-20.

Chamberlain, L. H. (2004). "Detergents as tools for the purification and classification of lipid rafts." FEBS Lett **559**(1-3): 1-5.

Christian, A. E., M. P. Haynes, M. C. Phillips and G. H. Rothblat (1997). "Use of cyclodextrins for manipulating cellular cholesterol content." J Lipid Res **38**(11): 2264-72.

Civenni, G., S. T. Test, U. Brodbeck and P. Butikofer (1998). "In vitro incorporation of GPI-anchored proteins into human erythrocytes and their fate in the membrane." Blood **91**(5): 1784-92.

Coates, P. J., R. Nenutil, A. McGregor, S. M. Picksley, D. H. Crouch, P. A. Hall and E. G. Wright (2001). "Mammalian prohibitin proteins respond to mitochondrial stress and decrease during cellular senescence." Exp Cell Res **265**(2): 262-73.

Coles, S. E. and G. W. Stewart (1999). "Temperature effects on cation transport in hereditary stomatocytosis and allied disorders." Int J Exp Pathol **80**(5): 251-8.

Connor, J. and A. J. Schroit (1989). "Transbilayer movement of phosphatidylserine in nonhuman erythrocytes: evidence that the aminophospholipid transporter is a ubiquitous membrane protein." Biochemistry **28**(25): 9680-5.

Cordy, J. M., I. Hussain, C. Dingwall, N. M. Hooper and A. J. Turner (2003). "Exclusively targeting beta-secretase to lipid rafts by GPI-anchor addition up-regulates beta-site processing of the amyloid precursor protein." Proc Natl Acad Sci U S A **100**(20): 11735-40.

Dantas de Medeiros, T. M., K. C. Ortega, D. Mion, Jr., K. Nonoyama and O. C. Barretto (2002). "Normal erythrocyte calpain I activity on membrane proteins under near-physiological conditions in patients with essential hypertension." Sao Paulo Med J **120**(1): 5-8.

Delaunay, J. (2002). "Molecular basis of red cell membrane disorders." Acta Haematol **108**(4): 210-8.

Delaunay, J. (2004). "The hereditary stomatocytoses: genetic disorders of the red cell membrane permeability to monovalent cations." Semin Hematol **41**(2): 165-72.

Desneves, J., A. Berman, K. Dynon, N. La Greca, M. Foley and L. Tilley (1996). "Human erythrocyte band 7.2b is preferentially labeled by a photoreactive phospholipid." Biochem Biophys Res Commun **224**(1): 108-14.

Dietrich, C., L. A. Bagatolli, Z. N. Volovyk, N. L. Thompson, M. Levi, K. Jacobson and E. Gratton (2001). "Lipid rafts reconstituted in model membranes." Biophys J **80**(3): 1417-28.

Drenan, R. M., C. A. Doupnik, M. P. Boyle, L. J. Muglia, J. E. Huettner, M. E. Linder and K. J. Blumer (2005). "Palmitoylation regulates plasma membrane-nuclear shuttling of R7BP, a novel membrane anchor for the RGS7 family." J Cell Biol **169**(4): 623-33.

El-Husseini, A. E., S. E. Craven, D. M. Chetkovich, B. L. Firestein, E. Schnell, C. Aoki and D. S. Bredt (2000). "Dual palmitoylation of PSD-95 mediates its vesiculotubular sorting, postsynaptic targeting, and ion channel clustering." J Cell Biol **148**(1): 159-72.

Fairbanks, G., T. L. Steck and D. F. Wallach (1971). "Electrophoretic analysis of the major polypeptides of the human erythrocyte membrane." Biochemistry **10**(13): 2606-17.

Fenteany, G. and S. L. Schreiber (1998). "Lactacystin, proteasome function, and cell fate." J Biol Chem **273**(15): 8545-8.

Ferguson, M. A. (1999). "The structure, biosynthesis and functions of glycosylphosphatidylinositol anchors, and the contributions of trypanosome research." J Cell Sci **112 (Pt 17)**: 2799-809.

Foley, M. and L. Tilley (1997). "Quinoline antimalarials: mechanisms of action and resistance." Int J Parasitol **27**(2): 231-40.

Fricke, B., H. G. Jarvis, C. D. Reid, P. Aguilar-Martinez, A. Robert, P. Quittet, M. Chetty, A. Pizzey, T. Cynober, W. F. Lande, W. C. Mentzer, M. During, S. Winter, J. Delaunay and G. W. Stewart (2004). "Four new cases of stomatin-deficient hereditary stomatocytosis syndrome: association of the stomatin-deficient cryohydrocytosis variant with neurological dysfunction." Br J Haematol **125**(6): 796-803.

Fricke, B., A. C. Argent, M. C. Chetty, A. R. Pizzey, E. J. Turner, M. M. Ho, A. Iolascon, M. von During and G. W. Stewart (2003). "The "stomatin" gene and protein in overhydrated hereditary stomatocytosis." Blood **102**(6): 2268-77.

Fricke, B., R. Lints, G. Stewart, H. Drummond, G. Dodt, M. Driscoll and M. von During (2000). "Epithelial Na+ channels and stomatin are expressed in rat trigeminal mechanosensory neurons." Cell Tissue Res **299**(3): 327-34.

Fricke, B., S. F. Parsons, G. Knopfle, M. von During and G. W. Stewart (2005). "Stomatin is mis-trafficked in the erythrocytes of overhydrated hereditary stomatocytosis, and is absent from normal primitive yolk sac-derived erythrocytes." Br J Haematol **131**(2): 265-77.

Fu, G., T. Wang, B. Yang, F. Lv, C. Shi, X. Jiang, L. Tian, W. Yu and N. Hamasaki (2004). "Purification and characterization of the human erythrocyte band 3 protein C-terminal domain." Biochemistry **43**(6): 1633-8.

Gardner, J. D., A. Lapey, P. Simopoulos and E. L. Bravo (1971). "Abnormal membrane sodium transport in Liddle's syndrome." J Clin Invest **50**(11): 2253-8.

Gascard, P., W. Nunomura, G. Lee, L. D. Walensky, S. W. Krauss, Y. Takakuwa, J. A. Chasis, N. Mohandas and J. G. Conboy (1999). "Deciphering the nuclear import pathway for the cytoskeletal red cell protein 4.1R." Mol Biol Cell **10**(6): 1783-98.

Gaus, K., E. Gratton, E. P. Kable, A. S. Jones, I. Gelissen, L. Kritharides and W. Jessup (2003). "Visualizing lipid structure and raft domains in living cells with two-photon microscopy." Proc Natl Acad Sci U S A **100**(26): 15554-9.

Glebov, O. O. and B. J. Nichols (2004). "Distribution of lipid raft markers in live cells." Biochem Soc Trans **32**(Pt 5): 673-5.

Glebov, O. O. and B. J. Nichols (2004). "Lipid raft proteins have a random distribution during localized activation of the T-cell receptor." Nat Cell Biol **6**(3): 238-43.

Goll, D. E., V. F. Thompson, H. Li, W. Wei and J. Cong (2003). "The calpain system." Physiol Rev **83**(3): 731-801.

Gomez-Mouton, C., R. A. Lacalle, E. Mira, S. Jimenez-Baranda, D. F. Barber, A. C. Carrera, A. C. Martinez and S. Manes (2004). "Dynamic redistribution of raft domains as an organizing platform for signaling during cell chemotaxis." J Cell Biol **164**(5): 759-68.

Goodman, M. B., G. G. Ernstrom, D. S. Chelur, R. O'Hagan, C. A. Yao and M. Chalfie (2002). "MEC-2 regulates C. elegans DEG/ENaC channels needed for mechanosensation." Nature **415**(6875): 1039-42.

Green, J. B., B. Fricke, M. C. Chetty, M. von During, G. F. Preston and G. W. Stewart (2004). "Eukaryotic and prokaryotic stomatins: the proteolytic link." Blood Cells Mol Dis **32**(3): 411-22.

Gri, G., B. Molon, S. Manes, T. Pozzan and A. Viola (2004). "The inner side of T cell lipid rafts." Immunol Lett **94**(3): 247-52.

Haldar, K., B. U. Samuel, N. Mohandas, T. Harrison and N. L. Hiller (2001). "Transport mechanisms in Plasmodium-infected erythrocytes: lipid rafts and a tubovesicular network." Int J Parasitol **31**(12): 1393-401.

Hanada, K., M. Nishijima, Y. Akamatsu and R. E. Pagano (1995). "Both sphingolipids and cholesterol participate in the detergent insolubility of alkaline phosphatase, a glycosylphosphatidylinositol-anchored protein, in mammalian membranes." J Biol Chem **270**(11): 6254-60.

Hannan, L. A. and M. Edidin (1996). "Traffic, polarity, and detergent solubility of a glycosylphosphatidylinositol-anchored protein after LDL-deprivation of MDCK cells." J Cell Biol **133**(6): 1265-76.

Hao, M., S. Mukherjee and F. R. Maxfield (2001). "Cholesterol depletion induces large scale domain segregation in living cell membranes." Proc Natl Acad Sci U S A **98**(23): 13072-7.

Harder, T. and M. Kuhn (2000). "Selective accumulation of raft-associated membrane protein LAT in T cell receptor signaling assemblies." J Cell Biol **151**(2): 199-208.

Heerklotz, H. (2002). "Triton promotes domain formation in lipid raft mixtures." Biophys J **83**(5): 2693-701.

Henderson, R. M., J. M. Edwardson, N. A. Geisse and D. E. Saslowsky (2004). "Lipid rafts: feeling is believing." News Physiol Sci **19**: 39-43.

Hiebl-Dirschmied, C. M., G. R. Adolf and R. Prohaska (1991). "Isolation and partial characterization of the human erythrocyte band 7 integral membrane protein." Biochim Biophys Acta **1065**(2): 195-202.

Hiebl-Dirschmied, C. M., B. Entler, C. Glotzmann, I. Maurer-Fogy, C. Stratowa and R. Prohaska (1991). "Cloning and nucleotide sequence of cDNA encoding human erythrocyte band 7 integral membrane protein." Biochim Biophys Acta **1090**(1): 123-4.

Ho, M. M., A. Nicolaou, A. C. Argent and G. W. Stewart (1997). "Trans-bilayer phospholipid movements in human red blood cells deficient in the 32 kDa Band-7.2b membrane protein, 'stomatin'." Biochem Soc Trans **25**(3): 492S.

Hooper, N. M. (1999). "Detergent-insoluble glycosphingolipid/cholesterol-rich membrane domains, lipid rafts and caveolae (review)." Mol Membr Biol **16**(2): 145-56.

Hooper, N. M. (2005). "Roles of proteolysis and lipid rafts in the processing of the amyloid precursor protein and prion protein." Biochem Soc Trans **33**(Pt 2): 335-8.

Huang, M., G. Gu, E. L. Ferguson and M. Chalfie (1995). "A stomatin-like protein necessary for mechanosensation in C. elegans." Nature **378**(6554): 292-5.

Huber, T. B., M. Simons, B. Hartleben, L. Sernetz, M. Schmidts, E. Gundlach, M. A. Saleem, G. Walz and T. Benzing (2003). "Molecular basis of the functional podocin-nephrin complex: mutations in the NPHS2 gene disrupt nephrin targeting to lipid raft microdomains." Hum Mol Genet **12**(24): 3397-405.

Iida, K., M. B. Whitlow and V. Nussenzweig (1991). "Membrane vesiculation protects erythrocytes from destruction by complement." J Immunol **147**(8): 2638-42.

Ilangumaran, S. and D. C. Hoessli (1998). "Effects of cholesterol depletion by cyclodextrin on the sphingolipid microdomains of the plasma membrane." Biochem J **335 (Pt 2)**: 433-40.

Innes, D. S., J. H. Sinard, D. M. Gilligan, L. M. Snyder, P. G. Gallagher and J. S. Morrow (1999). "Exclusion of the stomatin, alpha-adducin and beta-adducin loci in a large kindred with dehydrated hereditary stomatocytosis." Am J Hematol **60**(1): 72-4.

Karlstrom, H., A. Bergman, U. Lendahl, J. Naslund and J. Lundkvist (2002). "A sensitive and quantitative assay for measuring cleavage of presenilin substrates." J Biol Chem **277**(9): 6763-6.

Kaser, M. and T. Langer (2000). "Protein degradation in mitochondria." Semin Cell Dev Biol **11**(3): 181-90.

Kenworthy, A. K., B. J. Nichols, C. L. Remmert, G. M. Hendrix, M. Kumar, J. Zimmerberg and J. Lippincott-Schwartz (2004). "Dynamics of putative raft-associated proteins at the cell surface." J Cell Biol **165**(5): 735-46.

Knowles, D. W., L. Tilley, N. Mohandas and J. A. Chasis (1997). "Erythrocyte membrane vesiculation: model for the molecular mechanism of protein sorting." Proc Natl Acad Sci U S A **94**(24): 12969-74.

Lafont, F. and F. G. van der Goot (2005). "Bacterial invasion via lipid rafts." Cell Microbiol **7**(5): 613-20.

Lande, W. M., P. V. Thiemann and W. C. Mentzer, Jr. (1982). "Missing band 7 membrane protein in two patients with high Na, low K erythrocytes." J Clin Invest **70**(6): 1273-80.

Langhorst, M. F., A. Reuter and C. A. Stuermer (2005). "Scaffolding microdomains and beyond: the function of reggie/flotillin proteins." Cell Mol Life Sci **62**(19-20): 2228-40.

Lawrence, J. C., D. E. Saslowsky, J. M. Edwardson and R. M. Henderson (2003). "Real-time analysis of the effects of cholesterol on lipid raft behavior using atomic force microscopy." Biophys J **84**(3): 1827-32.

Lawrence, J. G. and J. R. Roth (1996). "Selfish operons: horizontal transfer may drive the evolution of gene clusters." Genetics **143**(4): 1843-60.

Ledesma, M. D., J. S. Da Silva, A. Schevchenko, M. Wilm and C. G. Dotti (2003). "Proteomic characterisation of neuronal sphingolipid-cholesterol microdomains: role in plasminogen activation." Brain Res **987**(1): 107-16.

Lee, A. G. (1977). "Lipid phase transitions and phase diagrams. I. Lipid phase transitions." Biochim Biophys Acta **472**(2): 237-81.

Li, Q., V. Jungmann, A. Kiyatkin and P. S. Low (1996). "Prostaglandin E2 stimulates a Ca2+-dependent K+ channel in human erythrocytes and alters cell volume and filterability." J Biol Chem **271**(31): 18651-6.

Lichtenberg, D., F. M. Goni and H. Heerklotz (2005). "Detergent-resistant membranes should not be identified with membrane rafts." Trends Biochem Sci **30**(8): 430-6.

Liu, X. L., S. C. Done, K. Yan, P. Kilpelainen, T. Pikkarainen and K. Tryggvason (2004). "Defective trafficking of nephrin missense mutants rescued by a chemical chaperone." J Am Soc Nephrol **15**(7): 1731-8.

Liu, J., S. M. DeYoung, M. Zhang, L. H. Dold and A. R. Saltiel (2005). "The Stomatin/Prohibitin/Flotillin/HflK/C Domain of Flotillin-1 contains distinct sequences that direct plasma membrane localisation and protein interactions in 3T3-L1 adipocytes." J Biol Chem **280**(16): 16125-34.

Lock, S. P., R. S. Smith and R. M. Hardisty (1961). "Stomatocytosis: a hereditary red cell anomally associated with haemolytic anaemia." Br J Haematol **7**: 303-14.

London, E. and D. A. Brown (2000). "Insolubility of lipids in triton X-100: physical origin and relationship to sphingolipid/cholesterol membrane domains (rafts)." Biochim Biophys Acta **1508**(1-2): 182-95.

Low, P. S., D. Zhang and J. T. Bolin (2001). "Localization of mutations leading to altered cell shape and anion transport in the crystal structure of the cytoplasmic domain of band 3." Blood Cells Mol Dis **27**(1): 81-4.

Madore, N., K. L. Smith, C. H. Graham, A. Jen, K. Brady, S. Hall and R. Morris (1999). "Functionally different GPI proteins are organized in different domains on the neuronal surface." Embo J **18**(24): 6917-26.

Magee, A. I., J. Adler and I. Parmryd (2005). "Cold-induced coalescence of T-cell plasma membrane microdomains activates signalling pathways." J Cell Sci **118**(Pt 14): 3141-51.

Magnani, F., C. G. Tate, S. Wynne, C. Williams and J. Haase (2004). "Partitioning of the serotonin transporter into lipid microdomains modulates transport of serotonin." J Biol Chem **279**(37): 38770-8.

Mairhofer, M., M. Steiner, W. Mosgoeller, R. Prohaska and U. Salzer (2002). "Stomatin is a major lipid-raft component of platelet alpha granules." Blood **100**(3): 897-904.

Malinska, K., J. Malinsky, M. Opekarova and W. Tanner (2003). "Visualization of protein compartmentation within the plasma membrane of living yeast cells." Mol Biol Cell **14**(11): 4427-36.

Manjeshwar, S., D. E. Branam, M. R. Lerner, D. J. Brackett and E. R. Jupe (2003). "Tumor suppression by the prohibitin gene 3'untranslated region RNA in human breast cancer." Cancer Res **63**(17): 5251-6.

Manno, S., Y. Takakuwa and N. Mohandas (2002). "Identification of a functional role for lipid asymmetry in biological membranes: Phosphatidylserine-skeletal protein interactions modulate membrane stability." Proc Natl Acad Sci U S A **99**(4): 1943-8.

Manno, S., Y. Takakuwa and N. Mohandas (2005). "Modulation of erythrocyte membrane mechanical function by protein 4.1 phosphorylation." J Biol Chem **280**(9): 7581-7.

Mannsfeldt, A. G., P. Carroll, C. L. Stucky and G. R. Lewin (1999). "Stomatin, a MEC-2 like protein, is expressed by mammalian sensory neurons." Mol Cell Neurosci **13**(6): 391-404.

May, P., Y. K. Reddy and J. Herz (2002). "Proteolytic processing of low density lipoprotein receptor-related protein mediates regulated release of its intracellular domain." J Biol Chem **277**(21): 18736-43.

McMullin, M. F. (1999). "The molecular basis of disorders of the red cell membrane." J Clin Pathol **52**(4): 245-8.

Meder, D. and K. Simons (2005). "Cell biology. Ras on the roundabout." Science **307**(5716): 1731-3.

Meiri, K. F. (2005). "Lipid rafts and regulation of the cytoskeleton during T cell activation." Philos Trans R Soc Lond B Biol Sci **360**(1461): 1663-72.

Milhiet, P. E., C. Domec, M. C. Giocondi, N. Van Mau, F. Heitz and C. Le Grimellec (2001). "Domain formation in models of the renal brush border membrane outer leaflet." Biophys J **81**(1): 547-55.

Moore, R. B., M. V. Mankad, S. K. Shriver, V. N. Mankad and G. A. Plishker (1991). "Reconstitution of Ca(2+)-dependent K+ transport in erythrocyte membrane vesicles requires a cytoplasmic protein." J Biol Chem **266**(28): 18964-8.

Moore, R. B. and S. K. Shriver (1997). "Protein 7.2b of human erythrocyte membranes binds to calpromotin." Biochem Biophys Res Commun **232**(2): 294-7.

Morford, L. A., K. Forrest, B. Logan, L. K. Overstreet, J. Goebel, W. H. Brooks and T. L. Roszman (2002). "Calpain II colocalizes with detergent-insoluble rafts on human and Jurkat T-cells." Biochem Biophys Res Commun **295**(2): 540-6.

Morgan, B. P., J. R. Dankert and A. F. Esser (1987). "Recovery of human neutrophils from complement attack: removal of the membrane attack complex by endocytosis and exocytosis." J Immunol **138**(1): 246-53.

Murphy, S. C., B. U. Samuel, T. Harrison, K. D. Speicher, D. W. Speicher, M. E. Reid, R. Prohaska, P. S. Low, M. J. Tanner, N. Mohandas and K. Haldar (2004). "Erythrocyte detergent-resistant membrane proteins: their characterization and selective uptake during malarial infection." Blood **103**(5): 1920-8.

Neumann-Giesen, C., B. Falkenbach, P. Beicht, S. Claasen, G. Luers, C. A. Stuermer, V. Herzog and R. Tikkanen (2004). "Membrane and raft association of reggie-1/flotillin-2: role of myristoylation, palmitoylation and oligomerization and induction of filopodia by overexpression." Biochem J **378**(Pt 2): 509-18.

Nijtmans, L. G., S. M. Artal, L. A. Grivell and P. J. Coates (2002). "The mitochondrial PHB complex: roles in mitochondrial respiratory complex assembly, ageing and degenerative disease." Cell Mol Life Sci **59**(1): 143-55.

Padmakumar, V. C., T. Libotte, W. Lu, H. Zaim, S. Abraham, A. A. Noegel, J. Gotzmann, R. Foisner and I. Karakesisoglou (2005). "The inner nuclear membrane protein Sun1 mediates the anchorage of Nesprin-2 to the nuclear envelope." J Cell Sci **118**(Pt 15): 3419-30.

Parasassi, T., M. Loiero, M. Raimondi, G. Ravagnan and E. Gratton (1993). "Absence of lipid gel-phase domains in seven mammalian cell lines and in four primary cell types." Biochim Biophys Acta **1153**(2): 143-54.

Parfenov, V. N., D. S. Davis, G. N. Pochukalina, C. E. Sample, E. A. Bugaeva and K. G. Murti (1995). "Nuclear actin filaments and their topological changes in frog oocytes." Exp Cell Res **217**(2): 385-94.

Parsegian, V. A. (1995). "The cows or the fence?" Mol Membr Biol **12**(1): 5-7.

Pietiainen, V. M., V. Marjomaki, J. Heino and T. Hyypia (2005). "Viral entry, lipid rafts and caveosomes." Ann Med **37**(6): 394-403.

Pike, L. J. (2004). "Lipid rafts: heterogeneity on the high seas." Biochem J **378**(Pt 2): 281-92.

Price, M. P., R. J. Thompson, J. O. Eshcol, J. A. Wemmie and C. J. Benson (2004). "Stomatin modulates gating of acid-sensing ion channels." J Biol Chem **279**(51): 53886-91.

Rajalingam, K., C. Wunder, V. Brinkmann, Y. Churin, M. Hekman, C. Sievers, U. R. Rapp and T. Rudel (2005). "Prohibitin is required for Ras-induced Raf-MEK-ERK activation and epithelial cell migration." Nat Cell Biol **7**(8): 837-43.

Rajaram, S., M. M. Sedensky and P. G. Morgan (1998). "Unc-1: a stomatin homologue controls sensitivity to volatile anesthetics in Caenorhabditis elegans." Proc Natl Acad Sci U S A **95**(15): 8761-6.

Reliene, R., M. Mariani, A. Zanella, W. H. Reinhart, M. L. Ribeiro, E. M. del Giudice, S. Perrotta, A. Iolascon, S. Eber and H. U. Lutz (2002). "Splenectomy prolongs in vivo survival of erythrocytes differently in spectrin/ankyrin- and band 3-deficient hereditary spherocytosis." Blood **100**(6): 2208-15.

Richmond, T. D., M. Chohan and D. L. Barber (2005). "Turning cells red: signal transduction mediated by erythropoietin." Trends Cell Biol **15**(3): 146-55.

Rinia, H. A., M. M. Snel, J. P. van der Eerden and B. de Kruijff (2001). "Visualizing detergent resistant domains in model membranes with atomic force microscopy." FEBS Lett **501**(1): 92-6.

Rivas, M. G. and A. M. Gennaro (2003). "Detergent resistant domains in erythrocyte membranes survive after cell cholesterol depletion: an EPR spin label study." Chem Phys Lipids **122**(1-2): 165-9.

Roselli, S., L. Heidet, M. Sich, A. Henger, M. Kretzler, M. C. Gubler and C. Antignac (2004). "Early glomerular filtration defect and severe renal disease in podocin-deficient mice." Mol Cell Biol **24**(2): 550-60.

Rothberg, K. G., Y. S. Ying, B. A. Kamen and R. G. Anderson (1990). "Cholesterol controls the clustering of the glycophospholipid-anchored membrane receptor for 5-methyltetrahydrofolate." J Cell Biol **111**(6 Pt 2): 2931-8.

Sadowski, I., B. Bell, P. Broad and M. Hollis (1992). "GAL4 fusion vectors for expression in yeast or mammalian cells." Gene **118**(1): 137-41.

Sadowski, I., J. Ma, S. Triezenberg and M. Ptashne (1988). "GAL4-VP16 is an unusually potent transcriptional activator." Nature **335**(6190): 563-4.

Saikawa, N., Y. Akiyama and K. Ito (2004). "FtsH exists as an exceptionally large complex containing HflKC in the plasma membrane of Escherichia coli." J Struct Biol **146**(1-2): 123-9.

Salzer, U., H. Ahorn and R. Prohaska (1993). "Identification of the phosphorylation site on human erythrocyte band 7 integral membrane protein: implications for a monotopic protein structure." Biochim Biophys Acta **1151**(2): 149-52.

Salzer, U., P. Hinterdorfer, U. Hunger, C. Borken and R. Prohaska (2002). "Ca(++)-dependent vesicle release from erythrocytes involves stomatin-specific lipid rafts, synexin (annexin VII), and sorcin." Blood **99**(7): 2569-77.

Salzer, U., M. Kubicek and R. Prohaska (1999). "Isolation, molecular characterization, and tissue-specific expression of ECP-51 and ECP-54 (TIP49), two homologous, interacting erythroid cytosolic proteins." Biochim Biophys Acta **1446**(3): 365-70.

Salzer, U. and R. Prohaska (2001). "Stomatin, flotillin-1, and flotillin-2 are major integral proteins of erythrocyte lipid rafts." Blood **97**(4): 1141-3.

Samsonov, A. V., I. Mihalyov and F. S. Cohen (2001). "Characterization of cholesterol-sphingomyelin domains and their dynamics in bilayer membranes." Biophys J **81**(3): 1486-500.

Santamaria, A., E. Castellanos, V. Gomez, P. Benedit, J. Renau-Piqueras, J. Morote, J. Reventos, T. M. Thomson and R. Paciucci (2005). "PTOV1 enables the nuclear translocation and mitogenic activity of flotillin-1, a major protein of lipid rafts." Mol Cell Biol **25**(5): 1900-11.

Saslowsky, D. E., J. Lawrence, X. Ren, D. A. Brown, R. M. Henderson and J. M. Edwardson (2002). "Placental alkaline phosphatase is efficiently targeted to rafts in supported lipid bilayers." J Biol Chem **277**(30): 26966-70.

Scheiffele, P., M. G. Roth and K. Simons (1997). "Interaction of influenza virus haemagglutinin with sphingolipid-cholesterol membrane domains via its transmembrane domain." Embo J **16**(18): 5501-8.

Schnitzer, J. E., P. Oh, E. Pinney and J. Allard (1994). "Filipin-sensitive caveolae-mediated transport in endothelium: reduced transcytosis, scavenger endocytosis, and capillary permeability of select macromolecules." J Cell Biol **127**(5): 1217-32.

Schroeder, R. J., S. N. Ahmed, Y. Zhu, E. London and D. A. Brown (1998). "Cholesterol and sphingolipid enhance the Triton X-100 insolubility of glycosylphosphatidylinositol-anchored proteins by promoting the formation of detergent-insoluble ordered membrane domains." J Biol Chem **273**(2): 1150-7.

Schuck, S., M. Honsho, K. Ekroos, A. Shevchenko and K. Simons (2003). "Resistance of cell membranes to different detergents." Proc Natl Acad Sci U S A **100**(10): 5795-800.

Schwarz, K., M. Simons, J. Reiser, M. A. Saleem, C. Faul, W. Kriz, A. S. Shaw, L. B. Holzman and P. Mundel (2001). "Podocin, a raft-associated component of the glomerular slit diaphragm, interacts with CD2AP and nephrin." J Clin Invest **108**(11): 1621-9.

Sedensky, M. M., J. M. Siefker, J. Y. Koh, D. M. Miller, 3rd and P. G. Morgan (2004). "A stomatin and a degenerin interact in lipid rafts of the nervous system of Caenorhabditis elegans." Am J Physiol Cell Physiol **287**(2): C468-74.

Seidel, G. and R. Prohaska (1998). "Molecular cloning of hSLP-1, a novel human brain-specific member of the band 7/MEC-2 family similar to Caenorhabditis elegans UNC-24." Gene **225**(1-2): 23-9.

Sherf, B. A., Navarro, S. L., Hannah, R. R., and Wood, K. V. (1996). "Dual-Luciferase™ Reporter Assay: An Advanced Co-Reporter Technology Integrating Firefly and *Renilla* Luciferase Assays." Promega Notes Magazine **57**: 2-8.

Silvius, J. R. (2003). "Role of cholesterol in lipid raft formation: lessons from lipid model systems." Biochim Biophys Acta **1610**(2): 174-83.

Silvius, J. R., D. del Giudice and M. Lafleur (1996). "Cholesterol at different bilayer concentrations can promote or antagonize lateral segregation of phospholipids of differing acyl chain length." Biochemistry **35**(48): 15198-208.

Simons, K. and E. Ikonen (1997). "Functional rafts in cell membranes." Nature **387**(6633): 569-72.

Simons, K. and E. Ikonen (2000). "How cells handle cholesterol." Science **290**(5497): 1721-6.

Sims, P. J. and T. Wiedmer (1986). "Repolarization of the membrane potential of blood platelets after complement damage: evidence for a Ca++ -dependent exocytotic elimination of C5b-9 pores." Blood **68**(2): 556-61.

Smart, E. J., Y. S. Ying, P. A. Conrad and R. G. Anderson (1994). "Caveolin moves from caveolae to the Golgi apparatus in response to cholesterol oxidation." J Cell Biol **127**(5): 1185-97.

Smart, E. J., Y. S. Ying, C. Mineo and R. G. Anderson (1995). "A detergent-free method for purifying caveolae membrane from tissue culture cells." Proc Natl Acad Sci U S A **92**(22): 10104-8.

Smith, P. K., R. I. Krohn, G. T. Hermanson, A. K. Mallia, F. H. Gartner, M. D. Provenzano, E. K. Fujimoto, N. M. Goeke, B. J. Olson and D. C. Klenk (1985). "Measurement of protein using bicinchoninic acid." Anal Biochem **150**(1): 76-85.

Snyers, L., D. Thines-Sempoux and R. Prohaska (1997). "Colocalization of stomatin (band 7.2b) and actin microfilaments in UAC epithelial cells." Eur J Cell Biol **73**(3): 281-5.

Snyers, L., E. Umlauf and R. Prohaska (1998). "Oligomeric nature of the integral membrane protein stomatin." J Biol Chem **273**(27): 17221-6.

Snyers, L., E. Umlauf and R. Prohaska (1999). "Association of stomatin with lipid-protein complexes in the plasma membrane and the endocytic compartment." Eur J Cell Biol **78**(11): 802-12.

Snyers, L., E. Umlauf and R. Prohaska (1999). "Cysteine 29 is the major palmitoylation site on stomatin." FEBS Lett **449**(2-3): 101-4.

Staneva, G., M. Seigneuret, K. Koumanov, G. Trugnan and M. I. Angelova (2005). "Detergents induce raft-like domains budding and fission from giant unilamellar heterogeneous vesicles: a direct microscopy observation." Chem Phys Lipids **136**(1): 55-66.

Stewart, G. W. (2004). "Hemolytic disease due to membrane ion channel disorders." Curr Opin Hematol **11**(4): 244-50.

Stewart, G. W. (1997). "Stomatin." Int J Biochem Cell Biol **29**(2): 271-4.

Stewart, G. W., A. C. Argent and B. C. Dash (1993). "Stomatin: a putative cation transport regulator in the red cell membrane." Biochim Biophys Acta **1225**(1): 15-25.

Stewart, G. W., B. E. Hepworth-Jones, J. N. Keen, B. C. Dash, A. C. Argent and C. M. Casimir (1992). "Isolation of cDNA coding for an ubiquitous membrane protein deficient in high Na+, low K+ stomatocytic erythrocytes." Blood **79**(6): 1593-601.

Stewart, G. W. and E. J. Turner (1999). "The hereditary stomatocytoses and allied disorders: congenital disorders of erythrocyte membrane permeability to Na and K." Baillieres Best Pract Res Clin Haematol **12**(4): 707-27.

Struhl, G. and A. Adachi (1998). "Nuclear access and action of notch in vivo." Cell **93**(4): 649-60.

Suomalainen, M. (2002). "Lipid rafts and assembly of enveloped viruses." Traffic **3**(10): 705-9.

Suzuki, H., R. Kerr, L. Bianchi, C. Frokjaer-Jensen, D. Slone, J. Xue, B. Gerstbrein, M. Driscoll and W. R. Schafer (2003). "In vivo imaging of C. elegans mechanosensory neurons demonstrates a specific role for the MEC-4 channel in the process of gentle touch sensation." Neuron **39**(6): 1005-17.

Suzuki, K., S. Hata, Y. Kawabata and H. Sorimachi (2004). "Structure, activation, and biology of calpain." Diabetes **53 Suppl 1**: S12-8.

Takakuwa, Y. (2000). "Protein 4.1, a multifunctional protein of the erythrocyte membrane skeleton: structure and functions in erythrocytes and nonerythroid cells." Int J Hematol **72**(3): 298-309.

Tatsuta, T., K. Model and T. Langer (2005). "Formation of membrane-bound ring complexes by prohibitins in mitochondria." Mol Biol Cell **16**(1): 248-59.

Tavernarakis, N., M. Driscoll and N. C. Kyrpides (1999). "The SPFH domain: implicated in regulating targeted protein turnover in stomatins and other membrane-associated proteins." Trends Biochem Sci **24**(11): 425-7.

Tse, W. T. and S. E. Lux (1999). "Red blood cell membrane disorders." Br J Haematol **104**(1): 2-13.

Tsai, K. J., L. Y. Shih, et al. (1996). "Enhanced vesiculation exacerbates complement-dependent hemolysis in glucose-6-phosphate dehydrogenase deficient red blood cells." Life Sci **59**(10): 867-76.

Turner, E. J., H. G. Jarvis, M. C. Chetty, G. Landon, P. S. Rowley, M. M. Ho and G. W. Stewart (2003). "ATP-dependent vesiculation in red cell membranes from different hereditary stomatocytosis variants." Br J Haematol **120**(5): 894-902.

Umlauf, E., E. Csaszar, M. Moertelmaier, G. J. Schuetz, R. G. Parton and R. Prohaska (2004). "Association of stomatin with lipid bodies." J Biol Chem **279**(22): 23699-709.

Valensin, S., S. R. Paccani, C. Ulivieri, D. Mercati, S. Pacini, L. Patrussi, T. Hirst, P. Lupetti and C. T. Baldari (2002). "F-actin dynamics control segregation of the TCR signaling cascade to clustered lipid rafts." Eur J Immunol **32**(2): 435-46.

Vallet, V., C. Pfister, J. Loffing and B. C. Rossier (2002). "Cell-surface expression of the channel activating protease xCAP-1 is required for activation of ENaC in the Xenopus oocyte." J Am Soc Nephrol **13**(3): 588-94.

van Meer, G. (2001). "Caveolin, cholesterol, and lipid droplets?" J Cell Biol **152**(5): F29-34.

Varma, R. and S. Mayor (1998). "GPI-anchored proteins are organized in submicron domains at the cell surface." Nature **394**(6695): 798-801.

Vetrivel, K. S., H. Cheng, S. H. Kim, Y. Chen, N. Y. Barnes, A. T. Parent, S. S. Sisodia and G. Thinakaran (2005). "Spatial segregation of gamma-secretase and substrates in distinct membrane domains." J Biol Chem **280**(27): 25892-900.

Wang, D., W. C. Mentzer, T. Cameron and R. M. Johnson (1991). "Purification of band 7.2b, a 31-kDa integral phosphoprotein absent in hereditary stomatocytosis." J Biol Chem **266**(27): 17826-31.

Wang, S., G. Fusaro, J. Padmanabhan and S. P. Chellappan (2002). "Prohibitin co-localizes with Rb in the nucleus and recruits N-CoR and HDAC1 for transcriptional repression." Oncogene **21**(55): 8388-96.

Wang, Y. and J. S. Morrow (2000). "Identification and characterization of human SLP-2, a novel homologue of stomatin (band 7.2b) present in erythrocytes and other tissues." J Biol Chem **275**(11): 8062-71.

Wang, Z., W. Xie, F. Chi and C. Li (2005). "Identification of non-specific lipid transfer protein-1 as a calmodulin-binding protein in Arabidopsis." FEBS Lett **579**(7): 1683-7.

Whitlow, M., K. Iida, P. Marshall, R. Silber and V. Nussenzweig (1993). "Cells lacking glycan phosphatidylinositol-linked proteins have impaired ability to vesiculate." Blood **81**(2): 510-6.

Wiedmer, T., J. Zhao, M. Nanjundan and P. J. Sims (2003). "Palmitoylation of phospholipid scramblase 1 controls its distribution between nucleus and plasma membrane." Biochemistry **42**(5): 1227-33.

Wolfe, M. S. and R. Kopan (2004). "Intramembrane proteolysis: theme and variations." Science **305**(5687): 1119-23.

Wolfs, J. L., P. Comfurius, E. M. Bevers and R. F. Zwaal (2003). "Influence of erythrocyte shape on the rate of Ca2+-induced scrambling of phosphatidylserine." Mol Membr Biol **20**(1): 83-91.

Yokoyama, H. and I. Matsui (2005). "A novel thermostable membrane protease forming an operon with a stomatin homolog from the hyperthermophilic archaebacterium Pyrococcus horikoshii." J Biol Chem **280**(8): 6588-94.

Yuan, C., J. Furlong, P. Burgos and L. J. Johnston (2002). "The size of lipid rafts: an atomic force microscopy study of ganglioside GM1 domains in sphingomyelin/DOPC/cholesterol membranes." Biophys J **82**(5): 2526-35.

Zeyda, M., G. Staffler, V. Horejsi, W. Waldhausl and T. M. Stulnig (2002). "LAT displacement from lipid rafts as a molecular mechanism for the inhibition of T cell signaling by polyunsaturated fatty acids." J Biol Chem **277**(32): 28418-23.

Zhang, J. Z., W. Abbud, R. Prohaska and F. Ismail-Beigi (2001). "Overexpression of stomatin depresses GLUT-1 glucose transporter activity." Am J Physiol Cell Physiol **280**(5): C1277-83.

Zhang, J. Z., H. Hayashi, Y. Ebina, R. Prohaska and F. Ismail-Beigi (1999). "Association of stomatin (band 7.2b) with Glut1 glucose transporter." Arch Biochem Biophys **372**(1): 173-8.

Zhang, L. Y., F. Ding, Z. M. Liu, W. D. Li, Z. H. Liu and Y. D. Li (2005). "[Effect of stomatin-like protein 2 (SLP-2) gene on growth and proliferation of esophageal squamous carcinoma cell line TE12]." Ai Zheng **24**(2): 155-9.

Zhang, W., R. P. Trible and L. E. Samelson (1998). "LAT palmitoylation: its essential role in membrane microdomain targeting and tyrosine phosphorylation during T cell activation." Immunity **9**(2): 239-46.

Zhu, Y., C. Paszty, T. Turetsky, S. Tsai, F. A. Kuypers, G. Lee, P. Cooper, P. G. Gallagher, M. E. Stevens, E. Rubin, N. Mohandas and W. C. Mentzer (1999). "Stomatocytosis is absent in "stomatin"-deficient murine red blood cells." Blood **93**(7): 2404-10.

Zwaal, R. F. and A. J. Schroit (1997). "Pathophysiologic implications of membrane phospholipid asymmetry in blood cells." Blood **89**(4): 1121-32.